

(NASA-CR-124457) DEVELOPMENT, FABRICATION
AND EVALUATION OF COMPOSITE THERMAL
ENGINE INSULATION Final Report (Avco
Government Products Group) 101 p HC
\$7.25

N73-33458

Unclass

CSCL 11D G3/18 15722

DEVELOPMENT, FABRICATION AND EVALUATION OF
COMPOSITE THERMAL ENGINE INSULATION

FINAL REPORT

Prepared for

NATIONAL AERONAUTICS AND SPACE ADMINISTRATION
George C. Marshall Space Flight Center
Marshall Space Flight Center, Alabama 35812

Contract No. NAS8-29061



September 1973

AVCO GOVERNMENT PRODUCTS GROUP
SYSTEMS DIVISION
Lowell Industrial Park
Lowell, Massachusetts 01851



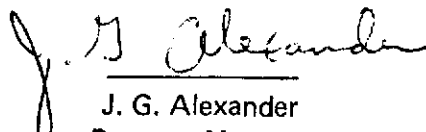
**DEVELOPMENT, FABRICATION AND EVALUATION OF
COMPOSITE THERMAL ENGINE INSULATION**

FINAL REPORT

Prepared for

NATIONAL AERONAUTICS AND SPACE ADMINISTRATION
George C. Marshall Space Flight Center
Marshall Space Flight Center, Alabama 35812

Contract No. NAS8-29061


J. G. Alexander
Program Manager

September 1973

AVCO GOVERNMENT PRODUCTS GROUP
SYSTEMS DIVISION
Lowell Industrial Park
Lowell, Massachusetts 01851



TABLE OF CONTENTS

1.0	INTRODUCTION	1
2.0	SUMMARY, CONCLUSIONS, AND RECOMMENDATIONS	3
3.0	TPS PANEL DESIGN	5
3.1	Description of 3DSX/Foil Concept	5
3.2	Design Environments	5
3.3	Selection of Materials	9
3.4	Enclosure Fabrication Studies	12
3.5	Structural Design Study	23
3.5.1	Foil Evaluation	23
3.5.2	Venting Pressure Loads	26
3.5.3	Thermomechanical Behavior	32
3.5.4	Enclosure Venting (Burst) Pressure Test	40
3.6	Thermal Sizing of 3DSX Insulation	47
3.7	Weight Analysis	51
4.0	EXPERIMENTAL DEMONSTRATION OF PERFORMANCE AND REUSE CAPABILITY ...	55
4.1	Thermal Testing and Design Development	55
4.2	Acoustic Testing	89
	REFERENCES	95

LIST OF FIGURES

Figure 1.1	Metallic Heat Shield Concepts	2
3.1	Schematic of 3DSX/Foil TPS System	6
3.2	3DSX Woven Silica Insulation	7
3.3	Rear of Foil Enclosure Illustrating Nut Strip Fastener Technique	8
3.4	Typical Foil Texture Patterns	13
3.5	Typical Beaded Surface Specimen	14
3.6	Beading Tool	14
3.7	Surface Stiffened by Spot-Welded Hat Sections	15
3.8	Tie-Strap Detail	16
3.9	Spot Weld Test Configuration	17
3.10	Electron Beam Seam Welds for Splicing Foil	19
3.11	Electron Beam Button Welds in Haynes 25	20
3.12	Box Fold for Corner of Enclosure	21
3.13	Sliding Joint Configuration for Floating Top Specimens	22
3.14	Typical Stress Strain Curve for Textured 5-mil Hastelloy Foil	25
3.15	Three Mil Textured Hastelloy Foil Venting Pressure Design Curves	27
3.16	Six Mil Textured Hastelloy Foil Venting Pressure Design Curves	28
3.17	Flutter Boundary for Simply Supported Plate	31
3.18	Effect of Top Stiffness on Thermal Stresses	35
3.19	Detail of Edge Pleat and Edge Stiffener in Specimen 11	36
3.20	Free Body Diagram and Deformation Behavior of Stiffened Edge Enclosures	38

LIST OF FIGURES (Cont'd)

Figure 3.21	Horizontal Stress (σ_x) at Center of A Restrained Plate (X = 0) for Different Plate Aspect Ratios (a/b) in terms of EaAT	39
3.22	Top Surface, Venting Pressure Test Fixture	41
3.23	Rear Surface, Venting Pressure Test Fixture	41
3.24	Venting Pressure Test Fixture Attachment and Instrumentation Locations	42
3.25	Venting Pressure Test Setup	43
3.26	Mid-Panel Foil Deflection versus Pressure, Venting Pressure Test	45
3.27	Mid-Panel Foil Deflection versus Pressure, Venting Pressure Test	46
3.28	Thermal Design Environment	48
3.29	Reentry Pressure History, PHI-2 Trajectory	48
3.30	3DSX Sizing for MSFC Test Heating Environment	49
3.31	3DSX Thickness Requirement for 350° F Maximum Structure Temperature	49
3.32	Unit Weight of 3DSX/Foil TPS	50
3.33	Effective Density of 3DSX/Foil Heat Shield	52
4.1	Simple Textured Box Design	57
4.2	Textured Box Specimens Installed on Substructure Panel	58
4.3	Bottom View of Substructure Panel	59
4.4	Chamber and Radiant Heater for Thermal Cycling Test	60
4.5	Room-Ambient Heater Facility	61
4.6	Three-mil Hastelloy-X, 6 lb/ft ³ , One Cycle to 1800° F (Specimen 3)	62
4.7	Post Test Condition of Panel after One Cycle to 1800° F (Specimens 1 through 6)	64

LIST OF FIGURES (Cont'd)

Figure 4.8	Damage Map of Panel after One 1800° F Thermal Cycle	65
4.9	Detail of Edge Crack in 3-mil Hastelloy-X after Second Cycle to 1800° F (Specimen 3)	66
4.10	Detail of Floating Top Specimen Design (Specimen 7)	67
4.11	Pretest Appearance of Floating Top Specimen and Reference Specimen (Specimens 7 and 8)	68
4.12	Post Test Appearance of Floating Top and Reference Specimens after Four Thermal Cycles (1200°, 1400°, 1600°, 1800° F) (Specimens 7 and 8)	69
4.13	Compressive Crippling of Side of Floating Top Specimen (Specimen 7)	70
4.14	End View of Specimens 7 and 8 Showing Compressive Crippling of Specimen 7	71
4.15	Post Test Appearance of Floating Top and Reference Specimens after Ten Thermal Cycles to 1800° F (Specimens 7 and 8)	73
4.16	Modified Configurations with Stiffened Edges and Flexible Sides	74
4.17	Detail of Beaded Design (Specimen 10)	75
4.18	Beaded Design Flat Layout and Finished Specimen (Specimen 10)	76
4.19	Beaded Design Prior to Installation of 3DSX Insulation (Specimen 10)	77
4.20	Pleated Side Design (Specimen 11)	78
4.21	Specimens 9 and 10 after Ten Thermal Cycles to 1800° F	80
4.22	Detail of Second Floating Top Design (Specimen 12)	81
4.23	Second Floating Top Specimen (Specimen 12)	82
4.24	Detail of Tension Top Design (Specimen 13)	83

LIST OF FIGURES (Concl'd)

Figure 4.25	Tension-Top Specimen (Specimen 13)	84
4.26	Post Test Appearance of Second Floating Top Specimen after One 1800° F Thermal Cycle (Specimen 12)	85
4.27	Post Test Appearance of Tension Top Specimen after One 1800° F Thermal Cycle (Specimen 13)	86
4.28	Thermocouple Locations	87
4.29	Structure Temperature Response Data (Specimen 7)	88
4.30	Acoustic/Thermal Test Panel Prior to First Acoustic Test	90
4.31	Fatigue Crack Location in Hex Pattern on Top of Specimen 9	91

LIST OF TABLES

Table	I	Acoustic Design Environments	9
	II	Candidate Ceramic Insulation Materials	10
	III	Candidate Foil Materials	10
	IV	Results of Reentry Cycling on Foils for 100 Cycles to 2200° F	11
	V	Weld Strength Data	18
	VI	High Temperature Properties of Hastelloy-X and Haynes 25 Superalloys	23
	VII	Flexure Properties of Textured Foil	24
	VIII	Foil Tie-Down Spacing to Prevent Aerodynamic Flutter	32
	IX	Foil Pressure Test Results	44
	X	Thermal Property Model for 3DSX Material	47
	XI	3DSX/Foil Weight Breakdown	53
	XII	Specimen Description and Test Summary	56
	XIII	Acoustic Calibration Data	92

1.0 INTRODUCTION

Many areas of the Space Shuttle are subjected to heating environments which produce skin temperatures in the range of 500° to 1800° F. A metallic re-radiative heat shield provides an efficient approach to thermal protection in these areas. (See Figure 1.1.) Conventional design approaches typically utilize secondary structural heat shield panels attached to the primary vehicle structure with standoffs which provide space for thermal insulation behind the panel. Surface pressures are reacted by the bending stiffness of the panel and transmitted to the primary structure through the standoffs.

The 3DSX/foil heat shield concept provides an alternate approach in which a three-dimensionally woven silica insulation is used as a structural member to transmit surface pressures directly to the primary structure. The insulation is packaged within a superalloy foil enclosure which is attached to substructure by tie wires which penetrate the insulation. The system combines the benefits of a rugged system with reusability, low weight, and good thermal performance.

The overall objective of this program was the development of the 3DSX/foil concept to specific workable configurations and the demonstration of the multiple reuse capability of these configurations in a representative thermal and acoustic environment. Specific objectives were to:

- a. Select suitable metallic foil and insulation materials.
- b. Define the optimum geometry of construction.
- c. Define attachment methods.
- d. Demonstrate fabricability.
- e. Demonstrate the reuse capability of the composite TPS.
- f. Deliver specimens for test by NASA.

This program was conducted under the direction of the Avco Space Shuttle Program Office, J. W. Graham, Manager. The program manager was J. G. Alexander. Structural analyses were performed by P. J. Roy and R. H. Brown. Detail design of specimen configurations was performed by D. A. Mosher. The technical monitor for NASA/MSFC was H. M. King.

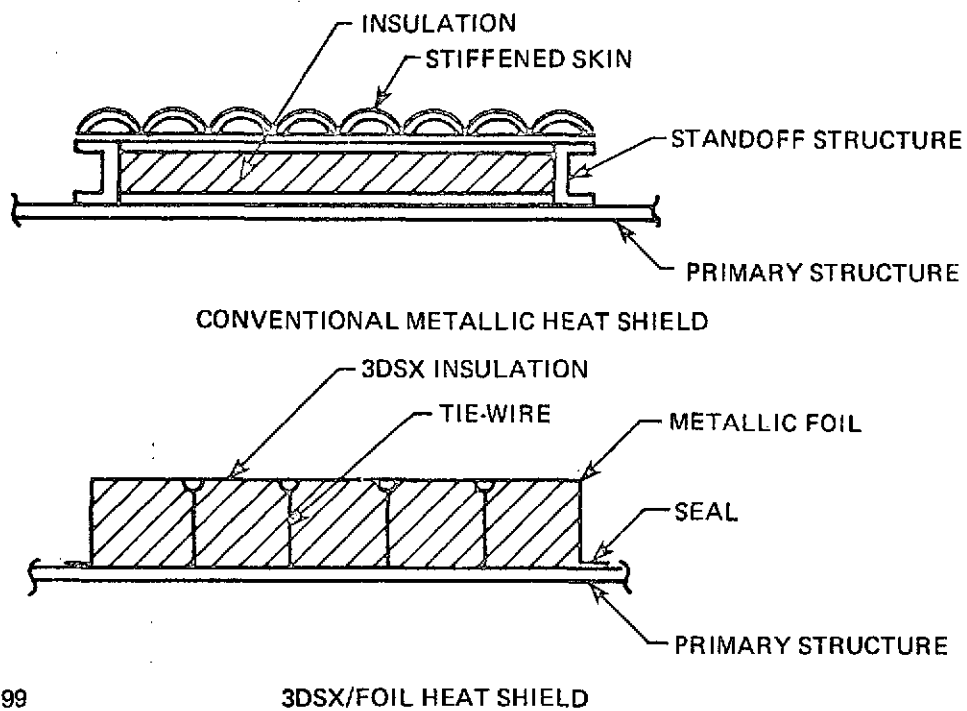


Figure 1.1 METALLIC HEAT SHIELD CONCEPTS

2.0 SUMMARY, CONCLUSIONS, AND RECOMMENDATIONS

2.1 Summary

A total of 14 specimens representing 10 variations of the foil enclosure configuration were fabricated and evaluated. Four configurations were subjected to ten 1800° F thermal cycles, and to acoustic exposures for as much as ten minutes duration at overall sound pressure levels of 154 db and 168 db for a demonstration of reuse capability.

The most significant design problem was that of controlling thermally introduced stresses which caused compressive crippling and subsequent fatigue cracking in areas of the enclosure subjected to severe temperature gradients. Designs incorporating selective stiffening in regions of the enclosure subjected to compressive loading were developed which satisfactorily resolved this difficulty. Elastic buckling caused by thermal expansion of the top surface of the enclosure was another problem area. Although elastically buckled areas were not subject to cracking, the foil deformations were considered undesirable because of the potential for application of the concept to aerodynamic surfaces. Two techniques were developed which were effective in improving or eliminating surface buckling. One utilized a two-piece design with the top of the enclosure structurally decoupled from the sides (floating top). The other incorporated stiffening members which deflected elastically on heating to load the top as a tension membrane. The two deliverable specimens which were fabricated for evaluation by NASA incorporated these features.

Specimens were fabricated using both Hastelloy-X and Haynes 25 superalloy foils in thicknesses ranging from 0.003 to 0.006 inch. There was little difference in the ease of fabrication (bending, welding, etc.) of enclosures using these materials. The Haynes 25 was more susceptible to development of cracks in crippled areas during the thermal and acoustic tests, however.

High purity fibrous silica components were used in the 3DSX insulation. Based on previous studies, no degradation was anticipated for cyclic exposure at the 1800° F temperature level. This was further substantiated by the reuse demonstration tests in which there was no apparent degradation of thermal or mechanical characteristics of the 3DSX caused by the thermal and acoustic exposures.

2.2 Conclusions

The major conclusions from the current effort are:

- a. 3DSX/foil design configurations which have multiple reuse capability at surface temperatures of at least 1800° F appear feasible.
- b. Hastelloy-X foil and high purity silica are credible candidate material components for surface temperatures to 1800° F.

- c. Compressive crippling of foil (caused by severe temperature gradients) must not be permitted because of rapid development of fatigue cracks in crippled areas.
- d. Thermally induced crippling and surface buckling can be eliminated by appropriate design configurations.
- e. The 3DSX/foil concept is not sensitive to acoustic environments representative of launch conditions for the Space Shuttle.

2.3 Recommendations

It is recommended that further thermal and acoustic cycling tests be performed on the final configurations evolved from this program with the objective of demonstrating a 100 mission capability. The two deliverable specimens are suitable for this purpose.

A comprehensive study is required to better define the aerodynamic flutter characteristics of the system and to optimize the surface stiffening method. A combined analytical and experimental program is suggested.

Scale-up of the final configurations to more realistic panel sizes (several square feet) should be accomplished. Additional thermal testing should be performed to establish that the thermal growth management concepts developed on this program are workable in realistic panel sizes.

3.0 THERMAL PROTECTION SYSTEM PANEL DESIGN

3.1 Description of 3DSX/Foil Concept

The principal features of the 3DSX/Foil configuration are illustrated in Figure 3.1. The 3DSX insulation material is comprised of thin layers of a high-purity silica felt (J.P. Stevens Astroquartz) which are precompacted in a fixture to a density of 5.8 lb/ft³. The felt layers are held in the compacted state by closely spaced stitching through the thickness using Astroquartz yarn. The resulting woven mat (Figure 3.2) possesses good handling characteristics and is an excellent low density, high temperature insulating material.

The insulation material is enclosed on the top surface and along four sides by a superalloy foil. The foil is sealed along the lower edges to the skin of the vehicle to provide a moisture resistant enclosure to protect the insulation material.

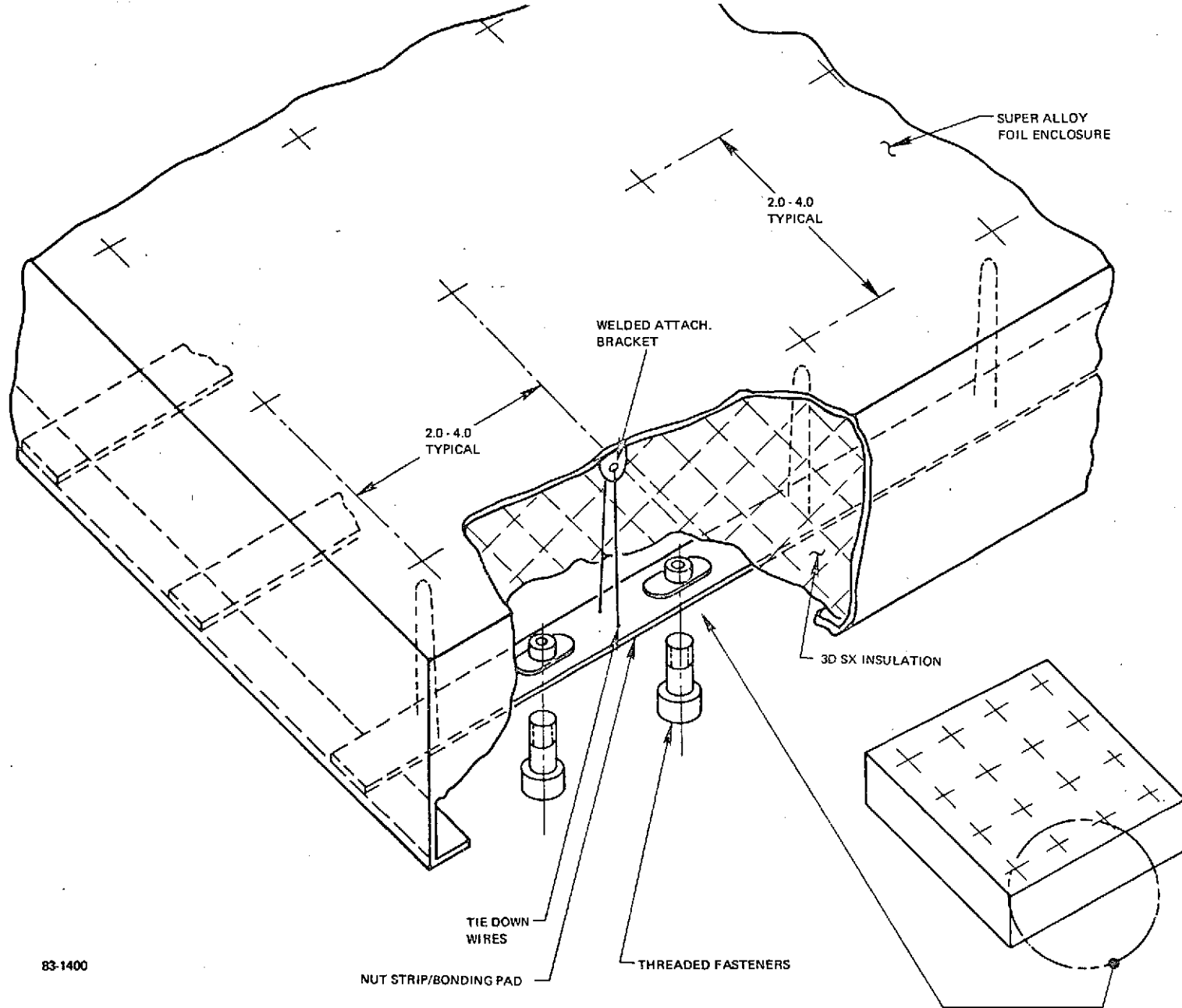
The foil enclosure was fabricated from nickel and cobalt base alloys in the thickness range of 3 to 6 mils which can be easily formed into a box shape with the corners made using a box fold for sealing purposes. To complete the assembly the 3DSX is placed into the foil enclosure and the two components are fastened together by tie-down wires. These wires are attached to the inner surface of the foil at discrete locations, pierce the 3DSX insulation, and attach at the back surface to nut strips (Figures 3.1 and 3.3), bonding pads, or directly to substructure. This then forms a complete self-contained metallic TPS system.

The novel feature of this concept is that it reduces the structural requirement of the metallic surface component by reacting the external pressure loads through direct compression of the compacted 3DSX insulation rather than through bending stiffness to the foil. All venting pressures, vibration and flutter loads are reacted by the vehicle structure through the discrete tie-down wires. This results in substantially lower system weight than a structural metallic heat shield would require.

During the course of the program several variations of the basic design concept were investigated. These latter systems used approaches which a) employed several top and side texturizing patterns, b) investigated various foil to substructure attachment methods, c) provided stiffeners at the top edges, and d) allowed for a "floating top".

3.2 Design Environments

A simplified thermal environment was specified which approximated a typical reentry heating trajectory. It consisted of a surface temperature history with a linear temperature rise to the maximum temperature during the first 300 seconds, a 900 second hold at the maximum surface temperature and a linear decay to room temperature over a 400 second period. Maximum surface temperatures were to be in the range 1200° to 1800° F.



83-1400

Figure 3.1 SCHEMATIC OF 3DSX/FOIL TPS SYSTEM

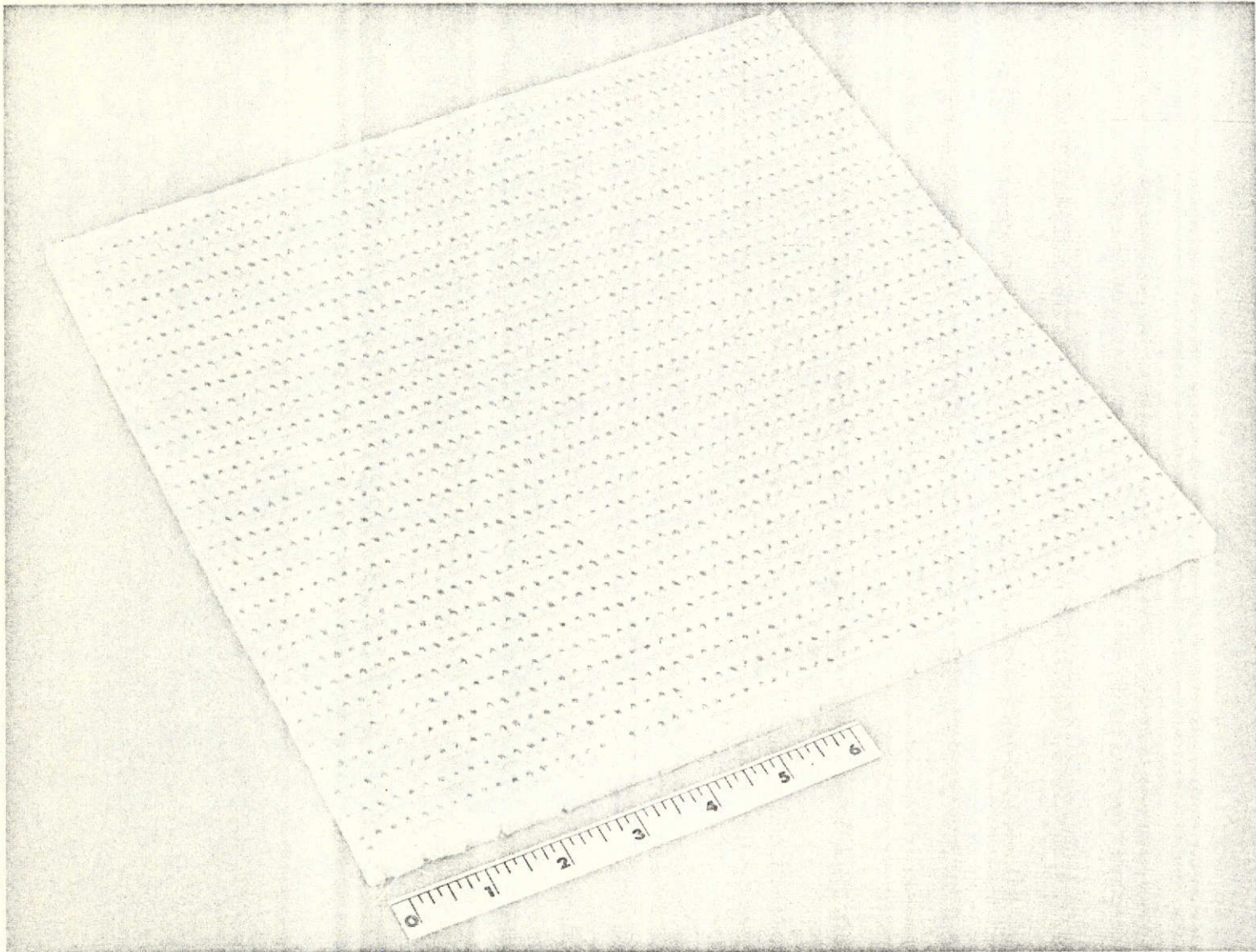


Figure 3.2 3DSX WOVEN SILICA INSULATION

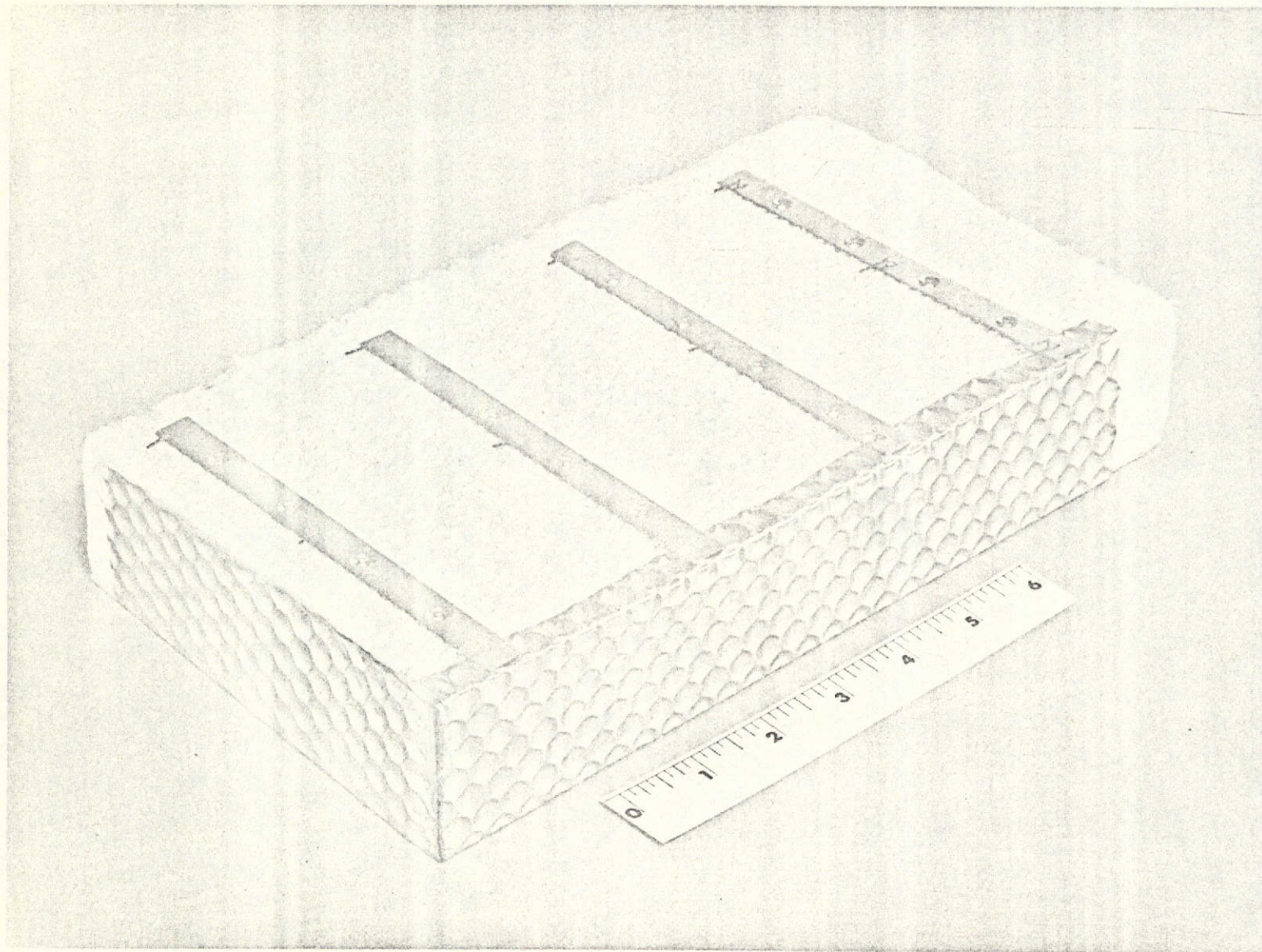


Figure 3.3 REAR OF FOIL ENCLOSURE ILLUSTRATING NUT STRIP FASTENER TECHNIQUE

The design acoustic environment specified was 154 dB overall sound pressure level with a spectrum as indicated in Table I. The acoustic levels were increased to an overall sound pressure level of 168 dB during the course of this program, corresponding to current design requirements for the base region of the orbiter during launch. Testing was performed in atmospheric air at both of these levels as discussed in Section 4.0.

TABLE I
DESIGN ACOUSTIC ENVIRONMENTS

Octave Band (Hz)	154 dB SPL		168 dB SPL	
	Noise Level* (dB)	Tolerance (dB)	Noise Level (dB)	Tolerance (dB)
23.8 - 47.2	133.7	+6, -2	152	(Not Specified)
47.2 - 92	139.3	+6, -2	155	
94 - 188	142.7	+5, -1	157	
183 - 375	146.8	+4, -1	157	
375 - 750	150.7	+4, -1	155	
750 - 1500	144.0	+5, -1	151	
1500 - 3000	139.7	+6, -2	146	
3000 - 6000	133.2	+6, -2	140	
Overall	154.0	+4, -0	168	

*Reference for dB level is 0.0002 dynes/cm² rms.

3.3 Selection of Materials

Tables II and III list metallic foil and ceramic fiber insulation materials which were considered viable candidates for the development of the 3DSX/foil concept.

A detailed evaluation of the long term high temperature stability and cyclic environmental capability of all candidates was not intended in this program. The selection of foil and insulation component materials was based largely on results of a previous related program (Ref. 1) in which comprehensive experimental evaluations were performed. In that program, a number of candidate metallic foils and ceramic fiber insulations were subjected to cyclic thermal and acoustic environments corresponding to 100 shuttle missions at surface temperatures as high as 2500° F.

It was immediately recognized that designing for the management of thermal growth and the related thermal stresses was a major development problem. It was decided to adopt a conservative approach to materials selection as related to temperature capability so that the concept development would not be hampered by chemical and structural changes within the materials themselves. Accordingly, 1800° F was selected as a maximum design temperature. Previous work on 3DSX insulation development (Refs. 2 and 3) as well as theoretical considerations

TABLE II

CANDIDATE CERAMIC INSULATION MATERIALS

Composition	Trade Name	Manufacturer	Maximum Use Temperature (°F)	Approximate Price Per lb (\$)
1. Fused SiO ₂	Astroquartz	J. P. Stevens Co. N.Y., N.Y.	2300	79
2. Fused SiO ₂	Irish Refrasil	H. I. Thompson Co. Gardena, Calif.	2500	30
3. Fused SiO ₂	Refrasil	H. I. Thompson Co. Gardena, Calif.	2300	25
4. Alumino Silicate	Thermoflex	Johns-Manville	2300	5
5. Alumino Silicate	Fiberfrax	Carborundum	2300	5
6. Sodium Calcium Silicate	Superglass	Eagle-Picher	1800	3

TABLE III

CANDIDATE FOIL MATERIALS

Material	Maximum Use Temperature (°F)
Type 321 stainless steel	1200
Inconel 702	1500
Inconel 601	1500
TD Nickel Chrome	2000
Hastelloy-X	2000
Haynes-25	2000

had demonstrated that high purity fused silica (e.g., J. P. Stevens Astroquartz) was capable of virtually unlimited temperature cycling to 1800° F. At temperatures exceeding 1800° F, silica is subject to phase transitions, particularly to α -cristobalite, with corresponding dimensional and structural changes. The transition occurs rather slowly, so that the actual cyclic temperature capability for typical shuttle trajectories may be considerably greater than 1800° F.

Reference 1 also indicated a distinct mechanical stability advantage of Astroquartz in severe acoustic environments. Consequently, Astroquartz components were selected for fabricating all the 3DSX insulation for this program. No significant advantage other than raw material cost was evident for the other candidate fibrous materials.

Reference 1 presented oxidation data for various metal foils with cyclic exposures corresponding to 100 shuttle missions at temperatures as high as 2200° F (Table IV). Hastelloy-X was the most favorable foil material both for oxidation resistance and for resistance to fatigue cracking. On this basis, Hastelloy-X was chosen as the primary foil candidate. It was considered the best of the available nickel-based superalloys for extended service at 1800° F.

TABLE IV*

RESULTS OF REENTRY CYCLING ON FOILS FOR 100 CYCLES TO 2200° F

Alloy	Substrate Thickness (in)	Max Thickness of Surface Oxides (in)
Hastelloy-X	0.0018	0.00012
Inconel 601	0.0036	0.00036
Inconel 702	0.0042	0.00070
TD Nickel Chrome	0.012	0.00040
On completion of above tests there was no visible cracking of the oxidized layer or foil.		

*Data from Reference 1.

It was decided to include a cobalt-based superalloy, Haynes 25, as a backup foil candidate. Haynes 25 was not evaluated in Reference 1, but was reported to have similar high temperature properties and superior oxidation resistance as compared to Hastelloy-X. Off-shelf availability of these materials in foil form of sufficient size for the desired specimens was a second major consideration in their selection for this program.

3.4 Enclosure Fabrication Studies

Some of the operations necessary for fabricating the superalloy foil enclosures required some minor technique development. These included methods for texturing, beading, folding, and welding Hastelloy-X and Haynes 25 in foil thicknesses ranging from 3 to 6 mils.

Three techniques were utilized for stiffening the top surface of the enclosure; texturing, beading, and welded stiffeners. Texturing the entire foil sheets between rollers prior to cutting and folding the enclosure was initially considered the most desirable method because it offered a low cost, high volume solution to the foil stiffening problem. Accordingly, the standard patterns of several textured metal fabricators were considered and samples were obtained for evaluation (Figure 3.4). These fabricators do not ordinarily texture material less than 15 mils in thickness. With the cooperation of Ardmore Textured Metals of Edison, N. J., some development work and experimentation was performed for texturing 3 to 6 mil superalloy foils. Gathering was a problem and pattern depth was limited depending on foil thickness, but several of the standard patterns were successfully textured in the thin foils. Ardmore's "Oxford" Pattern was selected for detailed evaluation. Texture depths up to 42 mils were successfully fabricated by Ardmore in 6-mil Hastelloy-X and 5-mil Haynes 25. Several textured sheets were obtained for structural evaluation.

The second approach to stiffening the thin foil was beading the surface (Figure 3.5). The desired pattern was machined in aluminum die plates and the foil pressed to conform using a rubber pad in contact with the foil (Figure 3.6). This method had the advantage that different bead patterns and bead orientations could be used on the top and sides of the specimens according to the structural requirements of the particular application.

The third approach for top stiffening used hat section stiffeners spot welded to the top surface (Figure 3.7). This was considered a less desirable stiffening approach because of cost and additional complexity of the configuration. Resistance spot-welding with a United 1-065-02 welder was successfully used for attaching stiffeners and tie-straps. Electrode and jaw modifications were necessary for particular applications where welding was performed on the inside surface of the folded enclosure.

Figure 3.8 illustrates the tie strap configuration for mechanical attachment of the foil to a substrate. A "U" shaped strap was spot-welded to the top surface of the enclosure and the legs of the "U" folded over. The folded construction of the strap adds rigidity and provides a rounded edge to reduce chaffing of the wire where it bears on the strap. The diameter of spot welds was approximately 1/16 inch and tensile strength of the welded joints exceeded 20 pounds. Figure 3.9 illustrates the weld test configuration and Table V presents weld strength data.

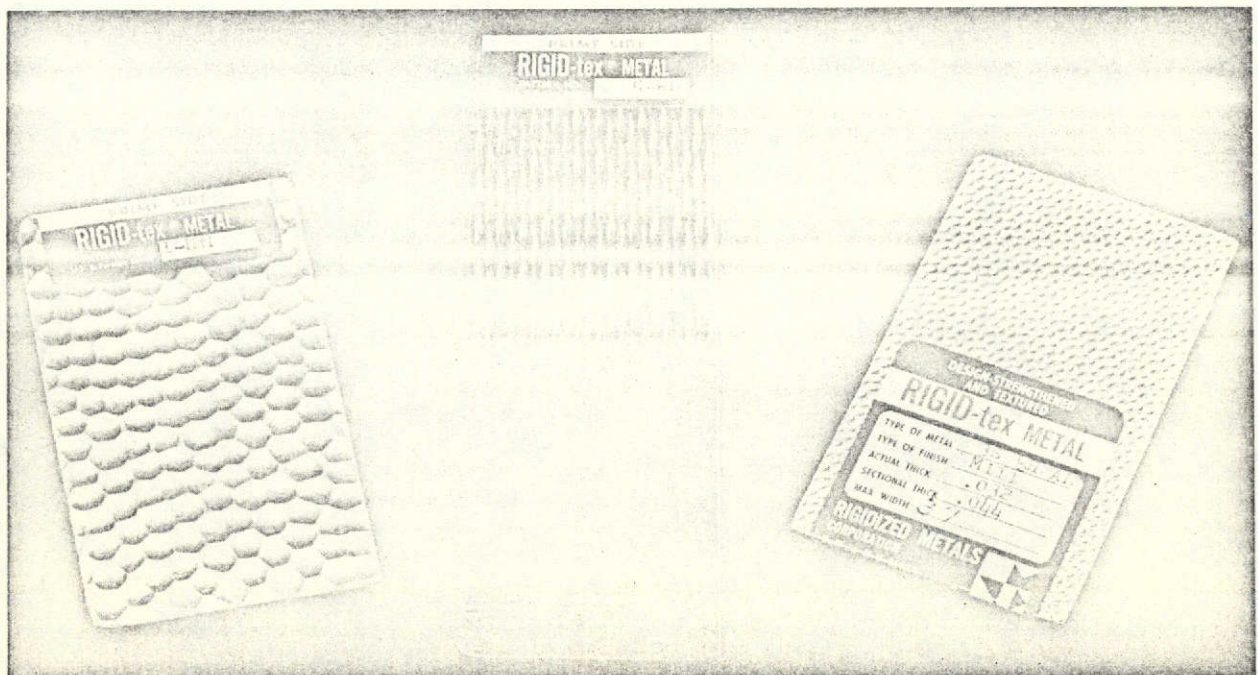
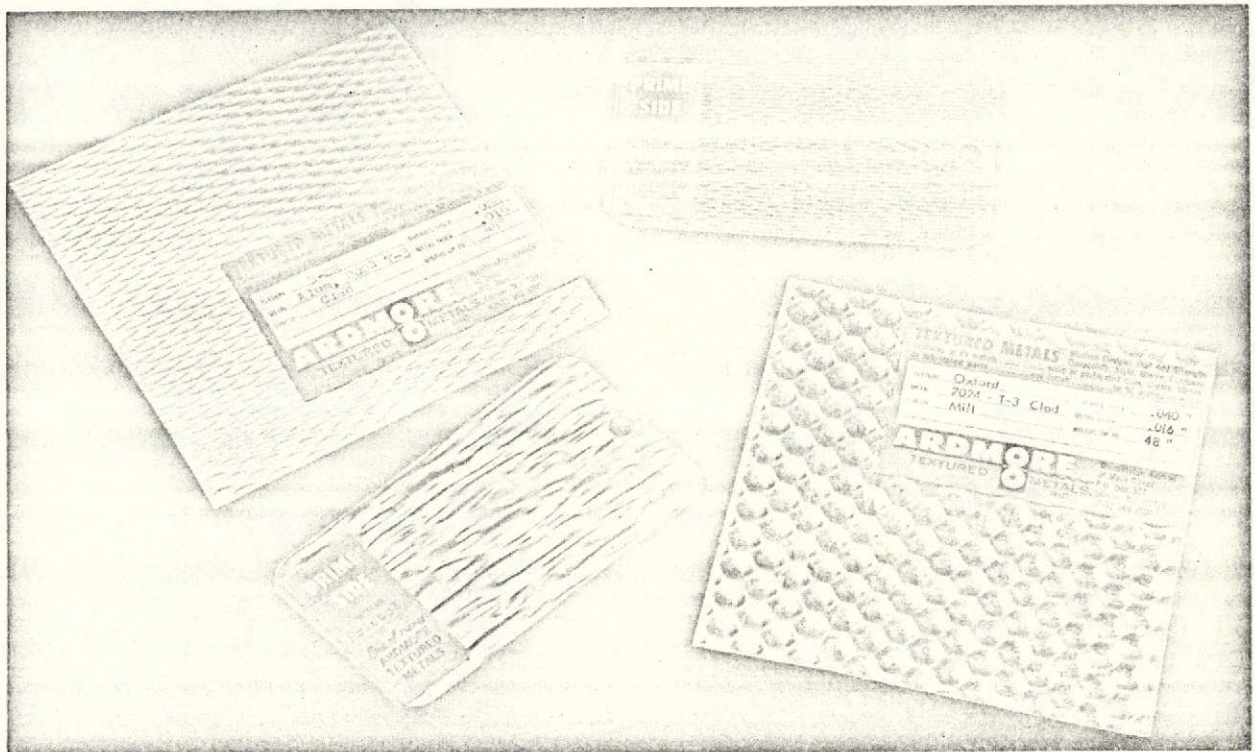


Figure 3.4 TYPICAL FOIL TEXTURE PATTERNS

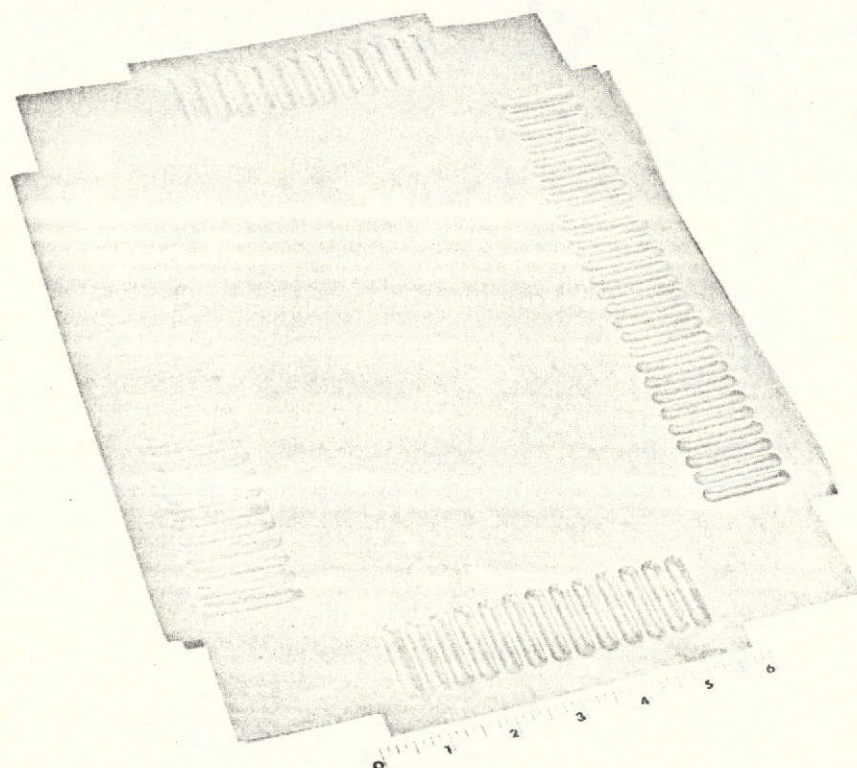
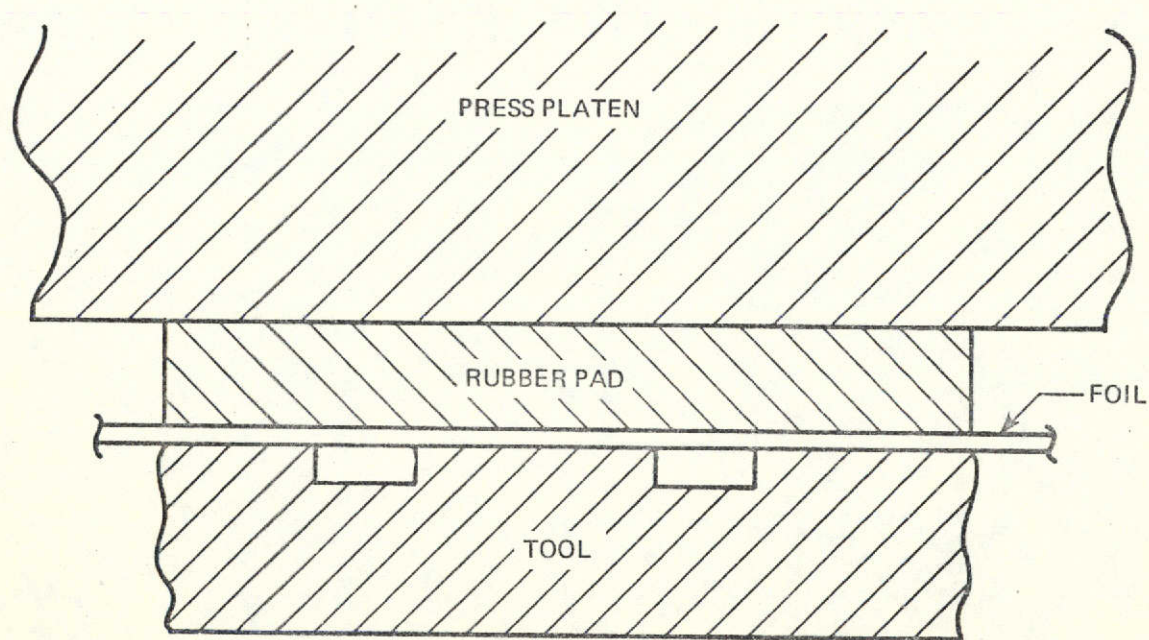


Figure 3.5 TYPICAL BEADED SURFACE SPECIMEN



83-1401

Figure 3.6 BEADING TOOL

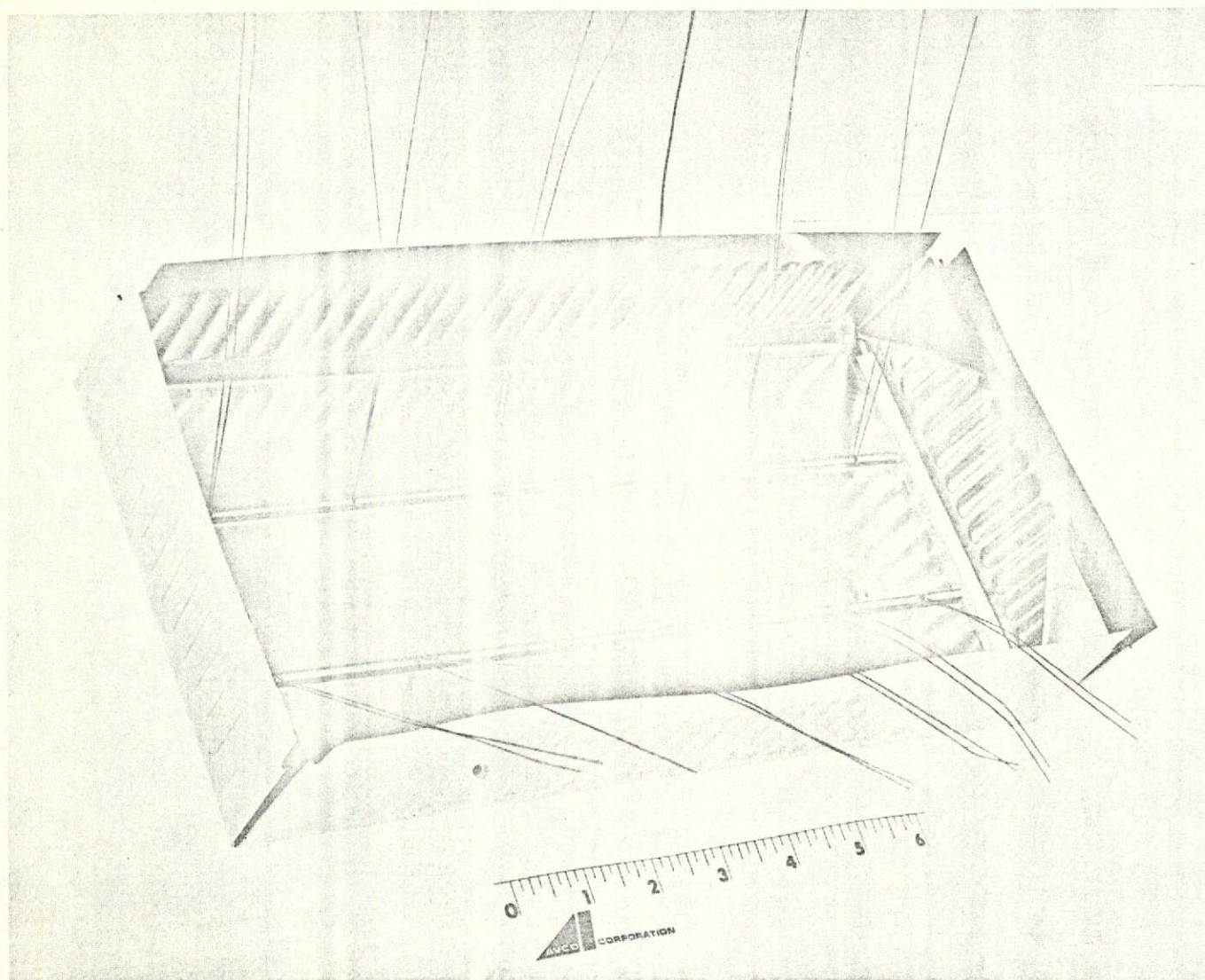
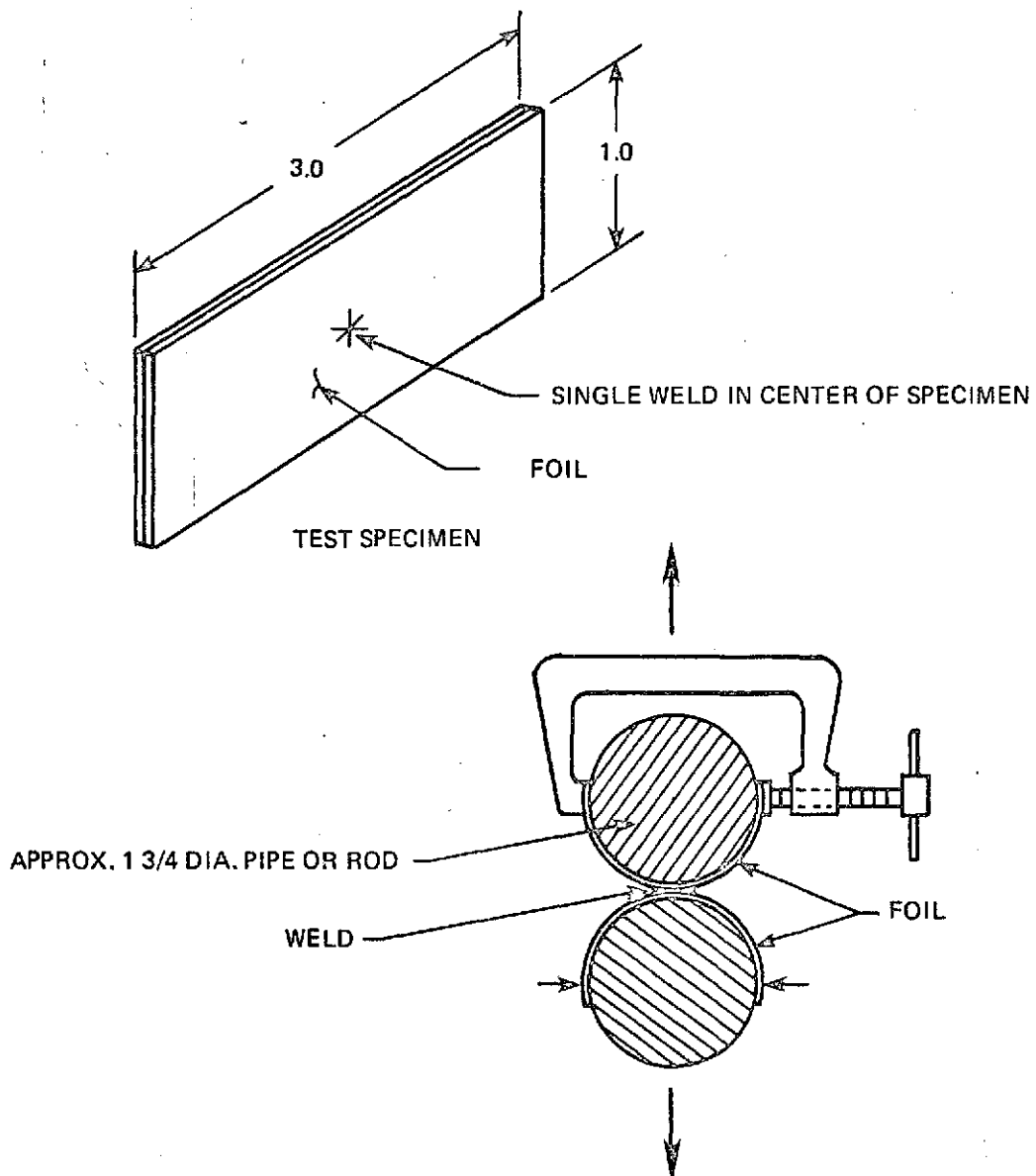


Figure 3.7 SURFACE STIFFENED BY SPOT-WELDED HAT SECTIONS



83-1403

Figure 3.9 SPOT WELD TEST CONFIGURATION

TABLE V

SPOT WELD STRENGTH DATA

Material	Type Weld	Vendor	Weld Strength (lbs)
.006 Hastelloy-X	1/8 Dia. Button Weld	Applied Energy	46 71 58 53
.006 Haynes 25	1/8 Dia. Button Weld	Applied Energy	67 68 56
.006 Hastelloy-X	1/16 Dia. Res. Spot	Avco - Wilmington	36 35 39 36
.006 Haynes 25	<1/16 Dia. Res. Spot	Avco - Wilmington	48 35 58 46
.003 Hastelloy-X	1/16 Dia. Res. Spot	Avco - Lowell	42 38
.003 Hastelloy-X	1/8 Dia. Res. Spot	Avco - Lowell	22 30
.003 Hastelloy-X	1/16 Dia. Res. Spot	Avco - Lowell	28 28 19
.003 Hastelloy-X	1/8 Dia. Res. Spot	Avco - Lowell	31 38 28 Repeats
.006 Haynes 25	1/8 Dia. Res. Spot	Avco - Lowell	24 23 68

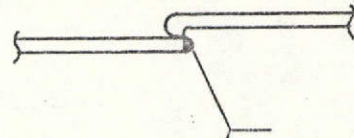
Hastelloy-X and Haynes 25 foils were not readily available in widths greater than 12 inches. Therefore methods for splicing foil sheets by electron beam seam welding were investigated. Figure 3.10 illustrates several foil splices fabricated in the foil materials by Applied Energy, Inc., of Burlington, Massachusetts. All of these were successfully texturized after welding. Tensile strengths of the splices approached that of unspliced sheets, even after texturing. The overlap weld appears most practical from the fabrication standpoint, because the other two configurations require high accuracy of cutting and alignment of the foils to achieve a satisfactory joint.

Electron beam "button" welds were considered as possible substitutes for resistance spot welds (Figure 3.11). The principal advantage of this method is that welding can be achieved with access from one side of the workpiece. Also the diameter of the "button" can be adjusted as desired to derive higher joint strengths. One problem noted with the technique is that good clamping of the workpiece is necessary to prevent local warping resulting in incomplete weld penetration as illustrated in Figure 3.11.

Even when textured, folding of the foil was readily accomplished for the simple box configurations. A standard box fold (Figure 3.12) was used in the corners of all the enclosures. A five-sided enclosure can be folded with this technique without cutting or welding joints; a most desirable feature from the aspect of cost, strength, and moisture sealing.

Two types of sliding joints were used for the two piece floating top designs (Figure 3.13). The textured floating top design (Specimens 7 and 12) utilized a stiffener spot-welded around the perimeter of the textured top

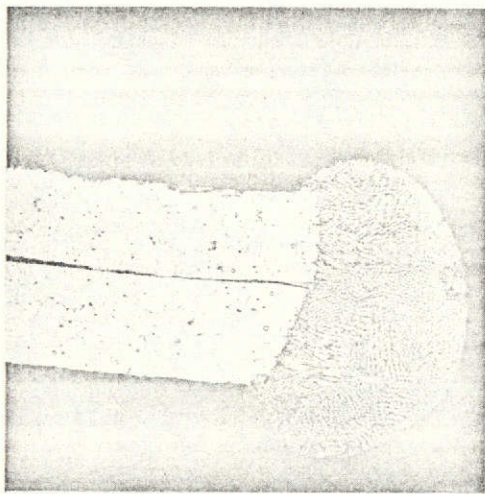
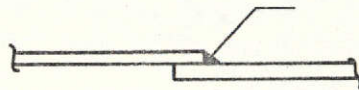
PARALLEL EDGE FOLD



BUTT WELD



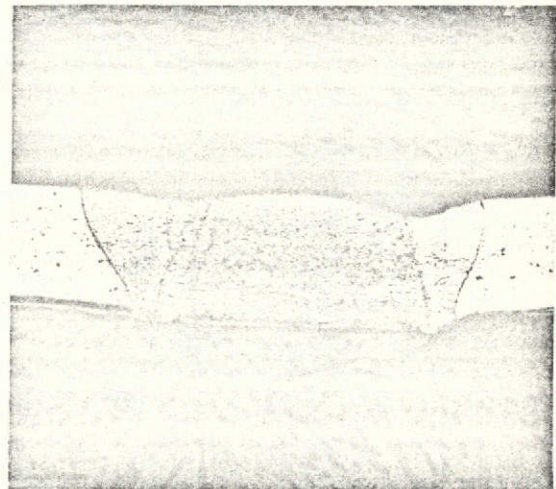
OVERLAP WELD



PL 5670-4

(a)

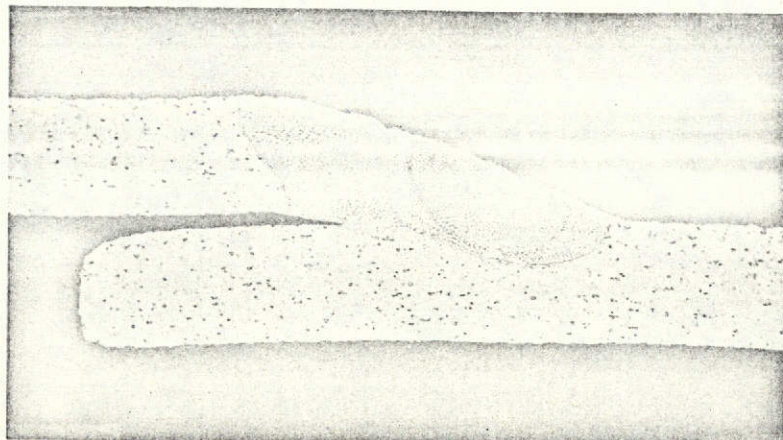
100X



PL 5670-7

(b)

100X



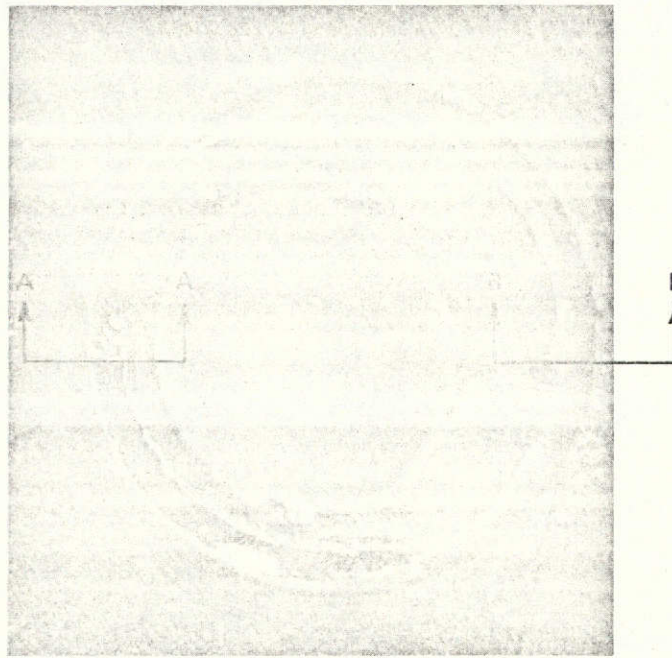
PL 5670-5

(c)

100X

83-1404

Figure 3.10 ELECTRON BEAM SEAM WELDS FOR SPLICING FOIL

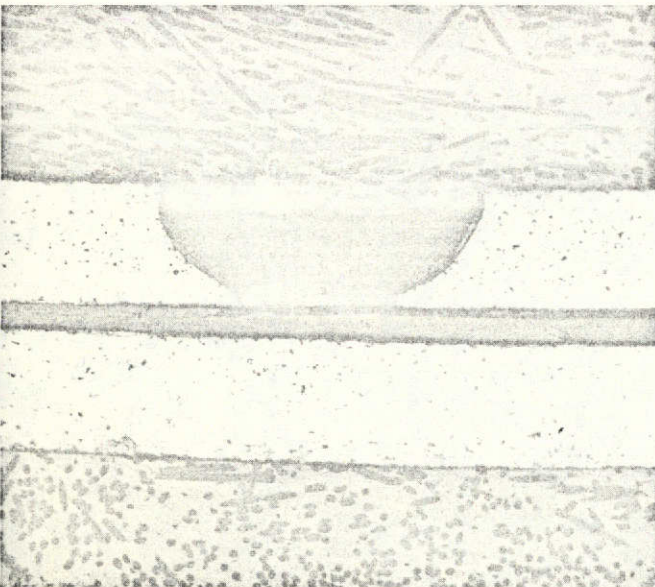


PL 5670-3A

(a)

(25X)

PLAN VIEW OF
BUTTON WELD

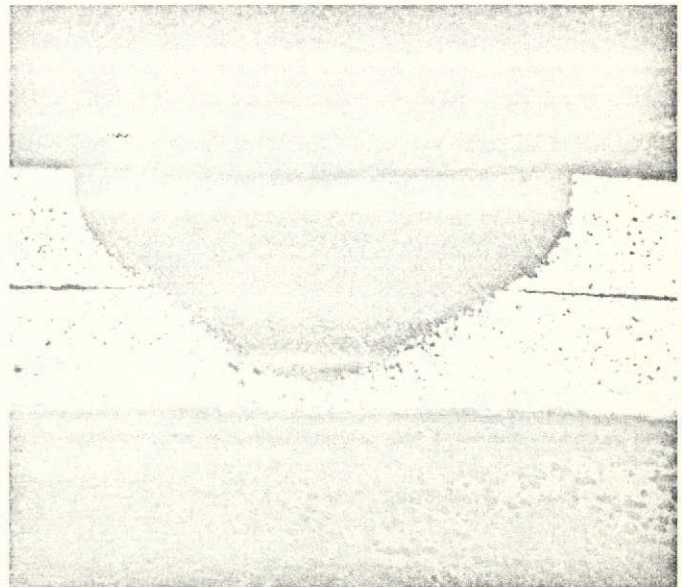


PL 5670-6A

(b)

100X

SECTION A-A INCOMPLETE WELD DUE
TO POOR CLAMPING (100X)



PL 5670-6

(c)

100X

SECTION B-B SUCCESSFUL WELD (100X)

33-1405

Figure 3.11 ELECTRON BEAM BUTTON WELDS IN HAYNES 25

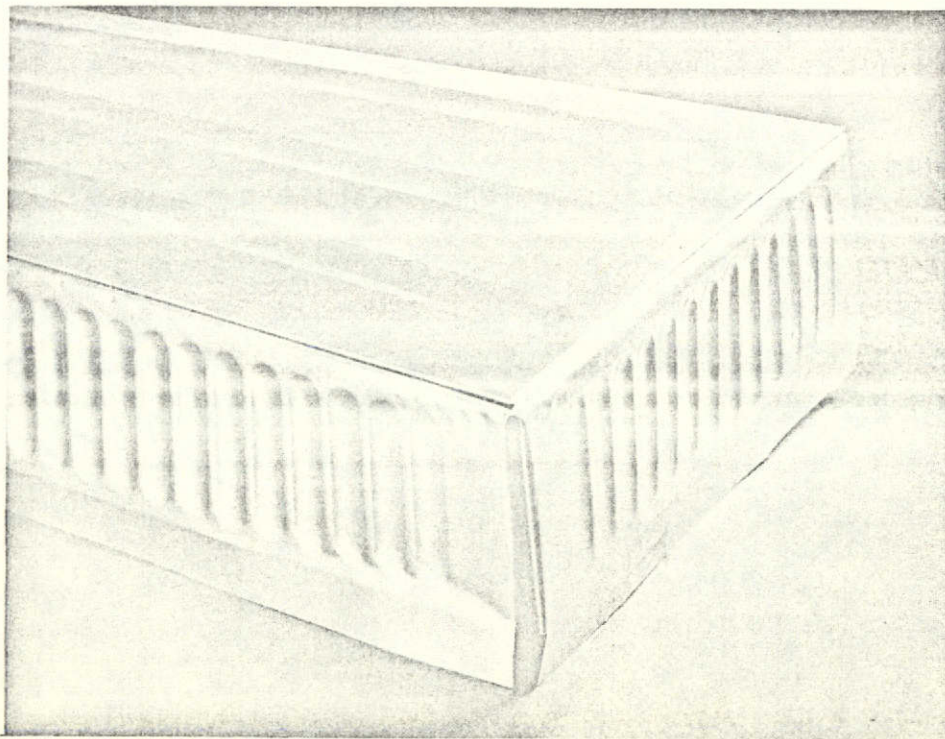
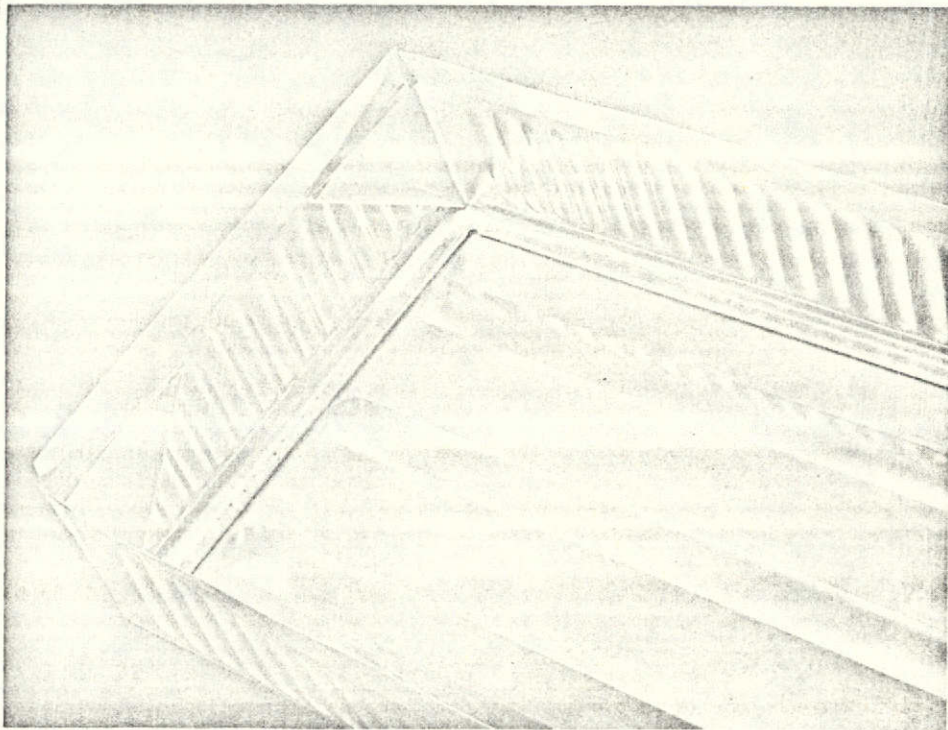
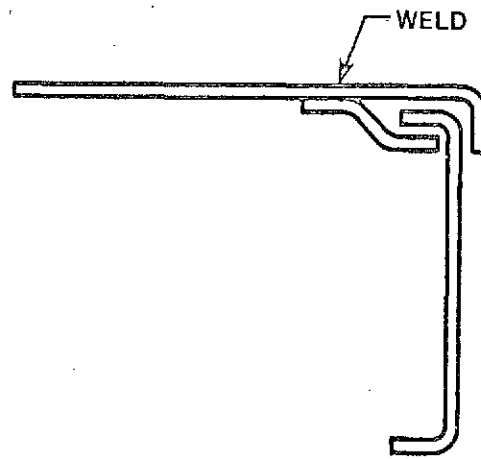
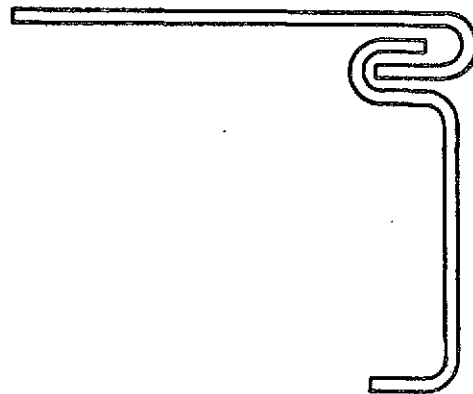


Figure 3.12 BOX FOLD FOR CORNER OF ENCLOSURE



SPECIMENS 7 AND 12



SPECIMEN 14

83-1406

Figure 3.13 SLIDING JOINT CONFIGURATION FOR FLOATING TOP SPECIMENS

which interlocked with the sides of the enclosure. A more satisfactory joint from the standpoint of both structure and sealing is shown for Specimen 14. This type of joint required untextured foil and was used in conjunction with stiffening beads on the top of the enclosure.

3.5 Structural Design Study

3.5.1 Foil Stiffness Evaluation. - Hastelloy-X (nickel base alloy) and Haynes 25 (cobalt base alloy) were selected for evaluation as candidate enclosure materials. Typical properties for these two materials are presented in Table VI indicating that both materials are suitable for the 1800° F operating temperature.

TABLE VI
HIGH TEMPERATURE PROPERTIES OF HASTELLOY-X
AND HAYNES 25 SUPERALLOYS

Materials		Ultimate Tensile Strength, 1000 psi				Yield Strength 1000 psi				Elongation, %			
	Temp °F	RT	1200	1500	1800	RT	1200	1500	1800	RT	1200	1500	1800
Haynes 25 (sheet)		146	103	50	34	67	35	36	23	64	35	16	41
Hastelloy-X (sheet)		114	83	52	22	52	40	37	16	43	37	34	45

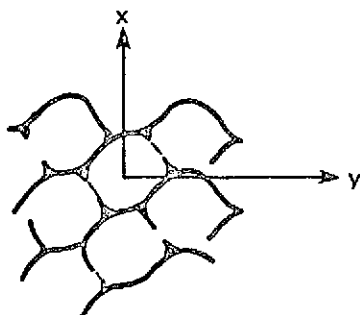
At the outset it was clear that one of the difficulties with using thin foils on the surface would be the effects of aerodynamic flutter. Ascent venting pressure also was of concern and these two factors combined would dictate the optimum foil thickness and tie down spacing. In both instances the problem could be traced to foil bending stiffness; the greater the foil bending stiffness the larger the tie down spacing thereby making a more tractable design. Therefore, experiments were required to evaluate the effectiveness of texturing for increasing foil stiffness.

3.5.1.1 Flexure Testing. - Ardmore's Oxford texture pattern was selected and a number of sheets were texturized varying the foil thickness and texture depth. These sheets were then cut into 3 x 3 inch plates and tested in flexure under quarter point bending to determine their flexural properties. The results are presented in Table VII; the values given represent an average taken from a minimum of four tests per direction. The flexural stiffness shown is the effective EI of the textured materials and as expected the texture pattern has different bending stiffnesses in the longitudinal and transverse directions.

TABLE VII

FLEXURE PROPERTIES OF TEXTURED FOILS
(ARDMORE'S OXFORD PATTERN)

Foil Material	Foil Thickness	Texture Depth	Flexure Stiffness		Texture Efficiency Factor (Ratio of Stiffness of Textured to Flat Foil)	
			lb-in ²			
Units	in.	in.	Longitudinal, X	Transverse, Y	Longitudinal, X	Transverse, Y
Hastelloy-X	.003	.037	.252	.406	3.9	6.1
Hastelloy-X	.006	.037	1.291	1.691	2.4	3.2
Haynes 25	.006	.017	.993	1.352	1.8	2.5
Haynes 25	.006	.037	1.564	2.401	2.8	4.4



The effectiveness of the texturing for increasing the foil bending stiffness can be determined from the data in the efficiency factor columns. Values shown indicate the increase in bending stiffness obtained by the texture pattern over that of an equivalent thickness flat sheet. Based upon the comparison between the two .006 inch thick Haynes 25 specimens, it is clear that the deeper texture pattern enhances the bending stiffness. As a result the .037 inch nominal texture depth was selected for all further studies. Using this texture depth in the Oxford pattern, increases in bending stiffness ranging from 2.4 to 6.1 were attained for thin foils.

3.5.1.2 Tensile Testing. - In addition to the flexure testing, several tensile tests were performed on .005 inch thick Hastelloy foil textured to the nominal .037 inch depth. Here, as with the flexure tests, specimen widths were selected to ensure that several repeating texture patterns were included in the gage section to obtain representative results. The purpose of these tests was to determine the effect of texturing on extensional stiffness. Typical results in the form of stress strain curves are presented in Figure 3.14. A stress strain curve for an untextured .005 inch thick foil is included for comparison. As expected these results show that the texturing reduces the initial extensional stiffness by as much as a factor of 4 in the strong direction and up to 6 in the weak texture direction. At higher stress levels a wider disparity is

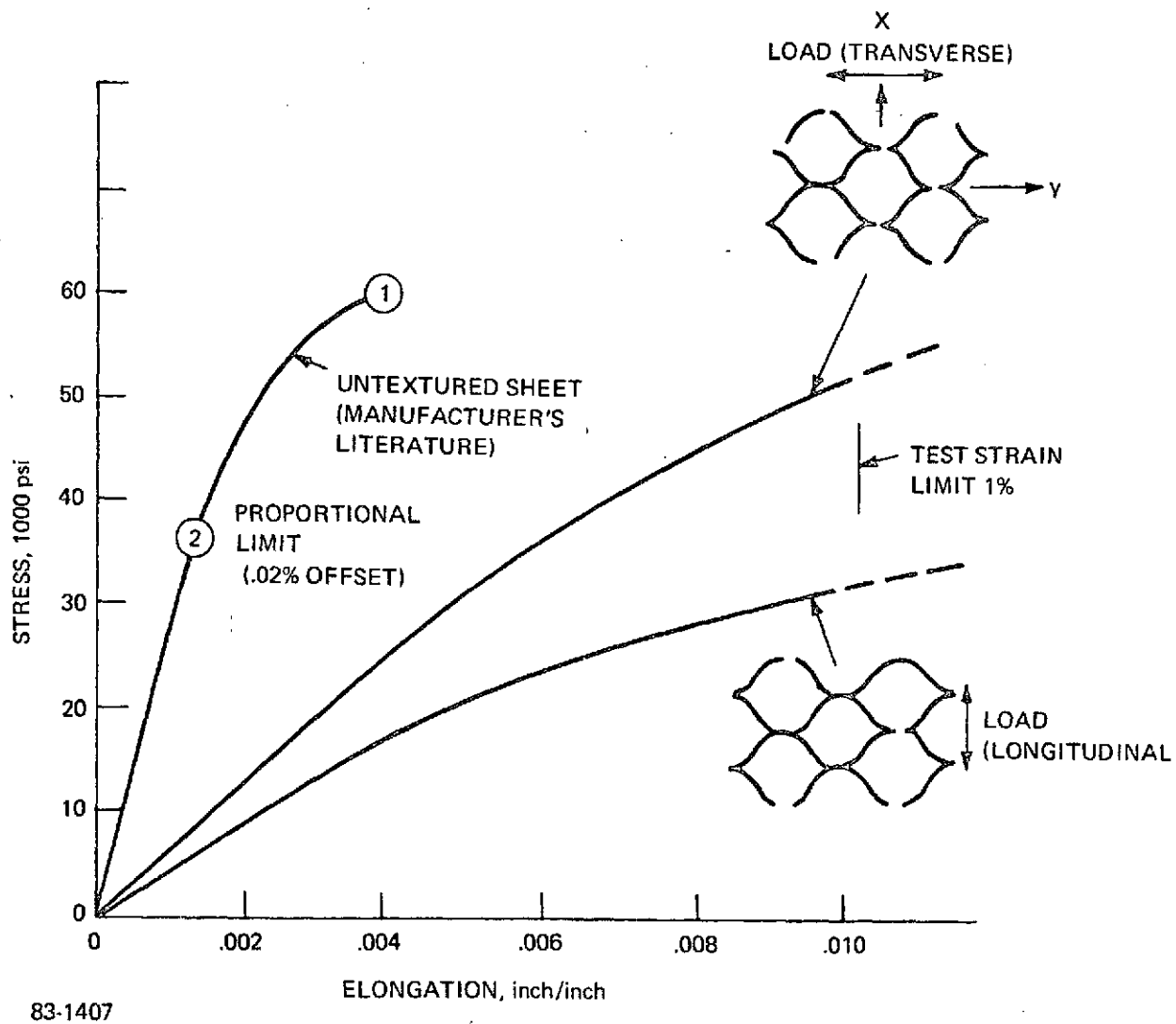


Figure 3.14 TYPICAL STRESS STRAIN CURVE FOR TEXTURED 5-mil HASTELLOY FOIL

noted. As expected, the textured foil has a much higher elongation than the untextured foil.

3.5.2 Enclosure Tie-Down Optimization. - One of the key elements in the design of the foil enclosure is the number and location of the tie-down wires required. Functionally, these wires retain the thin foil surface by drawing the foil down and precompressing the 3DSX insulation beneath. As long as these wires maintain a precompression between the foil and the insulation, the foil is stabilized by the insulation which acts as an elastic foundation.

Two factors influence the optimum tie down spacing; these are ascent venting (burst) pressures, and aerodynamic flutter. Although thermal mechanical loads exert a strong influence on the overall structural design of the enclosure their interaction with the design of the tie-down wires is minimal, therefore they are treated separately in Section 3.5.3. This section presents results of design tradeoff studies directed at selecting a satisfactory tie-down spacing.

3.5.2.1 Ascent Venting. - Failure modes associated with ascent venting include stress failure of the foil at or between the discrete ties, failure in the tie wires themselves or failure of the weld at the foil-wire attachment. Each of these failure conditions were evaluated parametrically in the form of allowable venting pressure versus tie down spacing. Results of this study are presented in Figures 3.15 and 3.16 for the 3- and 6-mil foils, respectively. In each figure, curves are presented for the allowable burst pressure considering either stress failure in the foil, stress failure in the wires or failure of the weld.

For the foil and wire calculations, a Hastelloy-X yield strength corresponding to 1500° F was used. This is believed to be a conservative estimate for the ascent phase where maximum venting pressures occur. A 20-mil diameter wire was used in the calculations (corresponding to the test specimen configuration). A weld strength of 15 pounds was assumed for the 3-mil foil and 50 pounds for the 6-mil foil (reflecting the results presented in Table V).

Stresses in the foil were determined using two different approximate solutions to provide bounds on the true solution. In one analysis the panel surface was treated as a continuous isotropic plate supported in a square pattern by discrete point supports and loaded by a uniform normal pressure. Directional variation of textured foil properties was not considered nor was the effect of in-plane membrane loads. Foil properties used for this and the subsequent analysis were taken from the flexure test data where the minimum flexural stiffnesses (weak direction) and a foil modulus of 27.5×10^6 psi were used to determine an equivalent thickness for the textured foil. This resulted in calculated equivalent thicknesses of 4.7 and 8.0 mils for the 3- and 6-mil foils, respectively. Tie-down spacings were then determined as a function of lateral pressure (assuming 1500° F properties for the foil) using data given in Reference 4. For this analysis the maximum bending stress occurred midway between tie wires.

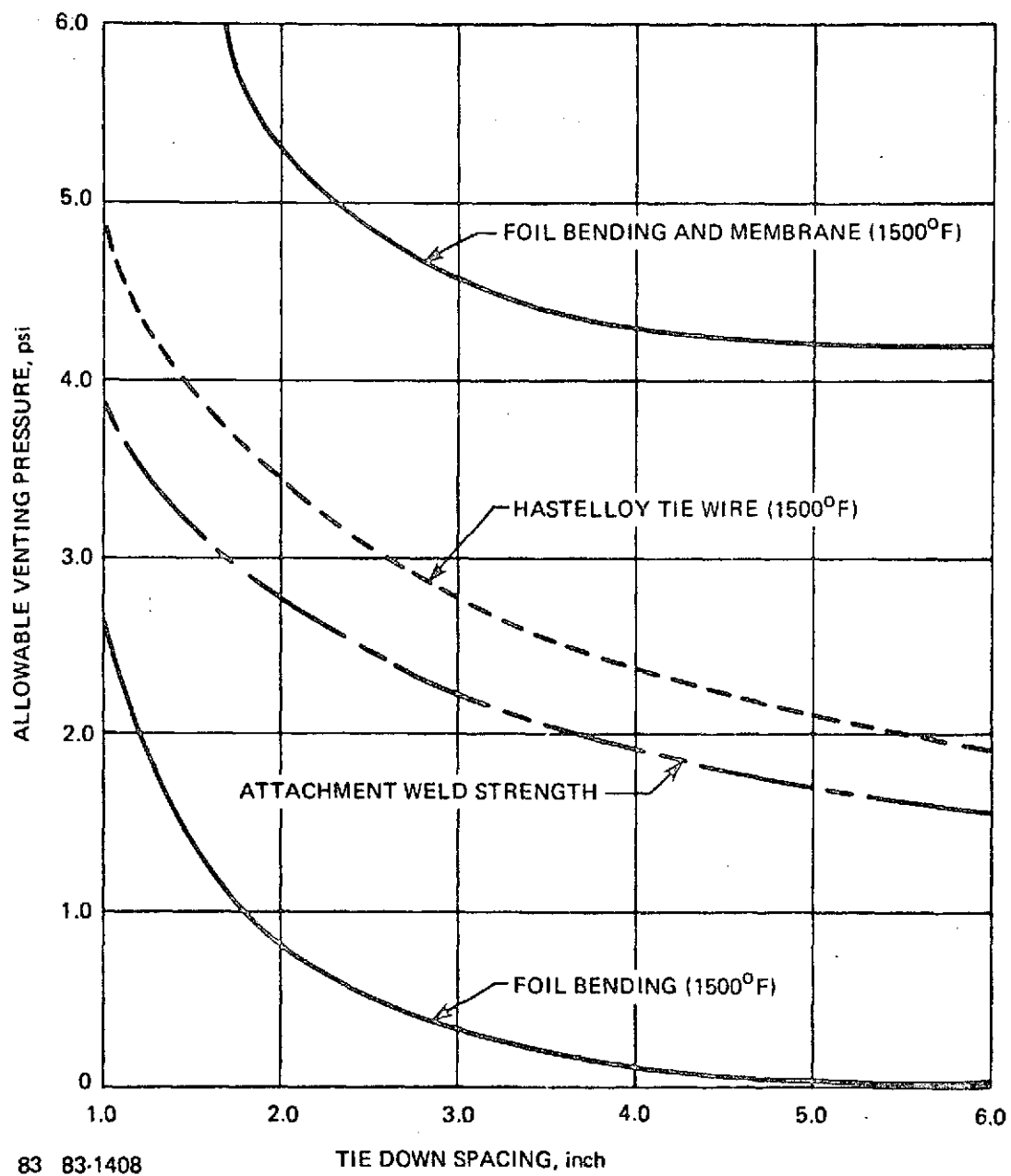


Figure 3.15 THREE MIL TEXTURED HASTELLOY FOIL VENTING PRESSURE DESIGN CURVES

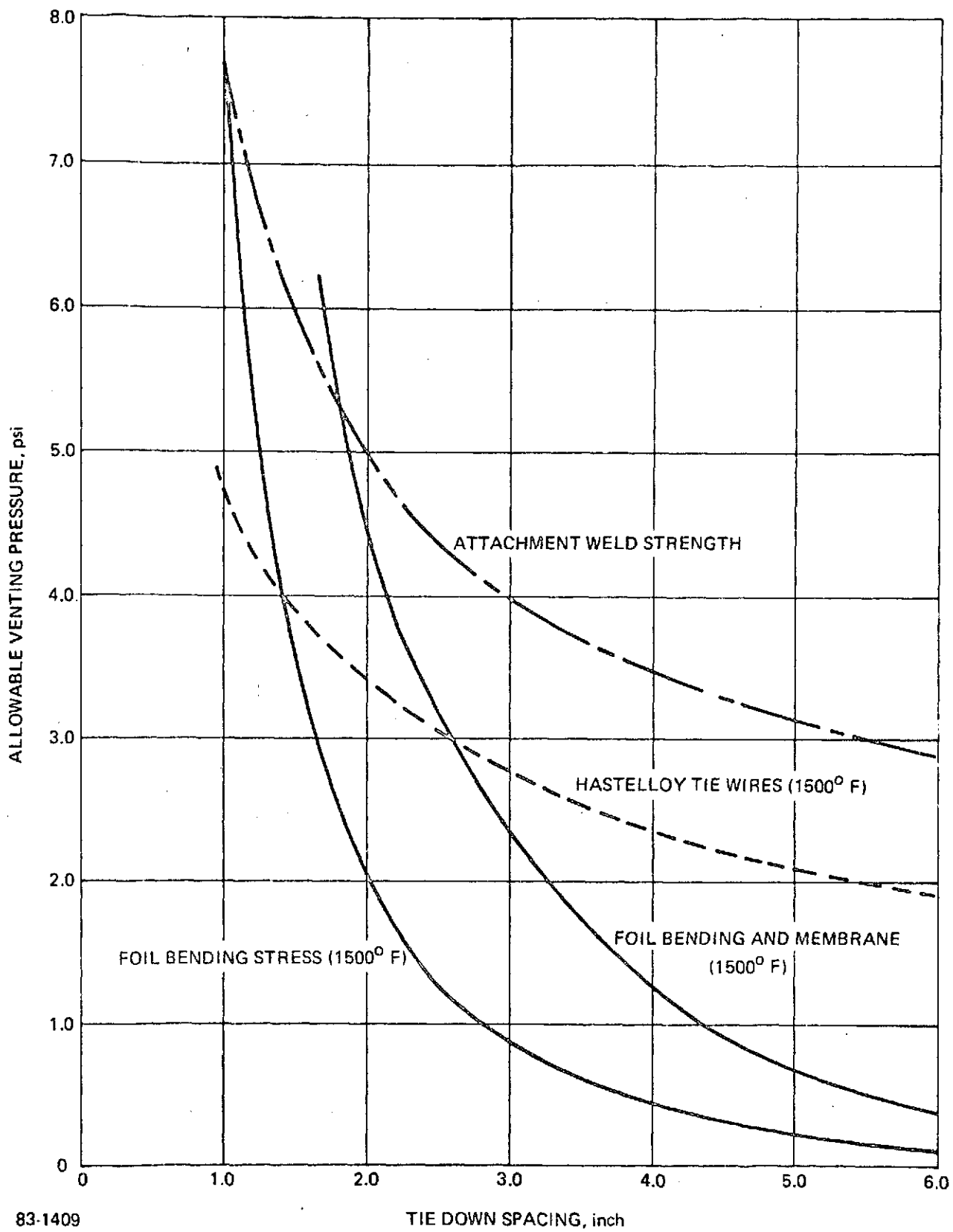


Figure 3.16 SIX MIL TEXTURED HASTELLOY FOIL VENTING PRESSURE DESIGN CURVES

This analysis provided a conservative estimate for the required tie-down spacing. In addition to neglecting the directional properties of the foil and using minimum foil bending stiffnesses for the stress analysis, further conservatism was included by ignoring the membrane tensile stresses in the bending analysis. These membrane stresses are developed in the surface because of the lateral pressure exerted on the enclosure sides and tend to counteract the effect of the normal pressure on the surface. Membrane stress effects would be most pronounced for the thinner (.003 inch) foil, which closely approaches a true membrane because of its lower bending stiffness. As the foil bending stiffness increases with the thicker foils, the positive effect of these membrane stresses becomes progressively smaller and the simple bending analysis yields reasonably accurate stress predictions.

To evaluate the significance of these membrane stresses on the tie-down spacing, a second series of analyses were performed considering both the lateral pressure and the inplane membrane loads. Because no solution was available which treated a continuous plate with discrete point supports under the combined action of lateral and in-plane loads, a simplified strip model was employed for this analysis. This model consisted of a unit strip with fixed ends, with the length adjusted to represent the spacing between the discrete tie downs. The fixed ends simulated the effect of the discrete ties because under lateral pressure there would be a zero slope in the actual enclosure surface. Furthermore, because the maximum stress in the point supported plate analysis occurred midway between the ties, the plate stress was closely approximated by the strip model for the degenerate case where the membrane stress was equated to zero.

Results for both analyses are presented in Figures 3.15 and 3.16, neither of which represent the true solution; however, it is reasonable to expect that they do bound the correct solution. Examining Figure 3.15 for the 3-mil textured foil considering all three failure conditions, it can be concluded that the governing design condition is either foil bending stress or the strength of the welds. Remembering that the foil stresses are bounded by the two stress curves it would seem that for the 3-mil foil the design condition should be the weld strength because it lies between the two stress curves.

The controlling parameter which dictates the tie down spacing for the 6-mil foil over the range of reasonable tie spacings is the stress in the foil. Both the wire strength and weld strength curves lie above the stress envelope throughout this range. Both 6-mil foil stress curves approach one another more closely than for the 3-mil foil. This is attributed to the higher bending stiffness of the 6-mil foil.

3.5.2.2 Surface Flutter Evaluation. - Available solutions to the aerodynamic flutter of plates subjected to supersonic flow are somewhat limited in that they treat a restricted range of elastic support and boundary conditions. Short of general design information given in Reference 5, which studied the effects of orientation of panel stiffening relative to the direction of flow, the literature provided little concrete information which could be applied directly to the foil enclosure. In Reference 5 it was observed from wind tunnel tests on stiffened panels that panels with their primary stiffness direction

oriented parallel to the flow direction were much less susceptible to flutter than those with crossflow stiffening.

Except for this important aspect, no complete solutions were obtained for either of the two models examined for the foil enclosure. One model consisted of a thin plate supported by a continuous elastic foundation. This model assumed that the tie wires were spaced sufficiently close together to provide an initial compression between the foil surface and the 3DSX insulation such that the insulation would act as an elastic foundation for the foil. The obvious weakness in this approach was that to ensure the existence of a pre-compression with the thin foils the tie wires would have to be spaced at very close intervals (i.e., less than 1 inch apart). Calculations modeling a beam on an elastic foundation (the 3DSX) indicated that larger wire spacings created local precompression in the region of the attachment only, with no overlap between adjacent attachment points. Furthermore, there appears to be some confusion relative to the stabilizing effects of elastic coupling to a substructure. In Reference 6, results are presented for the flutter boundary of two simply supported plates coupled by an elastic layer using a two mode Galerkin solution. These results indicate that in the low stiffness range, the elastic coupling has a destabilizing influence. As the stiffness increases there is a positive effect noted. A degenerate case of the above solution was investigated where the stiffness of the lower plate was infinite.

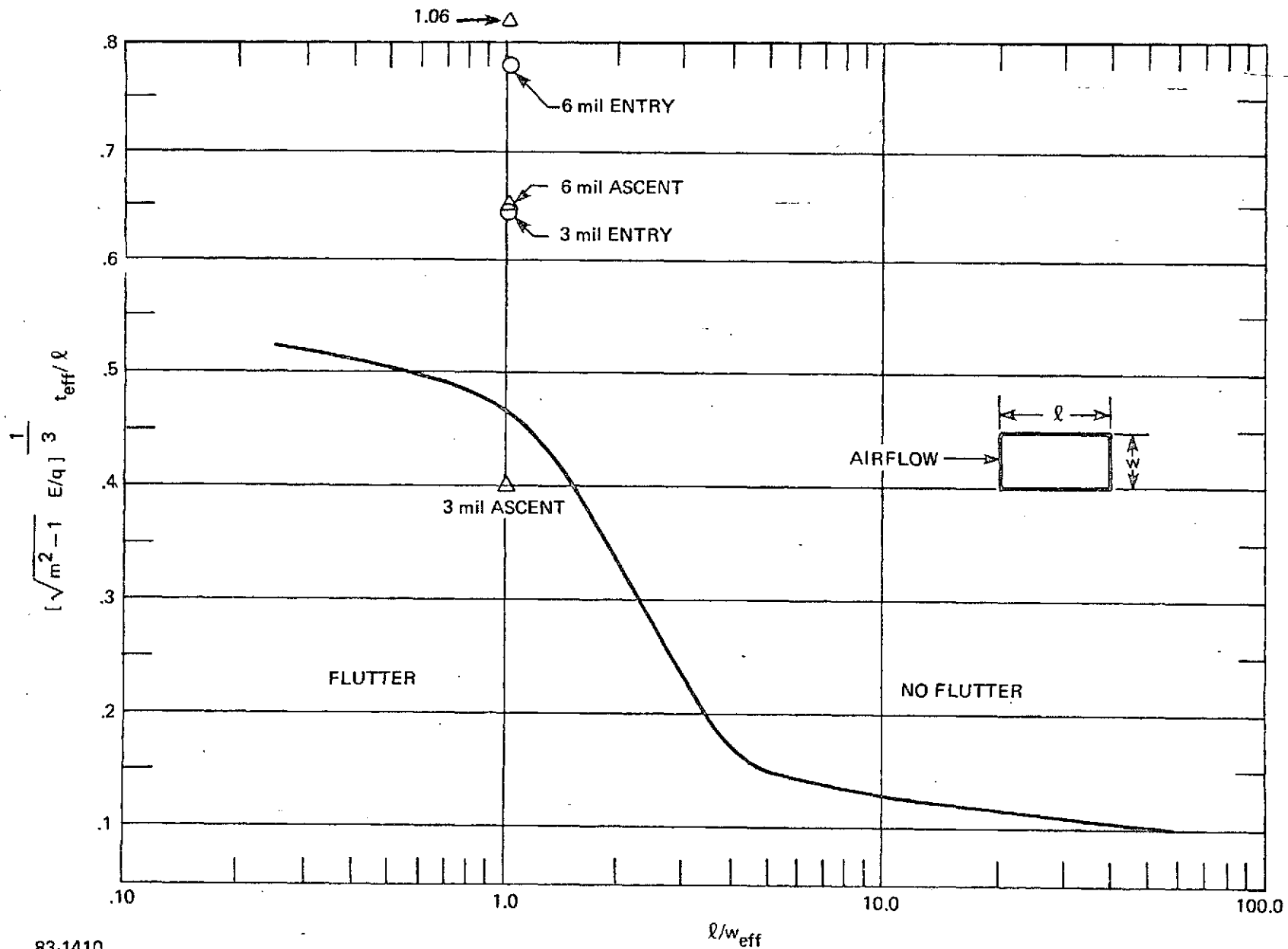
Results of this analysis (Refs. 7 and 8) using a similar two term Galerkin solution indicated that the elastic layer had no effect on the predicted flutter boundary. This is interpreted to mean that although the onset of flutter occurs at the same condition with or without the elastic foundation, the severity of the disturbance is diminished by the elastic support.

Because this analysis was only qualitative, a second approach was attempted to arrive at a suitable definition of tie-down spacing. As noted earlier for reasonable tie spacings with thin foils, the effect of precompression in the insulation is localized. The second model assumed that the surface between discrete ties could be idealized as a simply supported square plate. It was assumed that since the precompression around the wire covered a finite area in the region of the ties, the effective unrestrained distance between ties would be less than the actual tie spacing. For relatively closely spaced tie wires, a simply supported plate model with side lengths equal to the actual center-to-center spacing should provide a conservative estimate for the flutter boundary.

Using this configuration and a flutter envelope given in Reference 5 (presented here as Figure 3.17), calculations were made to determine the appropriate tie down spacing for the 3- and 6-mil textured foils to inhibit the onset of flutter. For a specified plate aspect ratio, the critical condition for aerodynamic flutter occurs when the parameter $\sqrt{M^2-1}/q^*$ is a minimum. For

*Symbol Definition:

M	=	Mach Number
q	=	Dynamic Pressure
$(l/w)_{eff}$	=	Effective Aspect Ratio
E	=	Modulus of Elasticity
t_{eff}	=	Effective thickness of textured foil



83-1410

Figure 3.17 FLUTTER BOUNDARY FOR SIMPLY SUPPORTED PLATE

For the "PHI-2" orbiter trajectory considered (Ref. 3) this occurs during ascent at a peak dynamic pressure (q) of 4.5 psi at a Mach number (M) of 1.1, resulting in a value of .1 for the parameter $\sqrt{M^2-1}/q$. For the entry condition the minimum value of this parameter was .45 clearly showing that the ascent case is more critical.

Utilizing these values for the ascent and entry conditions, and the equivalent foil properties given in Table VII, the required tie-down spacing was calculated for an aspect ratio $(\ell/W)_{\text{eff}}$ of 1.0. For an aspect ratio of 1.0, the flutter parameter, $(\sqrt{M^2-1}E/q)^{1/3} t_{\text{eff}}/\ell$, has a value of .47. This was solved directly for the tie spacing, ℓ . The results are presented in Table VIII for 3- and 6-mil textured Hastelloy foils and for both the ascent and entry trajectories. Based upon these results a common two inch spacing was selected for the test configurations. As shown in Figure 3.17, the 3-mil design is marginal and the 6-mil foil design has a substantial positive flutter margin during ascent. Both designs have positive margins during entry. Referring to Figures 3.15 and 3.16, the allowable venting pressure for the 3- and 6-mil enclosures would be 2.8 and 3.4 psi, respectively, with the selected 2 inch tie spacing.

TABLE VIII

FOIL TIE DOWN SPACING TO PREVENT AERODYNAMIC FLUTTER

Foil Description	Effective Thickness (t) (inch)	Maximum Tie-down Spacing	
		Ascent (inch)	Entry (inch)
3-mil Hastelloy-X (.040 nominal texture depth.)	.0055	1.65	4.78
6-mil Hastelloy-X (.040 nominal texture depth)	.0089	2.55	7.73

3.5.3 Thermomechanical Behavior. - Thermal stresses arise because of the temperature gradients which exist between the top of the enclosure and the sides. The top operates essentially at a uniform temperature peaking at approximately 1800° F whereas the sides are exposed to a temperature gradient ranging from 1800° F at the top edge to as low as 100° F along the lower edge. Consequently, if the top is integrally connected to the sides its expansion will be limited by the cooler sides giving rise to compressive stresses in the surface. These compressive stresses could cause the surface to buckle or fail in compression if the foil is not adequately stiffened. One method to relieve these stresses in the top is to allow it to expand freely relative to the sides by using a sliding joint along the edges as was employed in one test concept.

A second area of concern was the side near the top edge. Here again the problem is caused by thermal gradients where the top edge is restrained from expansion by the sides. In this instance, however, the failure can be more acute, whereas the top could buckle elastically because of thermal stresses and return to a flat configuration upon cool down, an edge failure would most likely involve a permanent deformation in the form of a crippling failure. Crippling failures are of a local nature and usually manifest themselves by local crushing at the top edge of the enclosure. Several different enclosure designs were fabricated and tested in an attempt to arrive at a design which could sustain the thermal environment without failure.

One Piece Textured Foil Enclosure. - The simplest, or reference concepts consisted of a one piece unit with textured foil in the Oxford pattern. A total of seven units of this type of enclosure were fabricated and tested varying the foil material and thickness. (The tests are described in Section 4.1.) This type of construction probably constituted the worst case for both surface buckling and edge crippling, but it represented the simplest and most practical enclosure. The objective in these tests was to determine if by varying the foil thickness within practical limits it might be possible to arrive at a thickness which could sustain the thermal strains without failure. For the foil thicknesses considered (i.e., .003 to .006) elastic buckling of the enclosure surface during heating was anticipated; however, it was assumed that upon cool down the surface would return to its original flat shape. This behavior was predicated on the condition that edge crippling did not occur. Consequently the crucial factor in these designs was whether or not the textured foil in the .003 to .006 inch thickness range when bent to form the enclosure edge would cripple during heating.

Simplified crippling models indicated that for an untextured foil the edge would most certainly cripple because thermal strains in the edge would approach 1.0 percent. This far exceeds even the room temperature yield stress of the untextured material (Figure 3.14). However, because the edge crippling stress is proportional to the yield strain of the material it was postulated that because of the higher yield strain exhibited by the textured foil, there was a possibility that it could absorb the thermal strains without failure.

Beginning with this as the reference concept, selected changes and modifications were made to improve upon the enclosures structural performance in the thermal environment. These modifications consisted of either changes in the top, the edge or the sides to prevent surface buckling or edge crippling. In many instances several of these innovations were incorporated in a single test article. The most significant design variations evaluated in this program are discussed below.

Floating Top. - Because the enclosure surface is exposed to uniform heating the most direct approach to relieve the thermally induced stresses in this area was to allow the top to expand freely as a flat plate. This was accomplished by making the enclosure in two separate pieces. The top was fastened to the sides using a sliding joint along the four edges to allow for free unrestrained expansion.

Stiffened Top. - One of the problems with the reference design was that its bending stiffness was insufficient to prevent buckling during heating. This surface buckling was not only cause for concern as it affected the aerodynamic characteristics of the surface, but it also tended to aggravate the edge crippling problem. This occurred because the top buckled at a very low stress level, making it ineffective in carrying any additional compressive load. Consequently, only a small area of the top, that in the proximity of the edge, continued to carry a load. Because the cross sectional area of the unbuckled edge was relatively small compared to the cooler sides it was effectively fully restrained from expansion by the sides. This is illustrated in Figure 3.18 which examines the thermal stresses in the center region of a two material restrained curvature model. In this figure the stresses in the heated top strip (panel edge) are plotted as a function of top-to-side stiffness ratio (EA_T/EA_S). Note that when the stiffness (EA_T) of the top strip is small relative to the side stiffness, the top is effectively fully restrained and attains its maximum thermal ($Ea\Delta T$) stress. As the stiffness of the top increases, the stresses diminish indicating that the top layer is beginning to do work on the side member.

Based upon this reasoning it was concluded that if the top of the enclosure could be suitably stiffened such that it did not buckle, this would not only produce a better aerodynamic surface but it would also tend to relieve the edge stresses. Two methods of stiffening the top were evaluated, one consisted of hat stiffeners welded to the under side of the surface and the other used beads embossed directly onto the surface of the foil. In both cases the stiffening was aligned with the long direction of the panel because in rectangular panels under in-plane compression, the buckling will usually occur with waves running along the length.

Edge Stiffening. - Edge crippling under the thermal/mechanical loads was one of the more serious problems because a failure of this type can quickly lead to the formation of a crack under thermal cycling or during acoustic excitation. In an attempt to prevent this occurrence, methods to stabilize the edges were examined. In general, crippling involves a local failure along the edge and around the 90° corner. Therefore, one approach examined to stabilize the edge was to incorporate a closure member across the inside edge of the enclosure as illustrated in Figure 3.19. This member tended to maximize the area available to resist crippling by providing an integral corner which stabilized the area enclosed by the stiffener as well as the immediately adjacent surface.

Edge stiffening of this type was also used to support the sides of one of the floating top designs. Without this added support the side behaved like a thin plate subjected to pure bending when subjected to the thermal gradient. As such the edge was prone to buckle laterally or cripple locally. With the internal edge stiffener the sides were stabilized in much the same way a flange stabilizes a compression member.

Internal edge stiffening provided sufficient crippling strength; however, it was noted that lateral inward buckling of the long side could occur because the thin foil surface was not sufficiently stiff in compression to stabilize

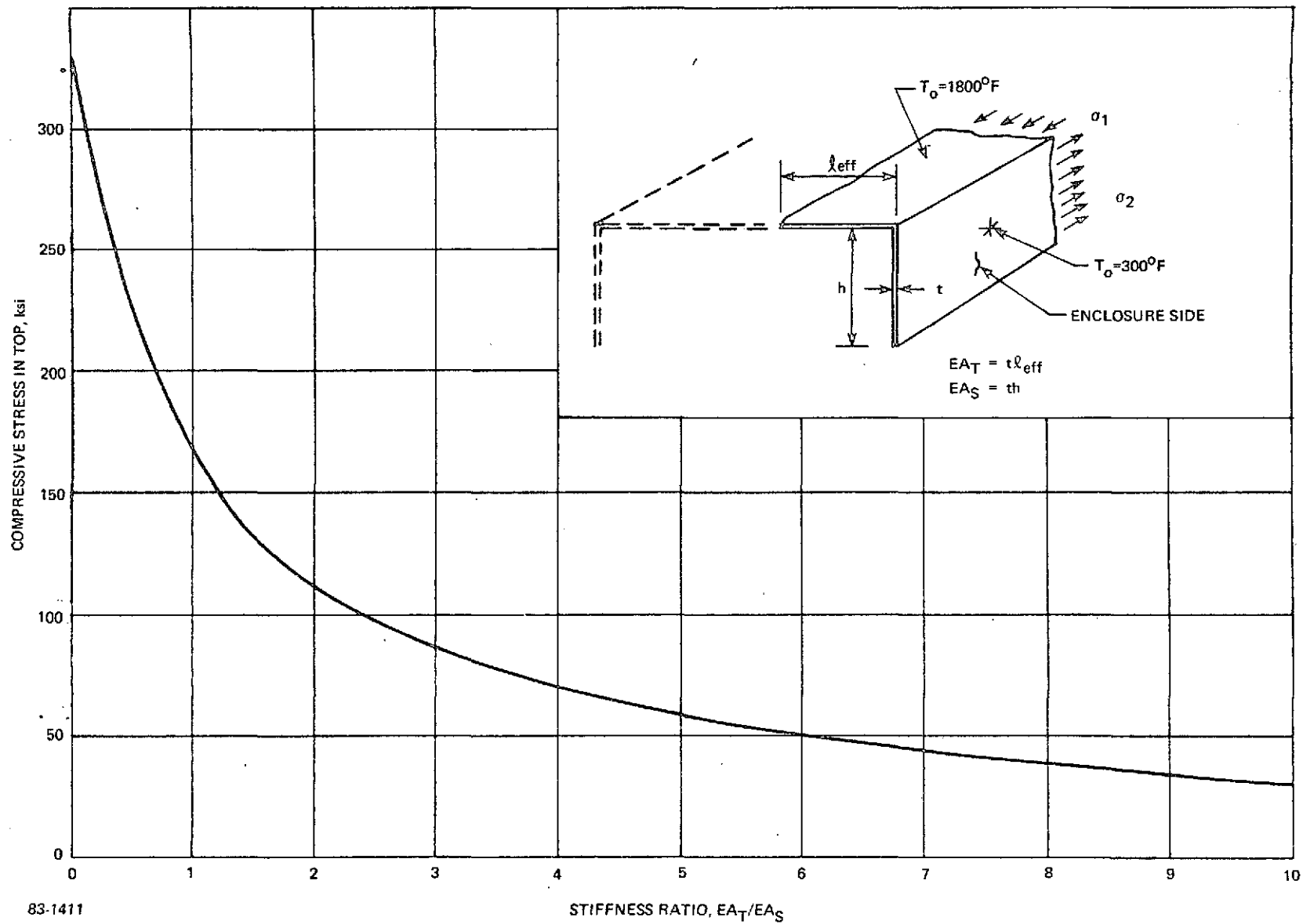


Figure 3.18 EFFECT OF TOP STIFFNESS ON THERMAL STRESSES

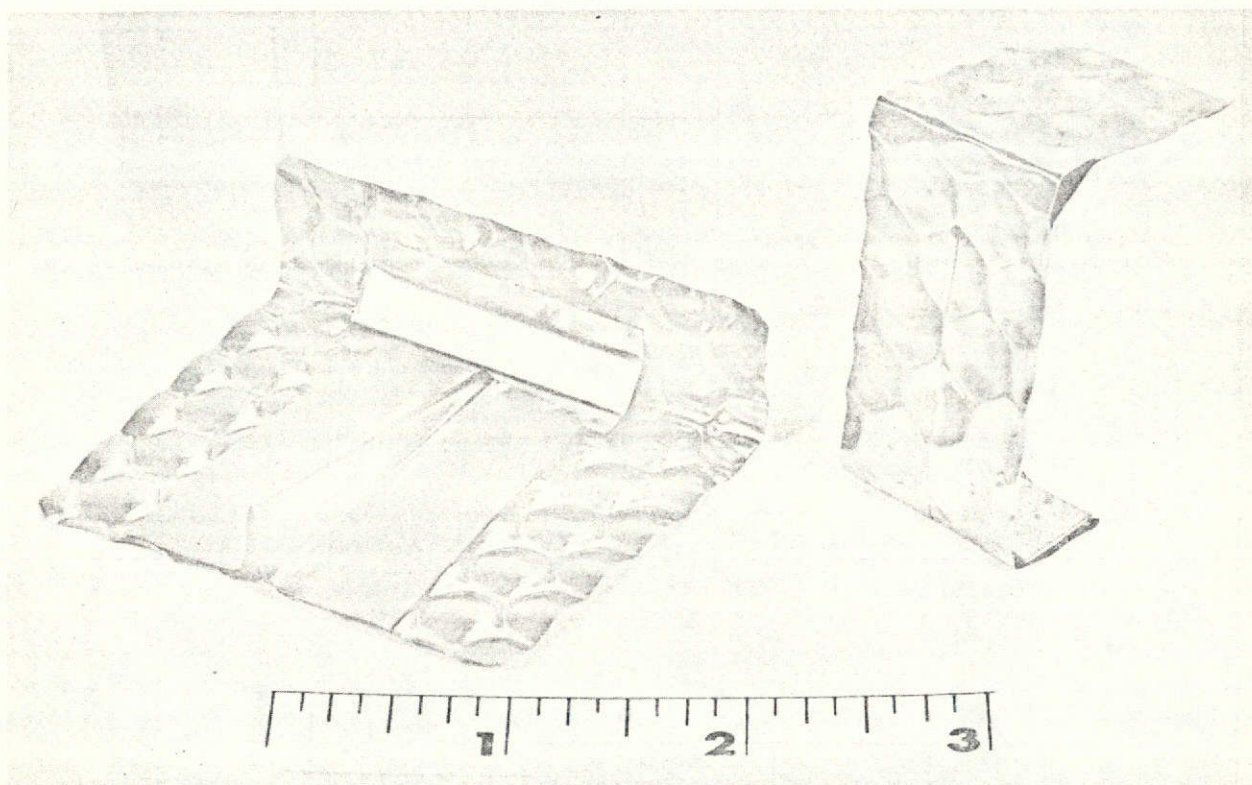


Figure 3.19 DETAIL OF EDGE PLEAT AND EDGE STIFFENER IN SPECIMEN 11

the sides over long lengths. (See Figure 3.20a.) An examination of this behavior lead to the conclusion that the edge member was loaded eccentrically which caused the edge to bend inward. This can be visualized by examining Figure 3.20b which shows the loads introduced into the edge member of a floating top design. The compressive load in the edge is induced by the restraint offered by the side. However, the compressive load is developed by shear stresses which occur over a finite length at the ends of the sides as shown in Figure 3.20. Usually, these shear stresses are neglected by appealing to St. Venant's principle which in effect attributes these to local effects that are not of importance except in the local area at the ends. In any event, the location of the shear restraint is of concern here because it is eccentric to the center of gravity of the edge closure. Therefore, for axial equilibrium this shear must be balanced by an axial compressive load and a moment about the c.g. of the edge member as illustrated in the figure. As a result the edge is subjected to a bending moment which causes the edge to bend inward.

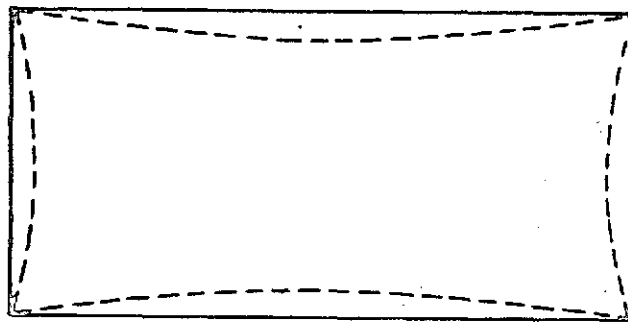
This condition was alleviated by fabricating a design which incorporated an edge stiffener on the outside of the enclosure as shown in Figure 3.20c. With this design the eccentricity is reversed and the moment tends to bow the sides outward. The magnitude of the bow is restrained by the surface which is now placed in tension.

Reduced Extensional Stiffness of Sides. - Figure 3.18 shows that the surface and edge compressive stresses are caused by the side restraint. Furthermore, this figure shows that if the effective stiffness of the surface is greater than the sides then the top could expand more easily. The important factor is the relative stiffness of the top and the sides. Previously, methods for stiffening the top were discussed; as a corollary to this, methods of making the sides flexible were also investigated.

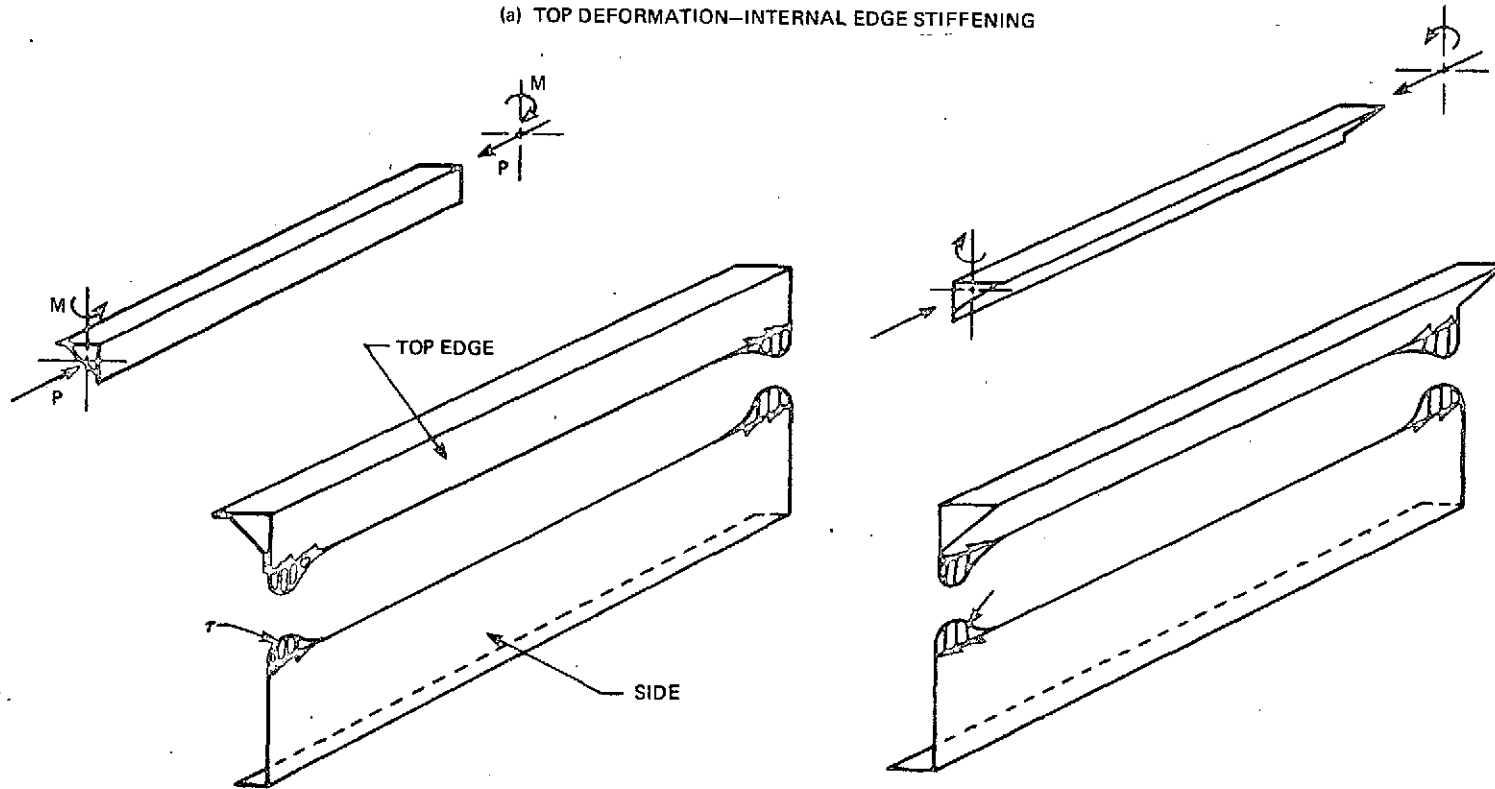
The first approach consisted of taking advantage of the directional nature of the foil. As shown in Figure 3.14 the extensional stiffness of the foil in the transverse direction is about one half the stiffness in the axial direction. The first enclosures fabricated in this program were assembled with the stiff foil direction oriented along the length of the enclosure and the same texture pattern was carried down the long sides. The short sides (width) had the pattern reversed. A subsequent enclosure was fabricated with the same texture orientation on the surface, but the pattern on the long sides was reversed such that the more flexible direction was aligned with the length. The short sides remained unchanged, retaining their flexibility.

A second technique employed to make the sides flexible was to use beads embossed vertically in the sides in an attempt to achieve a bellows action.

Pleated Sides. - Results obtained from the study of thermal stresses in isothermally heated flat plates with two edges restrained led to another approach for relieving the stresses in the surface of the enclosure. Figure 3.21 presents a series of plots taken from Reference 9 for the compressive stress in a heated plate considering various plate aspect ratios. These figures show that even for a fully restrained boundary the stresses at the center of



(a) TOP DEFORMATION—INTERNAL EDGE STIFFENING

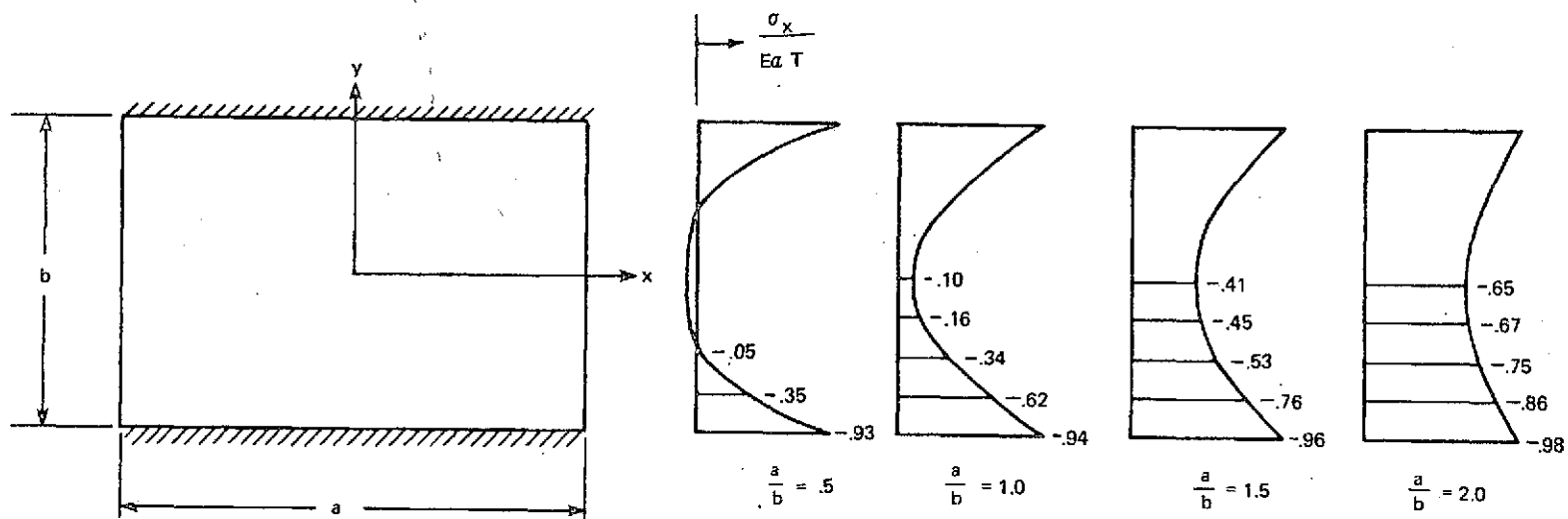


83-1412

(b) FREE BODY DIAGRAM—TOP EDGE INTERNAL STIFFENING

(c) FREE BODY DIAGRAM—TOP EDGE EXTERNAL STIFFENING

Figure 3.20 FREE BODY DIAGRAM AND DEFORMATION BEHAVIOR OF STIFFENED EDGE ENCLOSURES



83-1412

Figure 3.21 HORIZONTAL STRESS (σ_x) AT CENTER OF A RESTRAINED PLATE ($X = 0$) FOR DIFFERENT PLATE ASPECT RATIOS (a/b) IN TERMS OF $E\alpha\Delta T$

the plate are significantly reduced from the maximum plane stress condition (i.e., $Ea\Delta T$) for aspect ratios as great as $a/b = 2$. For aspect ratios of 1.0 or less the compressive stresses are less than one third the maximum value over 50 percent of the plate width. If one were to factor in the partial edge restraint representative of the sides these stresses would be reduced further.

This suggested that if the edge restraint provided by the sides in the actual enclosure were made discontinuous, such that the aspect ratio of the surface of the enclosure between the side discontinuities were less than one, the stresses in the surface would be greatly reduced. To accomplish this the sides of the enclosure were cut at selected intervals to limit the length of the individual side segments. The cut sides were then sealed by placing pleats on the inside surface which would not take any axial loads in the plane of the side. (See Figure 3.19.)

The other point of interest shown in Figure 3.21 is that for all aspect ratios considered, high compressive stresses are predicted near the edge restraint. As a result this approach requires edge stiffening to prevent edge crippling.

3.5.4 Enclosure Venting (Burst) Pressure Test. - To evaluate the basic behavior of the enclosure surface and the tie down system under positive internal pressure a series of pressure tests were performed on simulated enclosures. For these tests a piece of textured foil was mounted in a fixture to form one side of a closed chamber. 3DSX insulation was placed beneath the foil. The foil was sealed around the edges and tied to the rear surface of the enclosure with standard tie wires. Figure 3.22 illustrates a typical test assembly, showing the 10-3/4 x 6-3/8 inch foil specimen in place. The rear surface with all the tie down wires fastened and sealed is shown in Figure 3.23.

Three pressure tests were performed using this fixture, one each for the .003 and .006 inch thick textured foil using a rectangular tie down spacing of 1.6 x 1.3 inch on centers as depicted in Figure 3.24. Considering the directional nature of the panel this spacing corresponded to a 1.4 inch square array for the isotropic model used in the venting analysis. A third test was performed on the .006 inch thick Hastelloy foil employing an enlarged tie down spacing of 3.2 x 2.6 inches which is approximately equivalent to a 2.9 inch square spacing for the isotropic model. All tests were instrumented with dial gages to record the surface deflections (Figure 3.25). Water pressure was applied in increments and deflection measurements were taken. Once the design pressure was reached the pressure was relieved in preselected increments and again deflection measurements were taken. In this manner both the loading and unloading history of the foil was examined.

The test results are summarized in Table IX. Design pressures given in this table were determined from Figures 3.15 and 3.16 using equivalent square array tie down spacing of 1.4 and 2.9 inches for the two test rectangular tie down spacings. The only failure observed in the 3-mil foil specimen was one tie wire failed in the weld attachment. This failure occurred at approximately 3 psi which correlates closely with the design curve in Figure 3.15 for a 1.4 inch tie down spacing. The 6-mil foil specimen with closely spaced tie wires

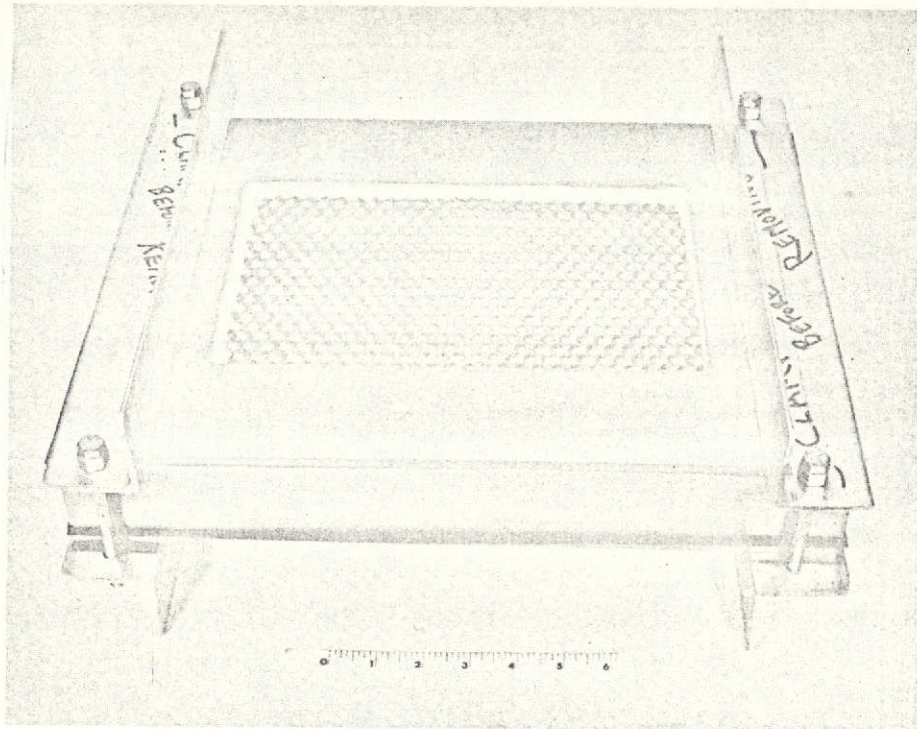


Figure 3.22 TOP SURFACE, VENTING PRESSURE TEST FIXTURE

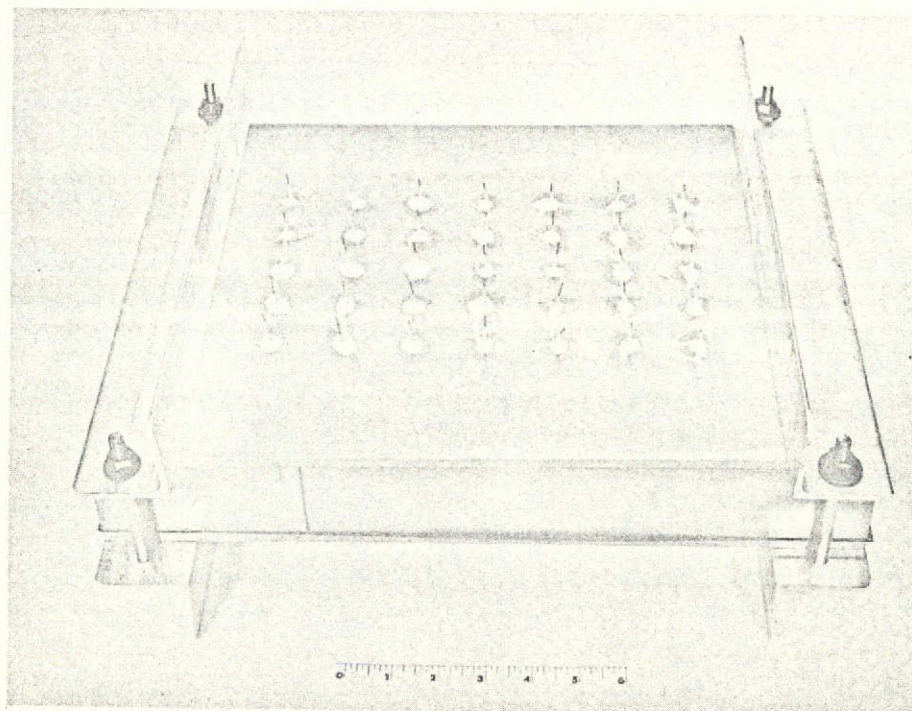
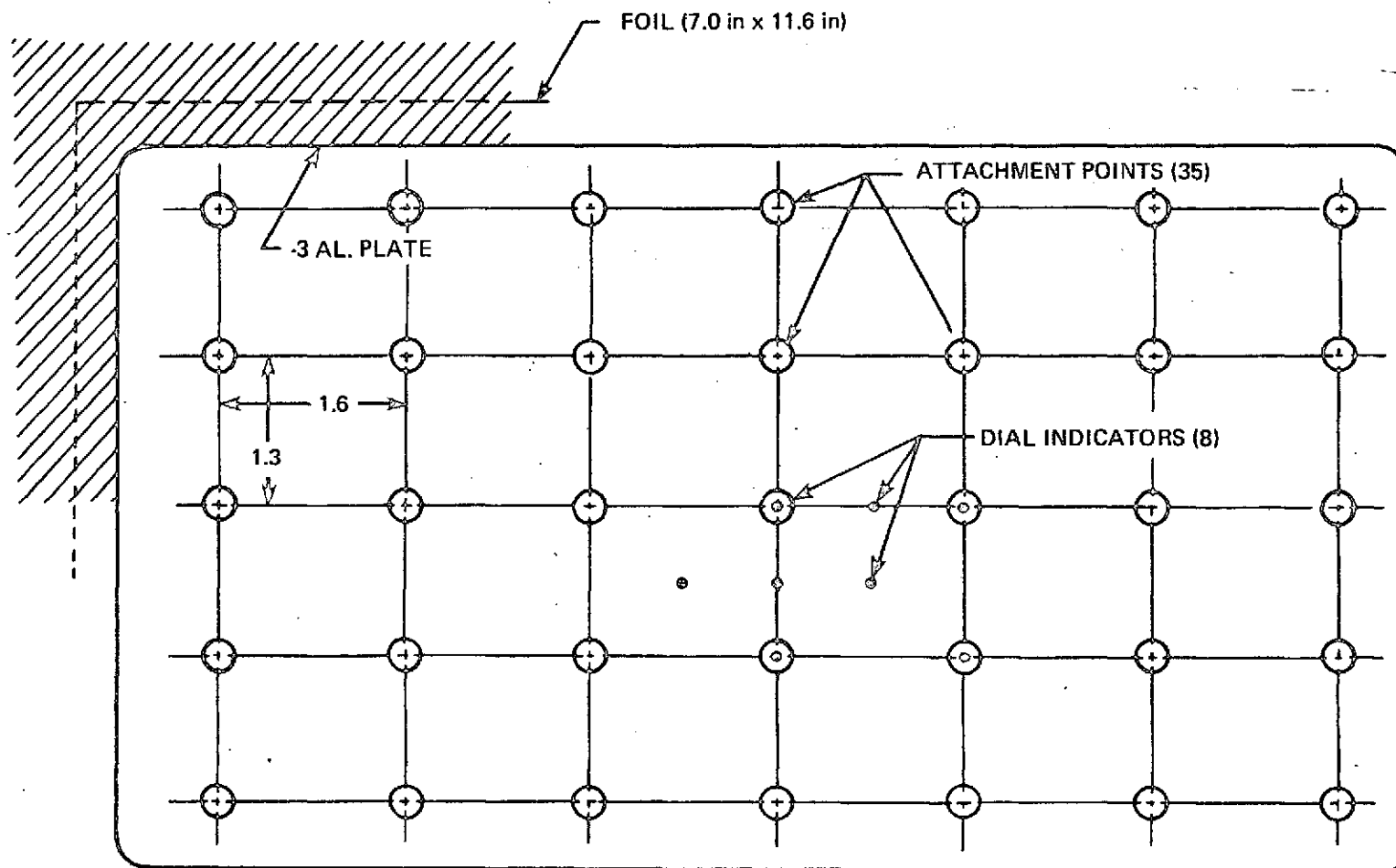


Figure 3.23 REAR SURFACE, VENTING PRESSURE TEST FIXTURE



NOTE: ALTERNATE CONFIGURATION WITH 2.6 x 3.2 INCH SPACING WAS ACHIEVED BY UTILIZING EVERY OTHER ATTACHMENT POINT.

83-1414

Figure 3.24 VENTING PRESSURE TEST FIXTURE ATTACHMENT AND INSTRUMENTATION LOCATIONS

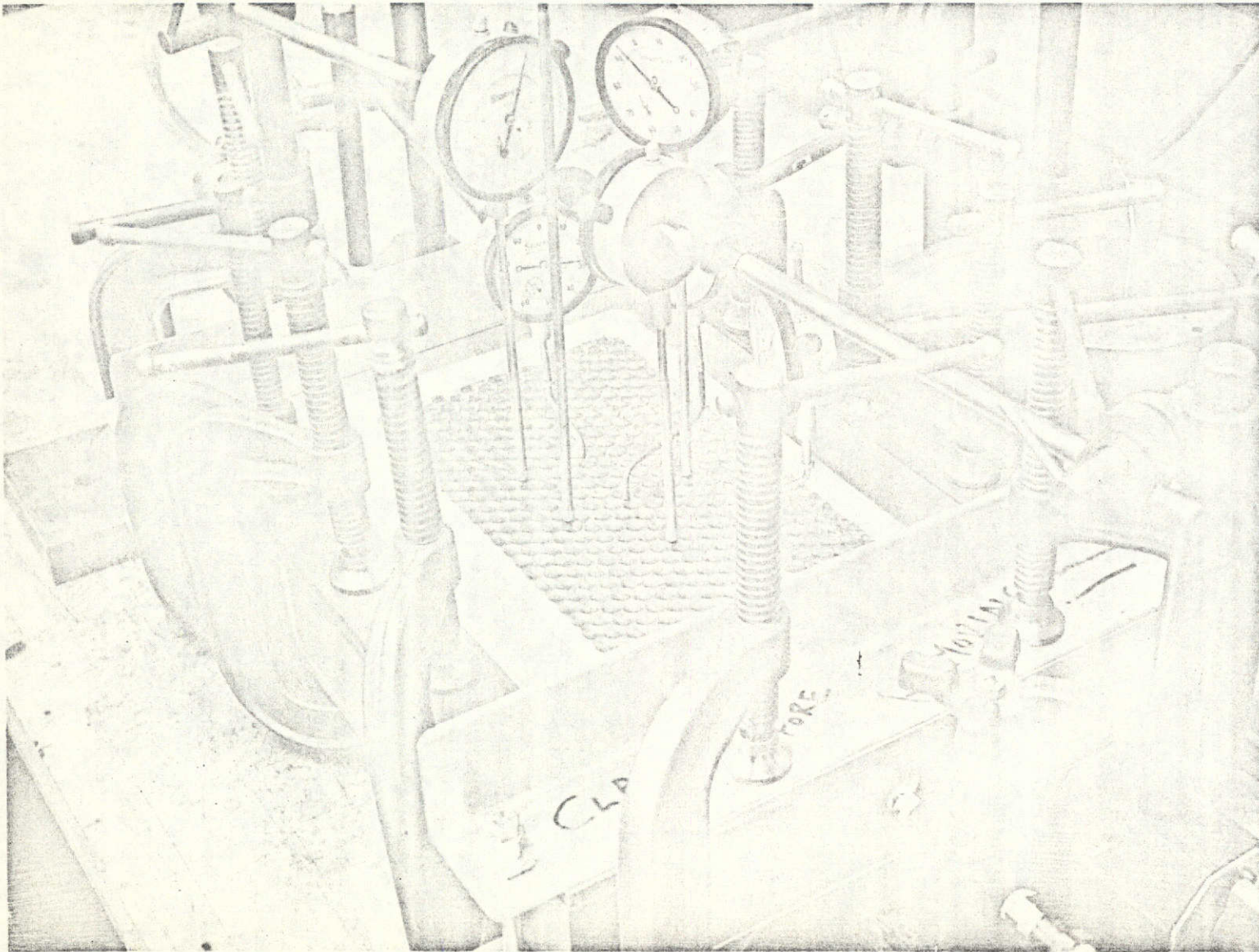


Figure 3.25 VENTING PRESSURE TEST SETUP

behaved perfectly up to the proof test pressure of 5 psi and no post test failures were detected. In fact, for the pressure test of the 6-mil foil with enlarged tie down spacing the same panel was employed with alternate tie wires removed. In this test the test pressure exceeded the design value by a factor of two.

TABLE IX
FOIL PRESSURE TEST RESULTS

Test No.	Foil Thickness (in)	Tie Spacing (in)	Design Pressure (psi)	Test Pressure (psi)	Remarks
1	.003	1.3 x 1.6	3.0	3.0	Weld failure at tie wire.
2	.006	1.3 x 1.6	4.0	5.0	No failures.
3	.006	2.6 x 3.2	2.0	4.0	Leak - No foil failure.

The intent was to determine the ultimate failure pressure, but the test had to be curtailed at 4.0 psi because of a water leak at the edge seal. The only failure noted was a weld which failed at approximately 3.5 psi, or slightly below the predicted value for an equivalent spacing of 2.9 inches.

Typical load-deflection curves taken at the center of each test panel for the loading and unloading cycles of Specimens 1 and 2 are presented in Figure 3.26. Note that each curve exhibits a non-linear hysteresis behavior with both curves indicating a slight permanent set. This was attributed to some slight slippage and bending in the tie system. Also note that the deformation of the 3-mil foil was approximately 1.5 times greater than the 6-mil foil for the same tie down spacing at 3 psi pressure.

The load deflection curve for the 6-mil foil with the 3.2 x 2.6 inch tie spacing is presented in Figure 3.27. Because of a pressure leak no unloading curve was obtained. The deformations with the larger tie spacing were substantially greater. At 3 psi these deflections are 5.2 times greater than Specimen 2, with closely spaced ties. This is slightly less than the factor of 8 which would have been predicted on the basis of the enlarged tie spacing using plate bending theory.

In general, the results of these tests were satisfactory in that they correlated reasonably with the predicted results and showed that the basic tie down concept could sustain acceptable venting pressures.

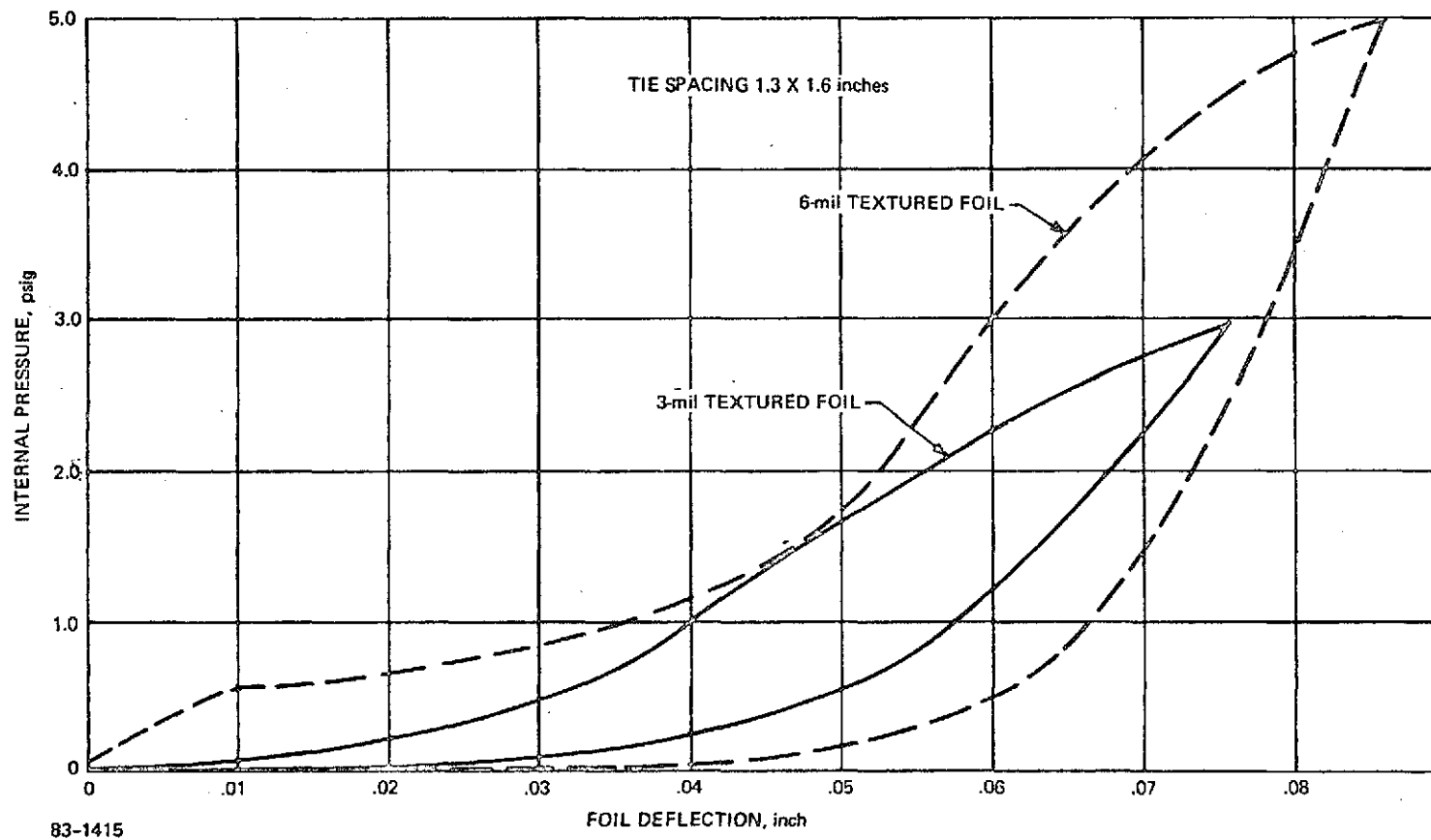
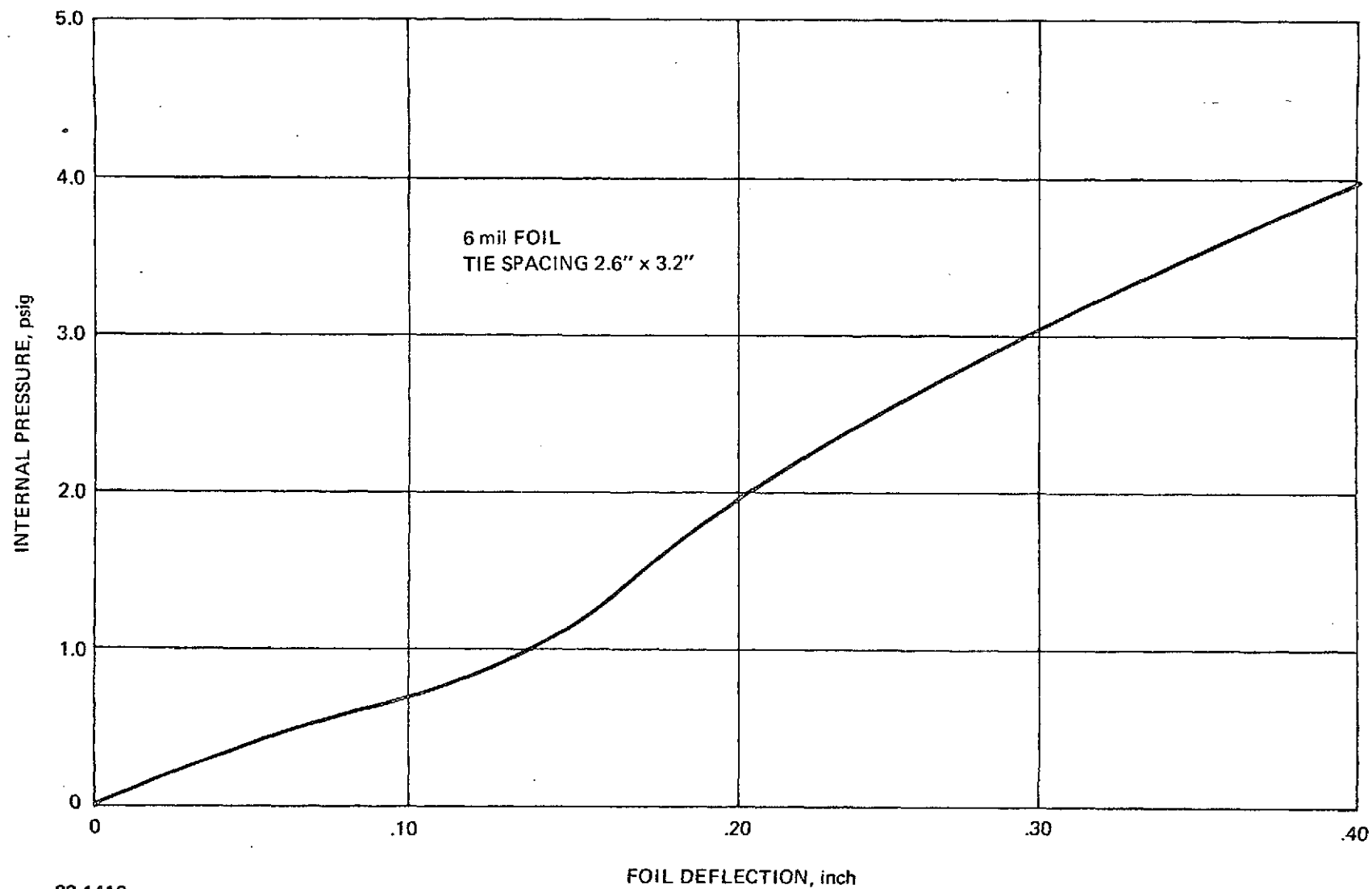


Figure 3.26 MID-PANEL FOIL DEFLECTION VERSUS PRESSURE,
VENTING PRESSURE TEST



83-1416

Figure 3.27 MID-PANEL FOIL DEFLECTION VERSUS PRESSURE,
VENTING PRESSURE TEST

3.6 Thermal Sizing of 3DSX Insulation

Representative insulation thickness requirements were established for the thermal environment specified by the contract document (Figure 3.28). Avco Corporation Program 2900 was utilized. This is a finite difference solution of a second order non-linear differential equation applicable to problems involving one-dimensional heat conduction.

Because the thermal conductivity of the 3DSX insulation is pressure dependent, a pressure history was also defined according to Figure 3.29 for Area 1. This is a typical orbiter lower surface pressure history for an entry trajectory (PHI-2) utilized in a previous study (Ref. 3) which has a thermal pulse similar to that specified by MSFC for the current program. The 3DSX thermal conduction properties used in the analysis are presented in Table X. A substructure heat capacity was assumed equivalent to a .10 inch thick aluminum alloy.

Figure 3.30 presents the effect of insulation thickness on the maximum structure temperature for the three trajectory heating pulses of Figure 3.28. A cross-plot relating insulation thickness to maximum surface temperature is presented in Figure 3.31 for a design allowable substructure temperature of 350° F.

TABLE X

THERMAL PROPERTY MODEL FOR 3DSX MATERIAL
(5.8 lb/ft³ Density)

Temperature (°F)	Specific Heat (Btu/lb-°F)	Thermal Conductivity At One Atm. (Btu/ft-hr-°F) 5.6 lb/ft ³ Material
80	.19	.033
200	.20	.035
500	.24	.043
1000	.27	.077
1500	.29	.124
2000	.30	.181
2500	.31	.247

PRESSURE MULTIPLIER FOR THERMAL CONDUCTIVITY

Pressure Torr	Multiplier
1.0	.55
10.0	.65
100.0	.90
760.0	1.00

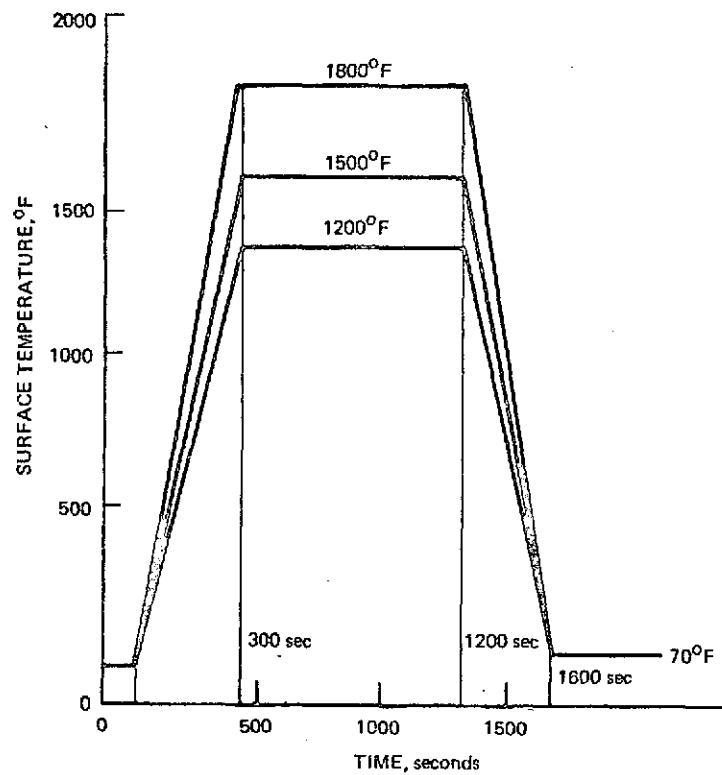


Figure 3.28 THERMAL DESIGN ENVIRONMENT

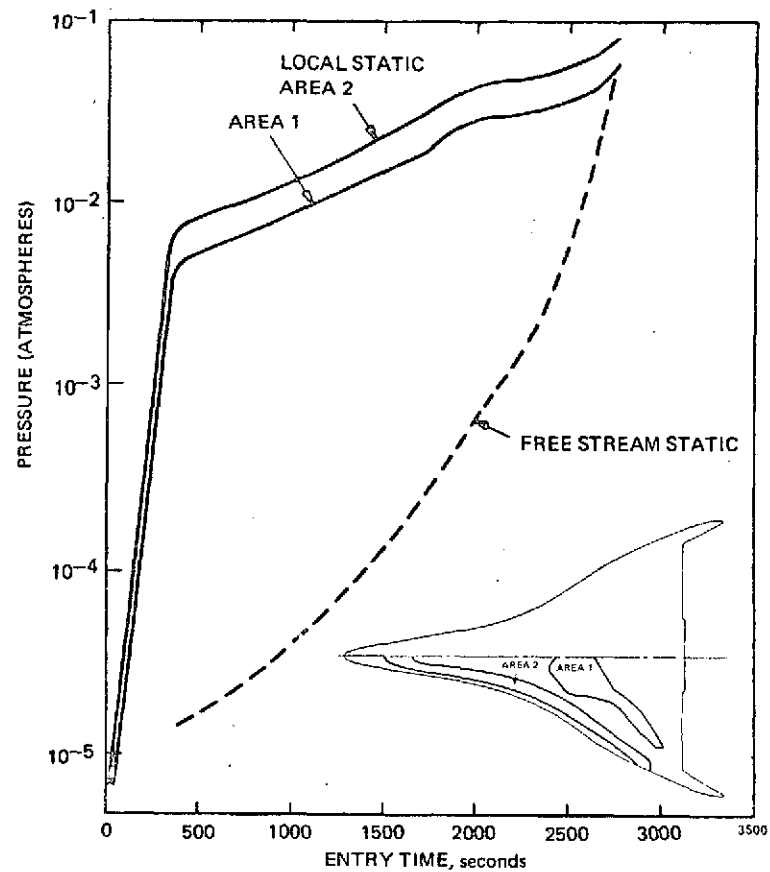


Figure 3.29 REENTRY PRESSURE HISTORY, PHI-2 TRAJECTORY

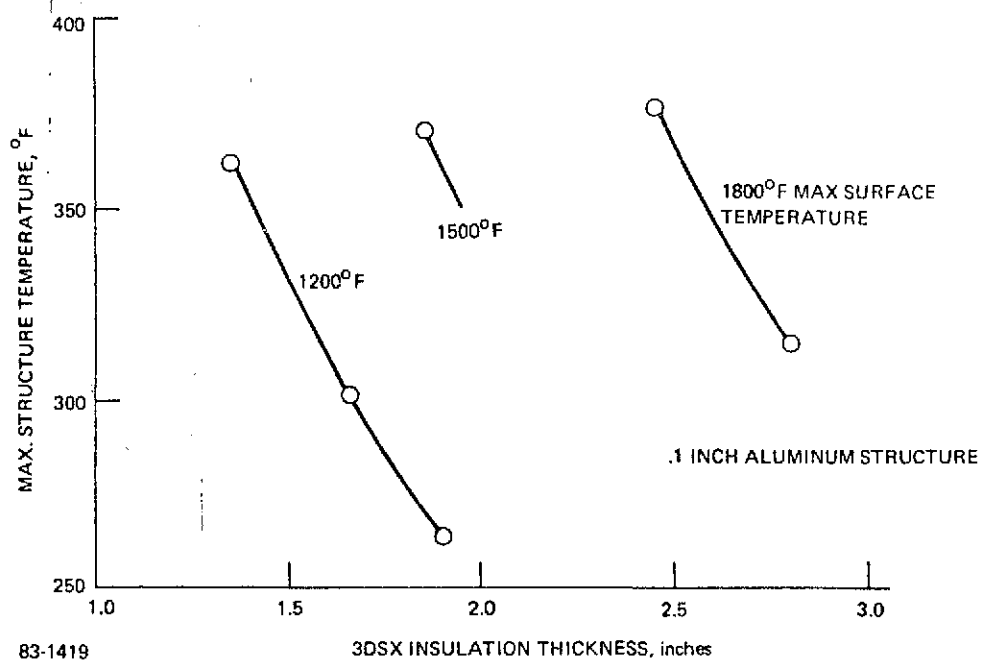


Figure 3.30 3DSX SIZING FOR MSFC TEST HEATING ENVIRONMENT

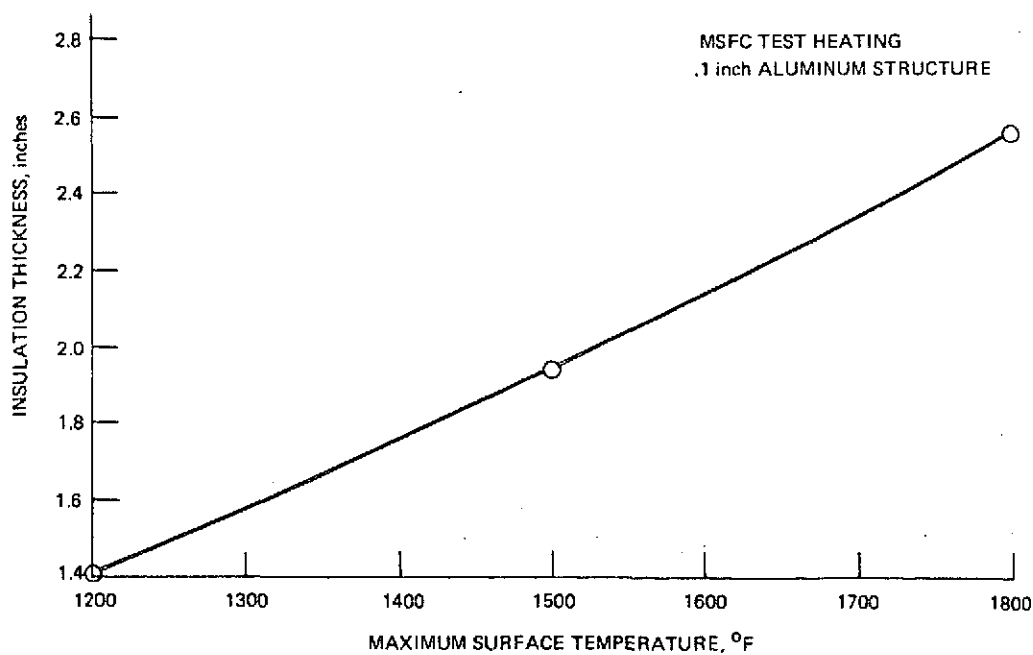


Figure 3.31 3DSX THICKNESS REQUIREMENT FOR 350°F MAXIMUM STRUCTURE TEMPERATURE

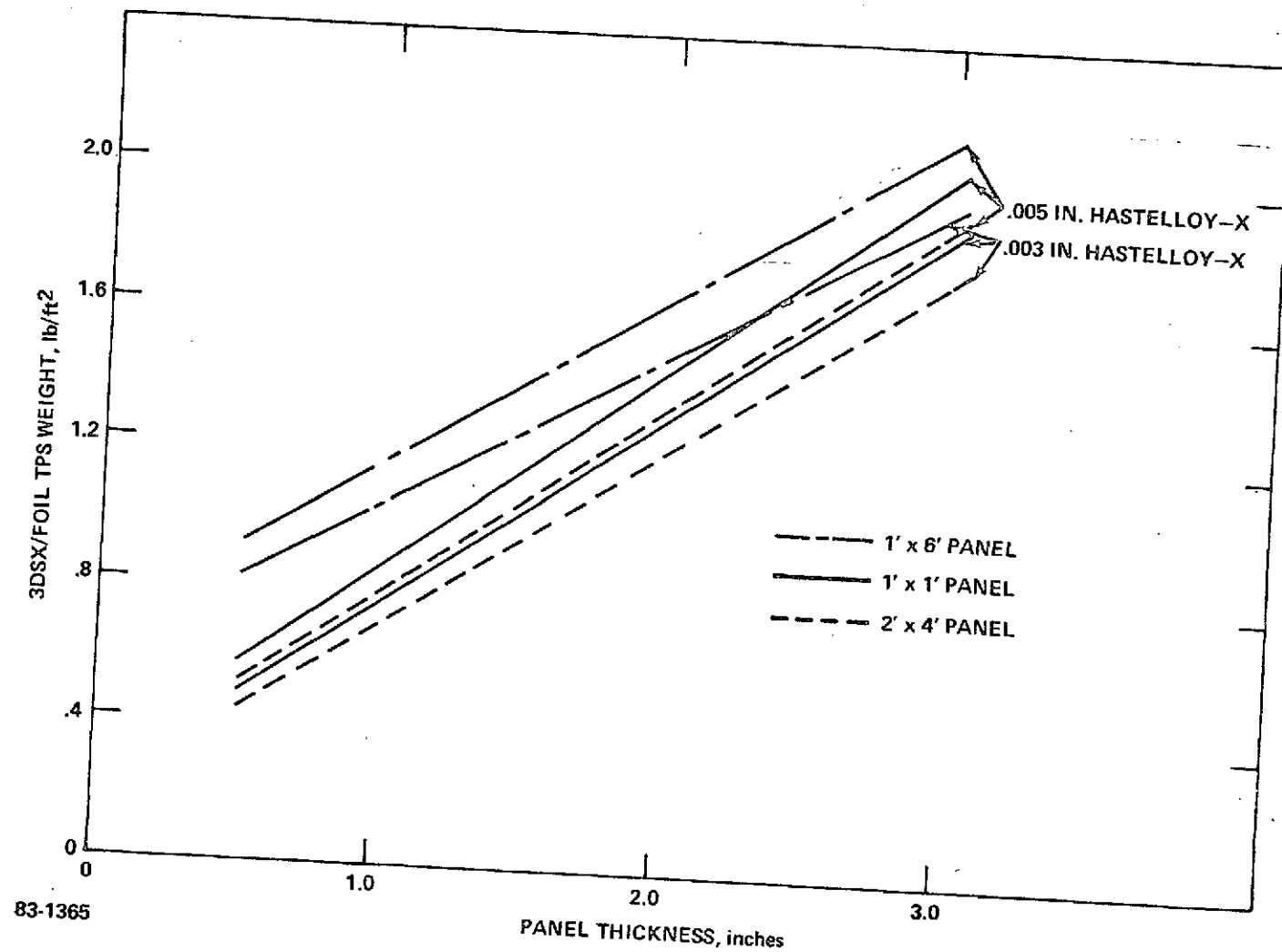


Figure 3.32 UNIT WEIGHT OF 3DSX/FOIL TPS

3.7 Weight Analysis

The weight of the 3DSX/Foil TPS includes several elements. In addition to the 3DSX insulation itself the foil (both top and sides), wires, straps and corner stiffeners must be included in the weight estimate. An additional parameter to be considered is the panel size (L x W x H) because the unit weight (lb/ft^2) will tend to decrease with increasing panel size for the same thickness.

Figure 3.32 shows the results of a tradeoff study conducted on a typical design using Hastelloy-X foil. The weight includes all the elements mentioned. The tradeoff includes variations in panel size and foil thickness. Several conclusions can be drawn from this figure:

1. Large size panels (of at least 1' x 1') are desirable because smaller tiles introduce significant weight penalties especially at the smaller thicknesses. Increasing the panel size from 1 x 1/2 to 1 x 1 foot reduces the weight by 45 percent at .50 inch to 5 percent at 3.0-inch thickness. Further increase in panel size to 2 x 4 feet increases the weight saving an additional 6 to 10 percent.
2. Reducing the foil thickness from 5 to 3 mils saves between 10 and 15 percent on weight.

Of additional interest is the "effective density" of the 3DSX/Foil concept as shown in Figure 3.33. As would be expected, this density remains relatively low ($\approx 8 \text{ lb}/\text{ft}^3$) at panel thicknesses exceeding one inch, but increases to $12 \text{ lb}/\text{ft}^3$ when the thickness requirements drop to approximately 0.50 inch. These data indicate the attractiveness of the 3DSX/Foil concept in that even at small thicknesses acceptable densities are obtained on the composite system.

Table XI presents a weight breakdown of the 3DSX/Foil TPS for the case of a maximum surface temperature of 1800°F and a 5-mil Hastelloy-X foil. The 3DSX insulation thickness (2.17 inches for 350°F structure temperature) was obtained from the thermal analysis described in Section 3.6 and the results are presented for two panel sizes.

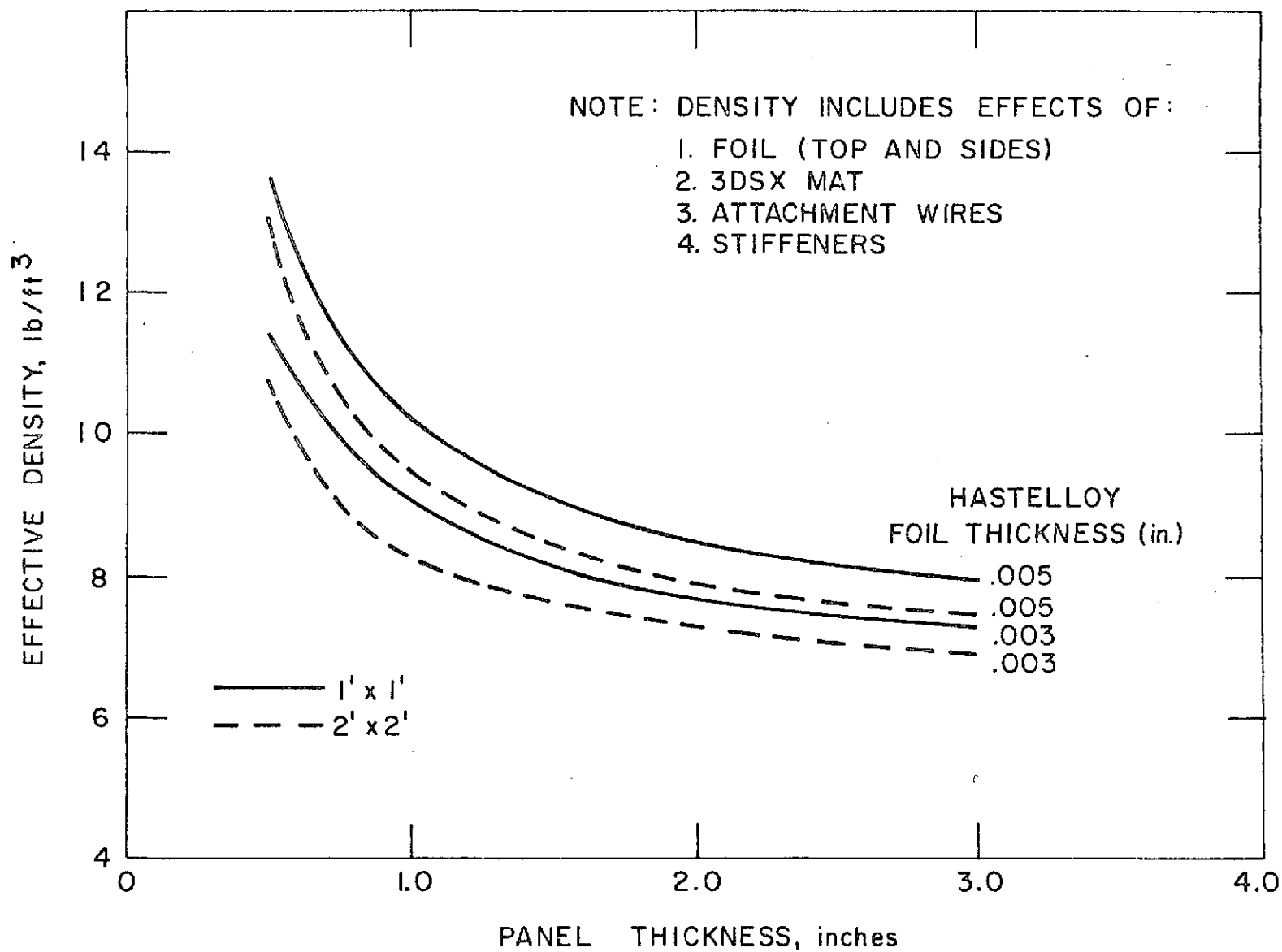


Figure 3.33 EFFECTIVE DENSITY OF 3DSX/FOIL HEAT SHIELD

TABLE XI

3DSX/FOIL WEIGHT BREAKDOWN

Maximum Surface Temperature = 1800° F		
Maximum Structure Temperature = 350° F		
5-Mil Hastelloy-X Foil		
Element	Weight (lbs)	
	1' x 1'	2' x 4'
3DSX Insulation (2.17 in. thick)	1.08	8.64
Foil (Top and Sides)	.37	2.16
Attachment Wires (.02 inch diameter)	.01	.12
Straps	.01	.06
Stiffener and Guide	.15	.45
Total Weight	1.62	11.43
Unit Weight (lbs/ft ²)	1.62	1.43

4.0 EXPERIMENTAL DEMONSTRATION OF PERFORMANCE AND REUSE CAPABILITY

4.1 Thermal Testing and Design Development

The thermal and acoustic cycling tests designed to demonstrate the performance and reuse capability of the 3DSX/foil concept are summarized in Table XII. Initially, the configuration was limited to the simple textured box, 6 x 12 x 2 inches thick, shown in Figure 4.1. Variations of the simple textured box design were limited to foil material and gage variations and to two densities of the 3DSX insulation.

Six specimens of this basic design were fabricated. (These are Specimens 1 through 6 of Table XII.) Specimens 1 and 2 were identical and were considered a reference configuration. They were made of 6-mil Hastelloy-X foil textured with Ardmore's Oxford pattern to a depth of 40 mils. The lower density (6 lb/ft³) 3DSX insulation was installed. A total of ten 20-mil diameter Hastelloy-X tie wires (spacing 2 x 2 inches) anchored the top foil to the structure. In addition, sheet metal screw fasteners and nutstrips tied down the bottom flange of the box.

Specimen 3 was identical to the reference except 3-mil Hastelloy-X foil was used. The texture pattern and depth were the same as Specimens 1 and 2. Specimens 4 and 5 were identical in configuration to the reference, but the foil material was 5-mil Haynes 25. Specimen 6 was identical to 4 and 5 except a higher density version of the 3DSX was used (nominal 10 lb/ft³).

Figures 4.2 and 4.3 illustrate the completed test panel. It consists of the six textured box specimens fastened to a 16 x 40 inch tee-stiffened aluminum alloy panel. The radiant heater facility is illustrated in Figure 4.4. It is shown installed in a closed chamber designed to permit reduced pressure testing.

The 3-mil Hastelloy-X panel was subjected to a preliminary test consisting of a single cycle to an 1800° F surface temperature in an open (room-ambient) heater facility illustrated in Figure 4.5. (This accounts for the darkened appearance of Specimen 3 in Figure 4.2.) The purpose of this test was to evaluate the general behavior of the configuration in the thermal environment prior to exposure of the six specimen panel. The specimen surface was subjected to a 300 second linear rise rate to 1800° F followed by a 300 second hold at 1800° F, at which time the specimen was permitted to cool naturally. Some permanent buckling of the top foil surfaces was apparent as seen in Figure 4.6, but the foil surface remained sealed.

The six specimen panel was then subjected to the initial thermal cycling test in the closed chamber. The chamber was evacuated to a pressure level of 10 torr (air) and filled with nitrogen to atmospheric pressure prior to initiation of the heating cycle. The intent of this procedure was to achieve an oxygen partial pressure representative of the reentry environment while maintaining reliable operation of the heating facility. Exposure to 1800° F in

TABLE XII

SPECIMEN DESCRIPTION AND TEST SUMMARY

Specimen	Description	Thermal Cycles No. 1 (Temp. ° F)	Acoustic Exposure (Min.)		Remarks
			154 dB	168 dB	
1	Textured Box 6-mil Hastelloy-X	1 (1800)	10	--	Specimens 1 through 6 had edge crippling and top buckling after one thermal cycle.
2	Textured Box 6-mil Hastelloy-X	1 (1800)	--	--	
3	Textured Box 3-mil Hastelloy-X	2 (1800)	--	--	Edge cracks after two thermal cycles.
4	Textured Box 5-mil Haynes 25	1 (1800)	5	--	Edge cracks after one thermal cycle.
5	Textured Box 5-mil Haynes 25	1 (1800)	5	--	Edge cracks after one thermal cycle.
6	Textured Box 5-mil Haynes 25 10 PCF 3DSX	1 (1800)	10	10	No cracks.
7	Textured Floating Top Plain Sides 4-mil Hastelloy-X Top 3-mil Hastelloy-X Sides	10 (1800)*	10	10	Very slight top deformation. Sides buckled.
8	Textured Box 6-mil Hastelloy-X	10 (1800)*	10	10	Edge crippled. Top buckled.
9	Textured Box, Stiffened Edge, Texture Rotated 90° 5-mil Hastelloy-X	10 (1800)	5	10	Top buckled, sides O.K. Cracks in top after acoustic test.
10	Beaded Sides, Flat Top with HAT Stiffeners, Stiffened Edge, 5-mil Hastelloy-X	10 (1800)	5	--	Top buckled, sides O.K.
11	Textured Box, Fluted Sides, Stiffened Edge 5-mil Hastelloy-X	1 (2300)	--	--	Overheat due to test malfunction. Top buckled and melted, sides O.K.
12	Textured Floating Top Beaded Sides, Stiffened Edge, 4-mil Hastelloy-X Top 5-mil Hastelloy-X Sides	1 (1800)	--	--	Top O.K. Sides O.K.
13	Tension - Top Design Beaded Sides and Top Externally Stiffened Edge	1 (1800)	--	--	Slight wrinkles in top. Sides O.K.

*Note: Specimens 7 and 8 were also subjected to one thermal cycle at 1200°, 1400°, and 1600° F.
Buckling of Specimen 8 occurred at 1400° F temperature level.

Figure 4.1 SIMPLE TEXTURED BOX DESIGN

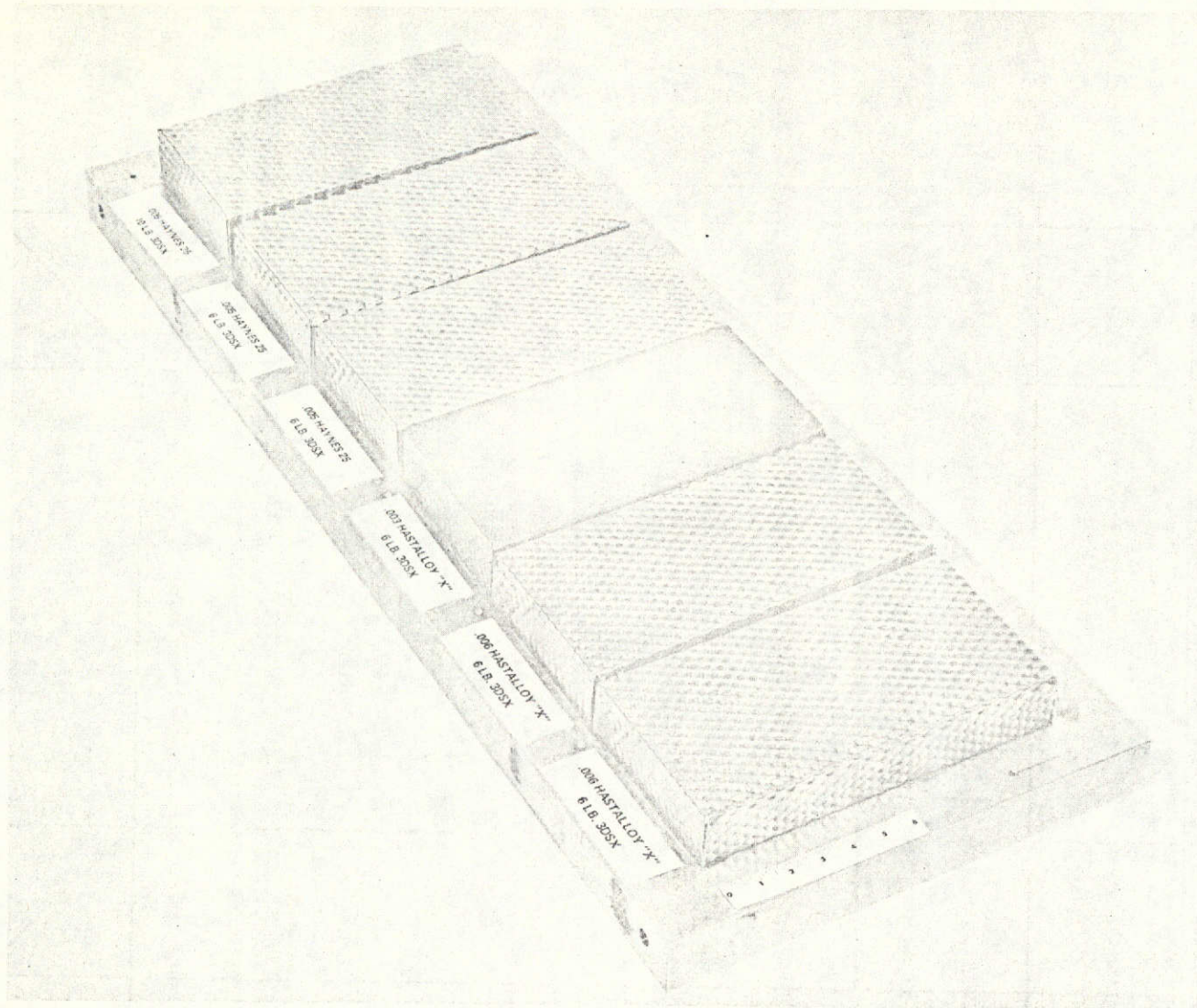


Figure 4.2 TEXTURED BOX SPECIMENS INSTALLED ON SUBSTRUCTURE PANEL

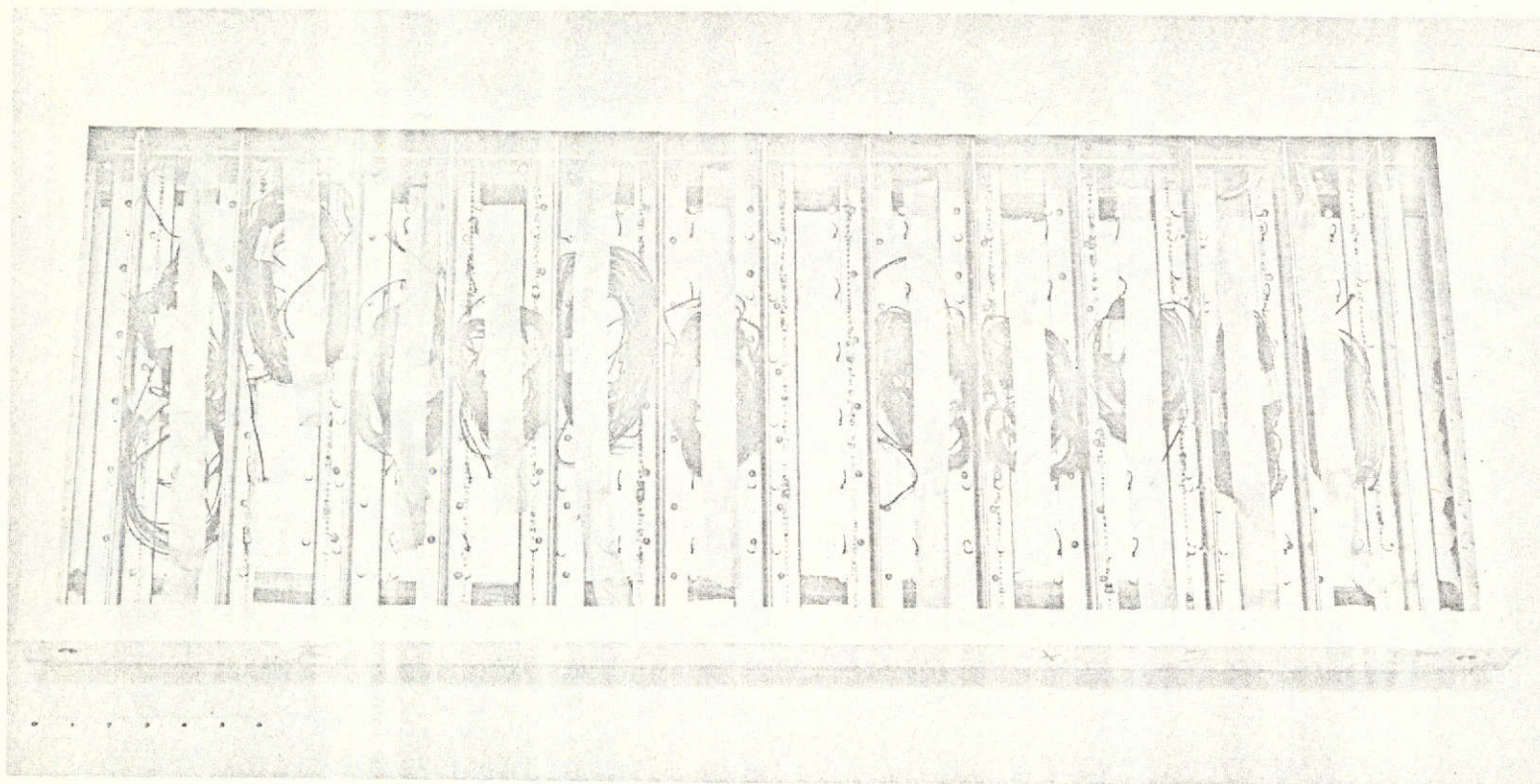


Figure 4.3 BOTTOM VIEW OF SUBSTRUCTURE PANEL

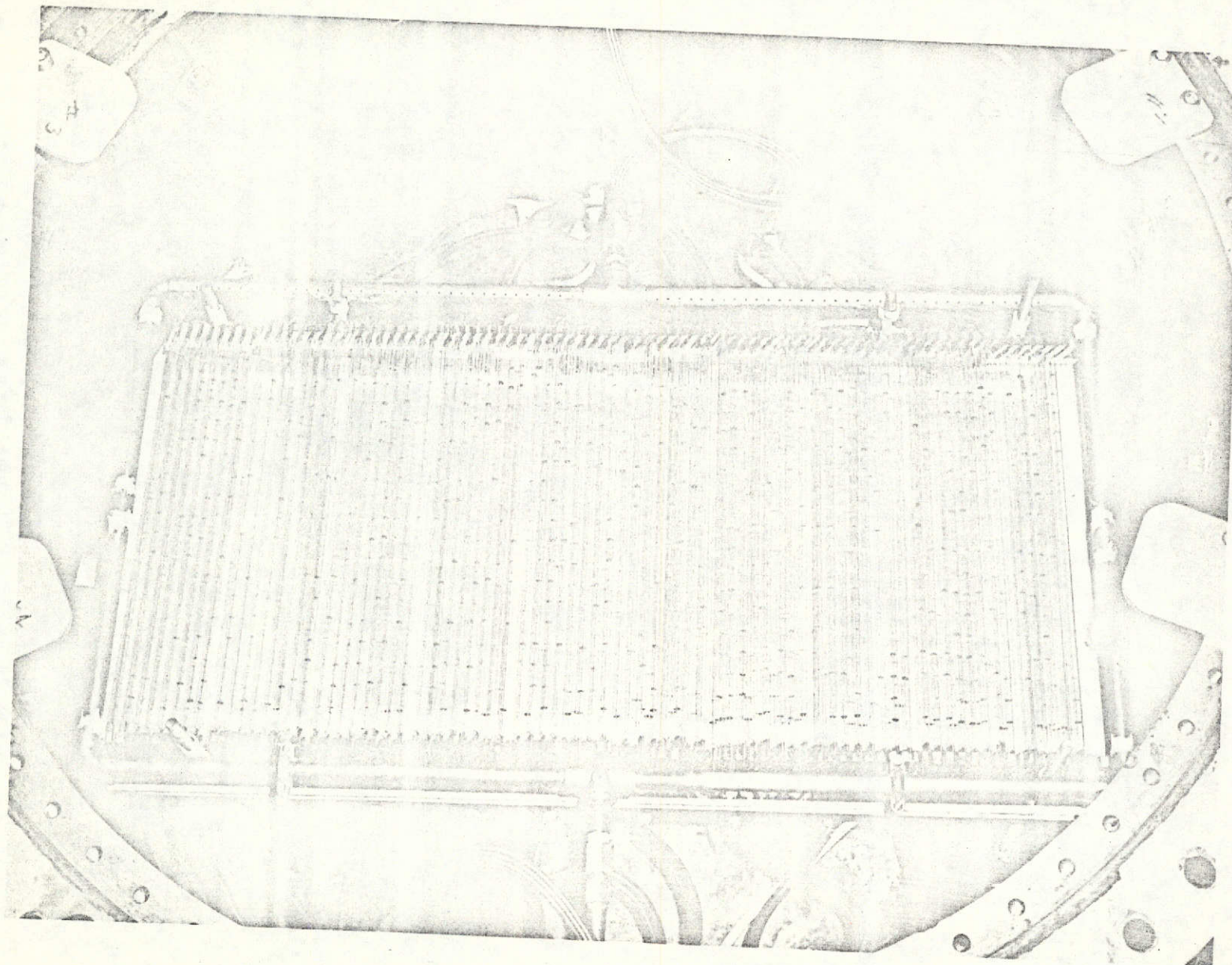


Figure 4.4 CHAMBER AND RADIANT HEATER FOR THERMAL CYCLING TEST

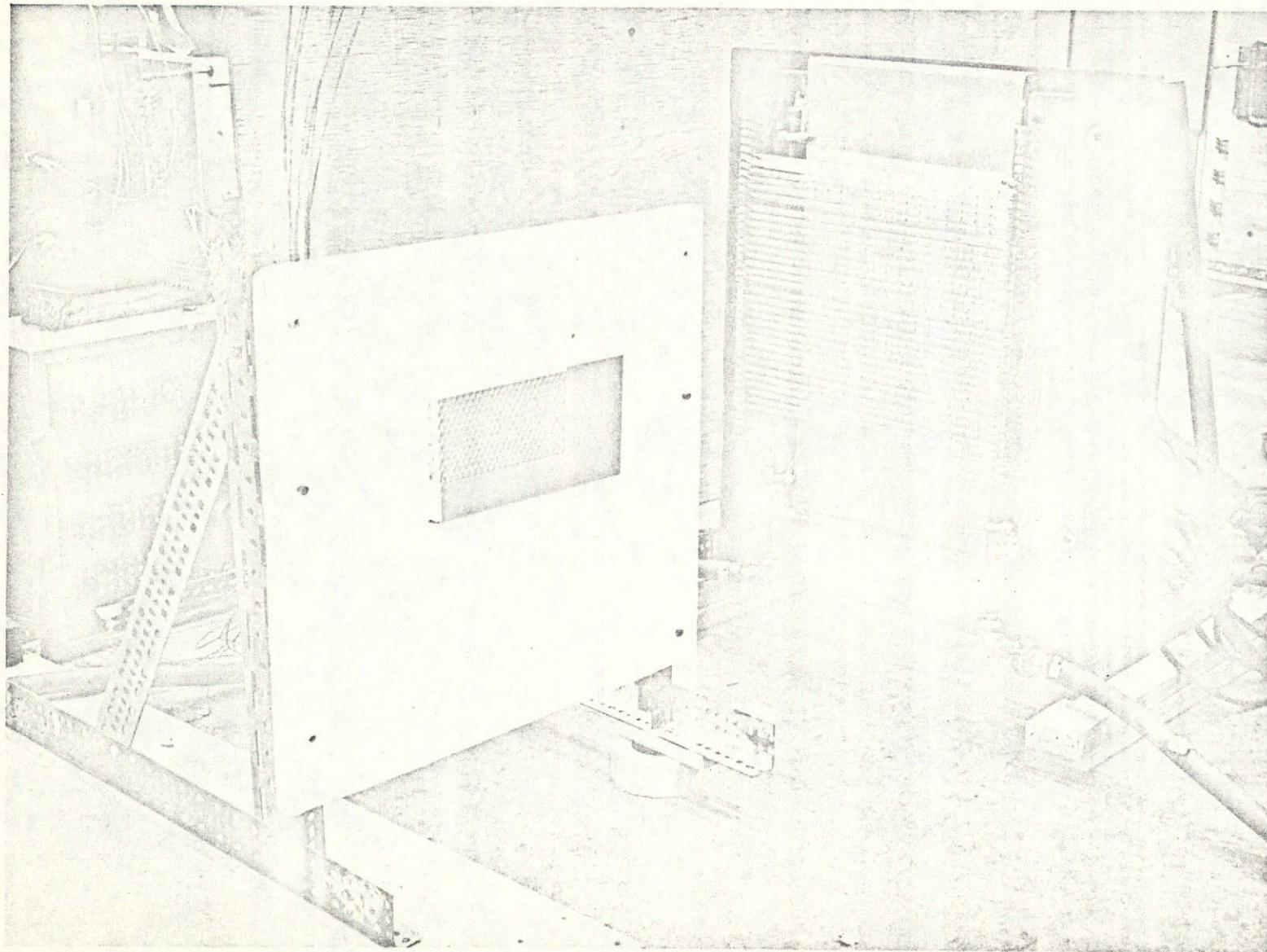


Figure 4.5 ROOM-AMBIENT HEATER FACILITY

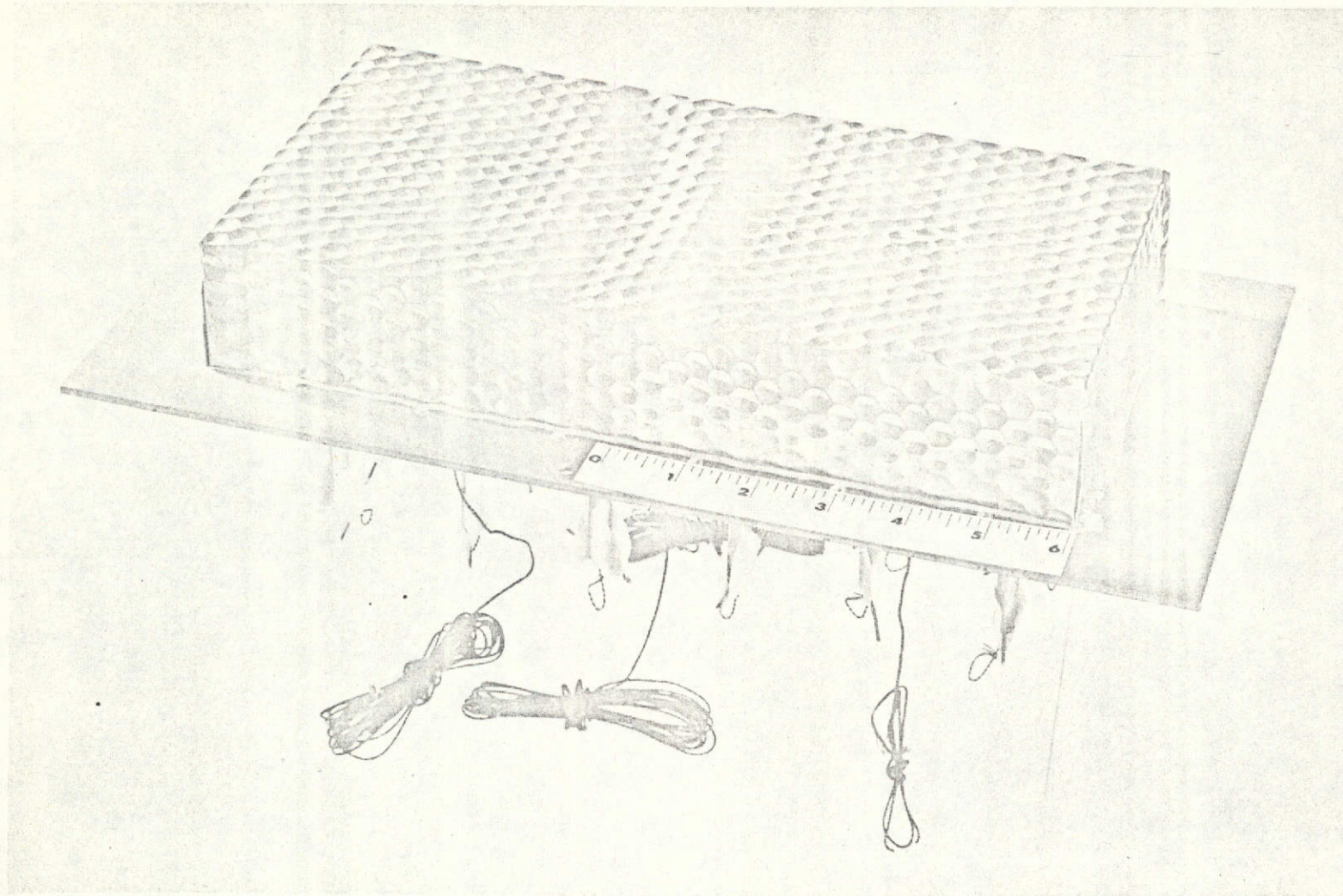


Figure 4.6 3-mil HASTELLOY-X, 6 LB/FT³, ONE CYCLE TO 1800° F (SPECIMEN 3)

atmospheric air would have been an overly severe oxidizing environment for the foil, considering the large number of thermal cycles planned. Operation of the facility in nitrogen at atmospheric pressure was required to prevent arcing and to provide adequate cooling to the lamps.

Figure 4.7 illustrates the test panel after the first heating cycle. The maximum surface temperature was 1750° F. All the specimens basically exhibited the same type of surface buckling on the top of the panel. Cracking failures occurred in the 3-mil Hastelloy-X specimen and in two of the 5-mil Haynes 25 specimens. (This was the second cycle for the 3-mil Hastelloy-X specimen.) These cracks were located at the upper (hot) edge between the top and side panels, near the center of the span (Figure 4.8). This edge appeared to have suffered local compressive crippling; the cracks were located in the crippled region. Figure 4.9 illustrates a typical crack failure.

At this point in the test program, it was apparent that the simple textured box design was inadequate for 1800° F service. Foil compression within the texture pattern was not sufficient to accommodate the thermal strain without local permanent deformation and resulting cracking. However, the simplicity of the configuration was sufficiently attractive to warrant evaluation at reduced temperature to define the level at which the crippling problem disappeared.

Two new specimens were fabricated for testing at reduced temperature levels. Specimen 8 was identical to the reference configuration (Specimens 1 and 2). Specimen 7 was made in two pieces with a "floating top" which was isolated from the untextured sides by a sliding joint detailed in Figure 4.10. The top of the specimen was 4-mil Hastelloy-X textured with the Oxford pattern. The sides were untextured 3-mil Hastelloy-X. Both specimens were mounted side by side on a 1 inch aluminum alloy panel for testing in the ambient environment heating fixture (Figure 4.11).

The two specimens were subjected to four thermal cycles with successively increasing peak surface temperatures at nominal levels of 1200°, 1400°, 1600°, and 1800° F. No permanent deformation of either specimen occurred at 1200° F. However, the characteristic buckling pattern in the top surface of the simple textured box (Specimen 8) was observed after the 1400° F exposure. The buckling was not apparent during heating but appeared to develop during cool down after the lamp exposure was terminated. Further cycling to the 1600° and 1800° F levels did not significantly change the damage pattern observed after the 1400° F exposure (Figure 4.12).

The top surface of the "floating top" specimen remained flat through the 1600° F cycle. A slight deformation of the top surface was observed after the 1800° F cycle which appeared to be caused by interference with the severely deformed side panel. Both the sides and ends of this specimen were compressively crippled at intervals of one to two inches (Figures 4.13 and 4.14). It was concluded that isolating the top from the side panels by a sliding joint was effective in preventing top surface buckling at the 1800° F level. It was also apparent that the untextured sides of the floating top specimen were much more susceptible to buckling than were the sides of the simple textured box specimens.

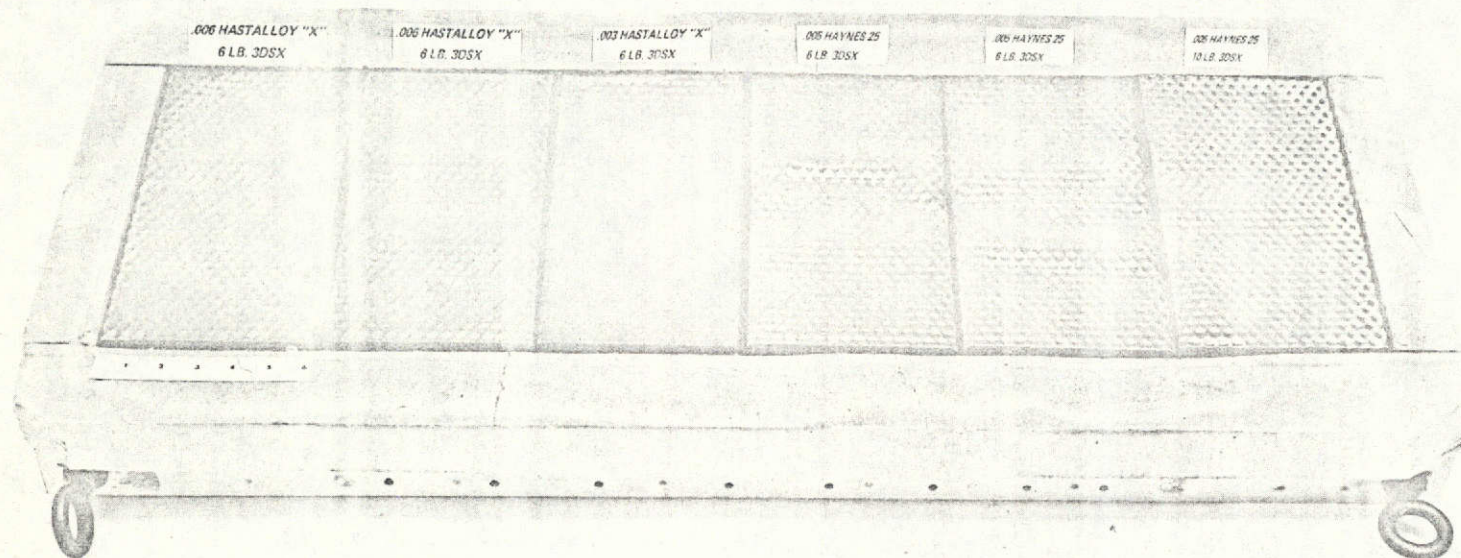
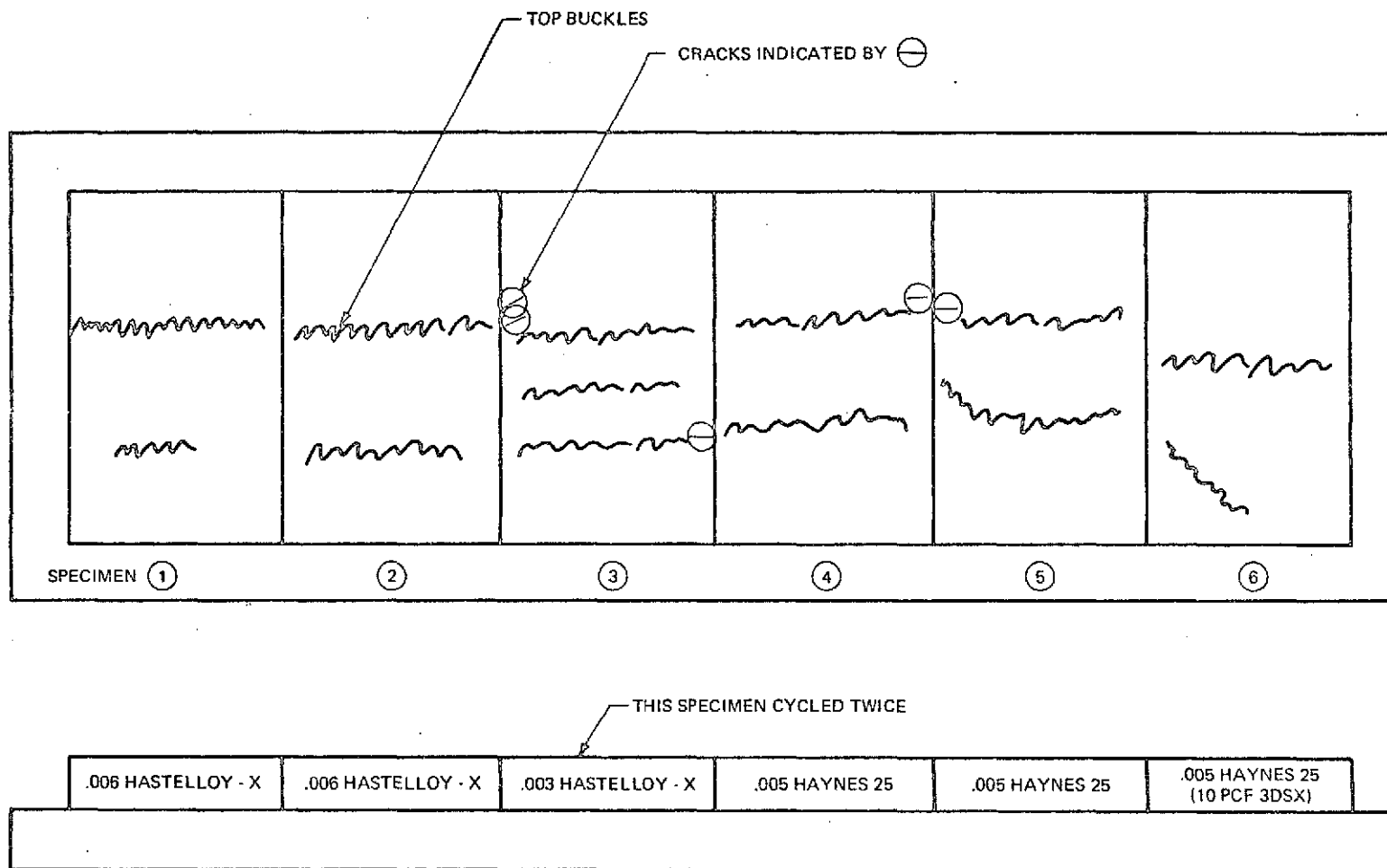


Figure 4.7 POST TEST CONDITION OF PANEL AFTER ONE CYCLE TO 1800° F
(SPECIMEN 1 THROUGH 6)



83-1423

Figure 4.8 DAMAGE MAP OF PANEL AFTER ONE 1800° F THERMAL CYCLE

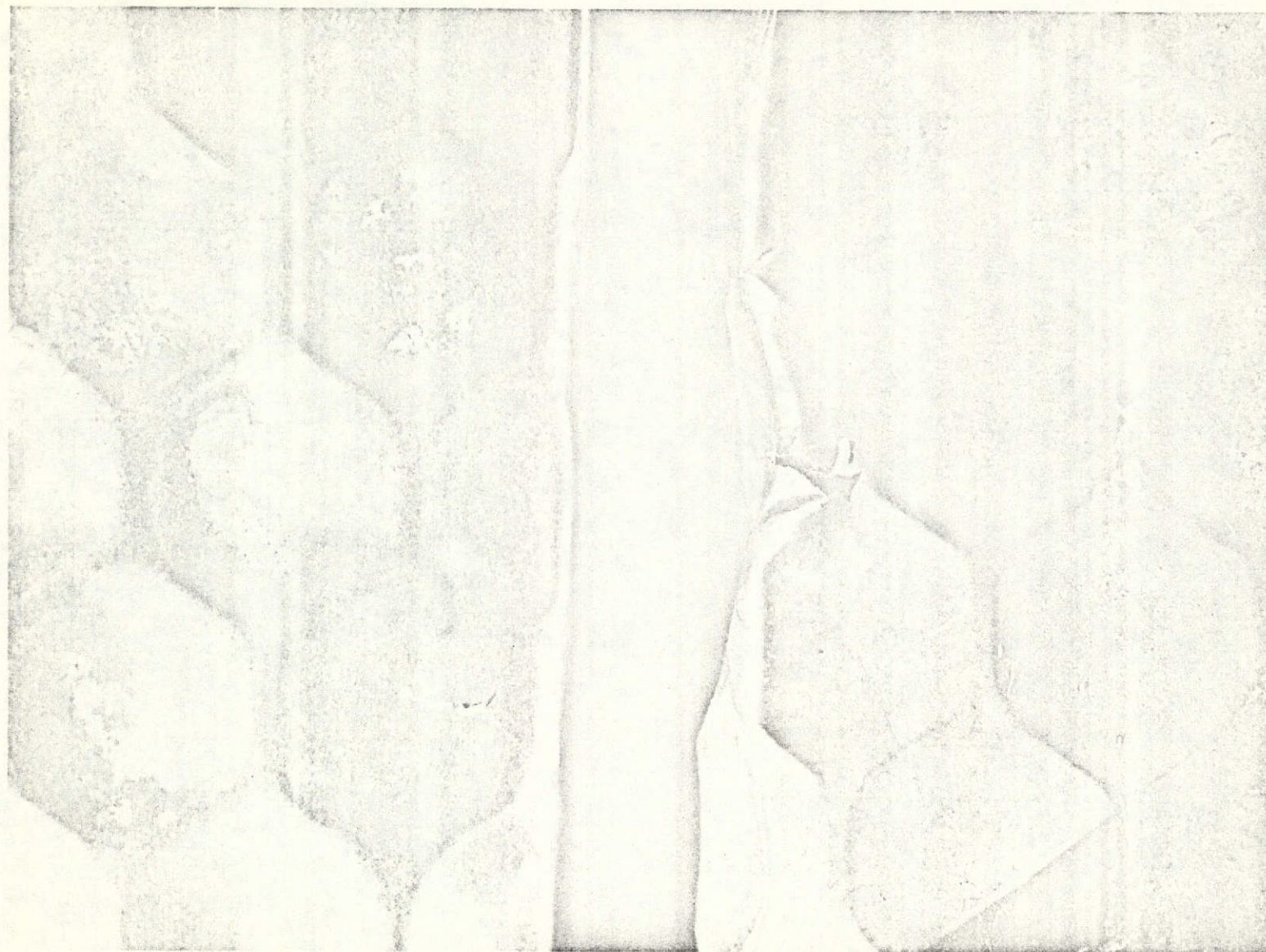


Figure 4.9 DETAIL OF EDGE CRACK IN 3-mil HASTELLOY-X AFTER SECOND CYCLE
TO 1800° F (SPECIMEN 3)

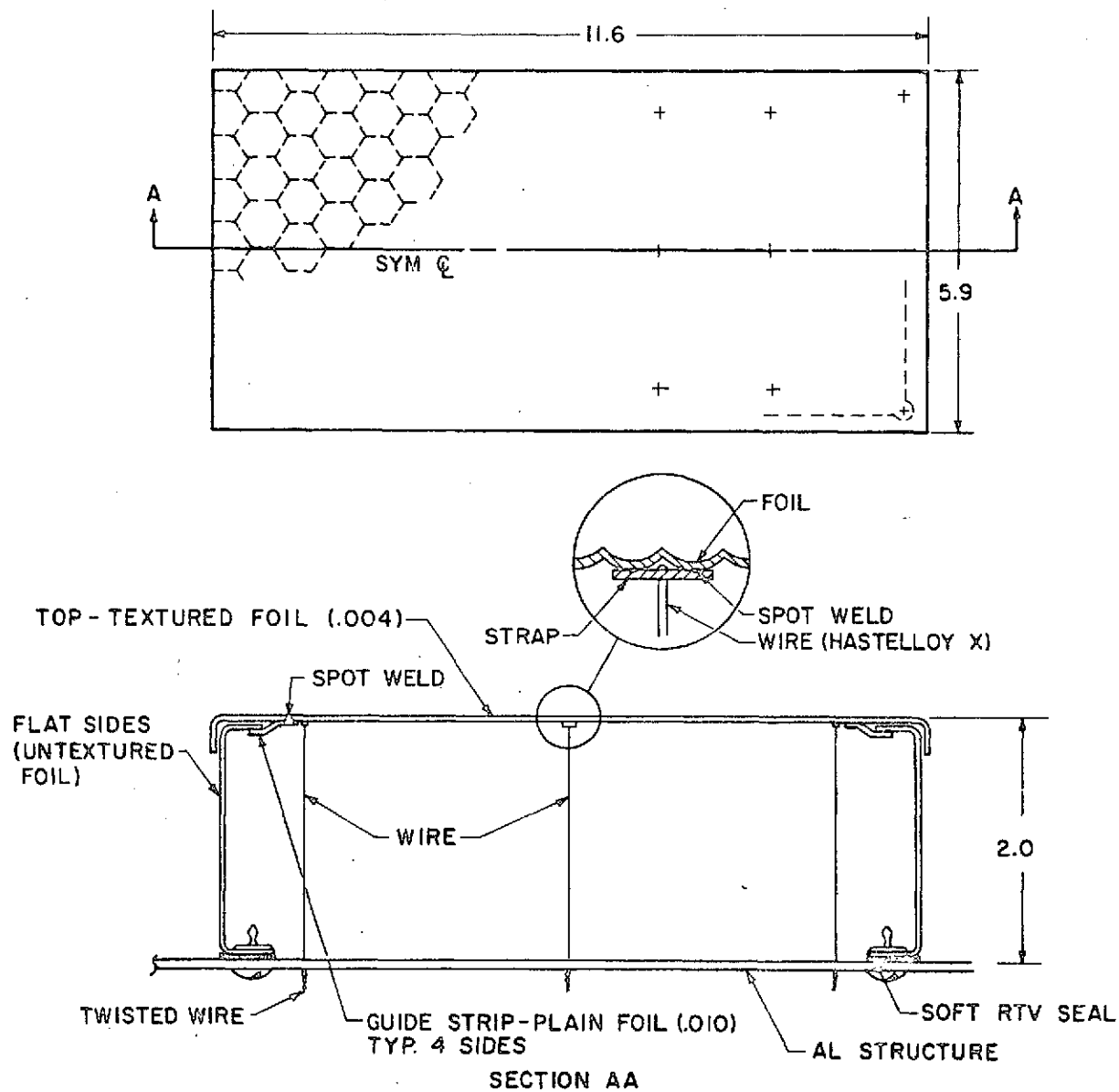


Figure 4.10 DETAIL OF FLOATING TOP SPECIMEN DESIGN (SPECIMEN 7)

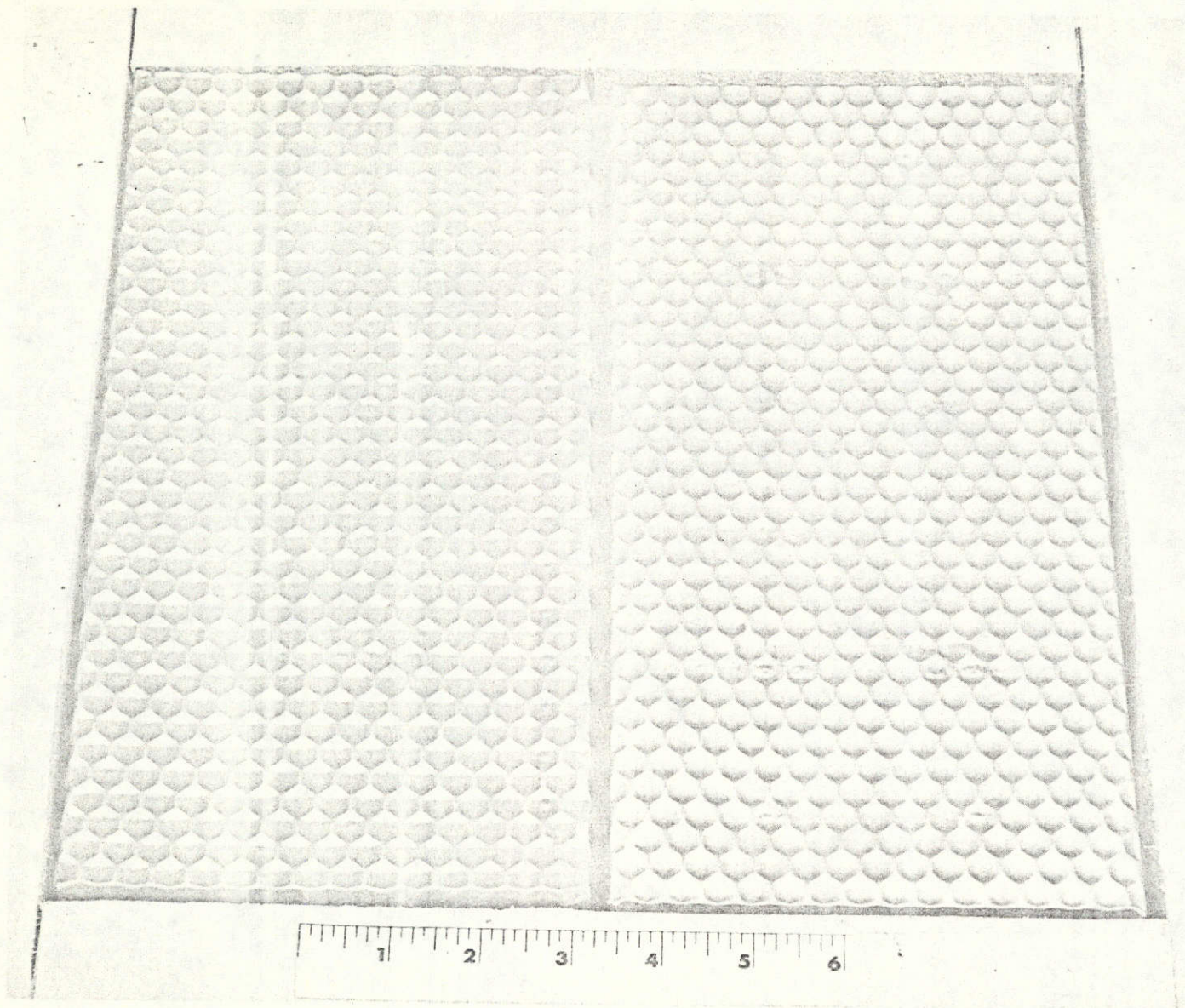


Figure 4.11 PRETEST APPEARANCE OF FLOATING TOP SPECIMEN AND REFERENCE SPECIMEN
(SPECIMENS 7 AND 8)

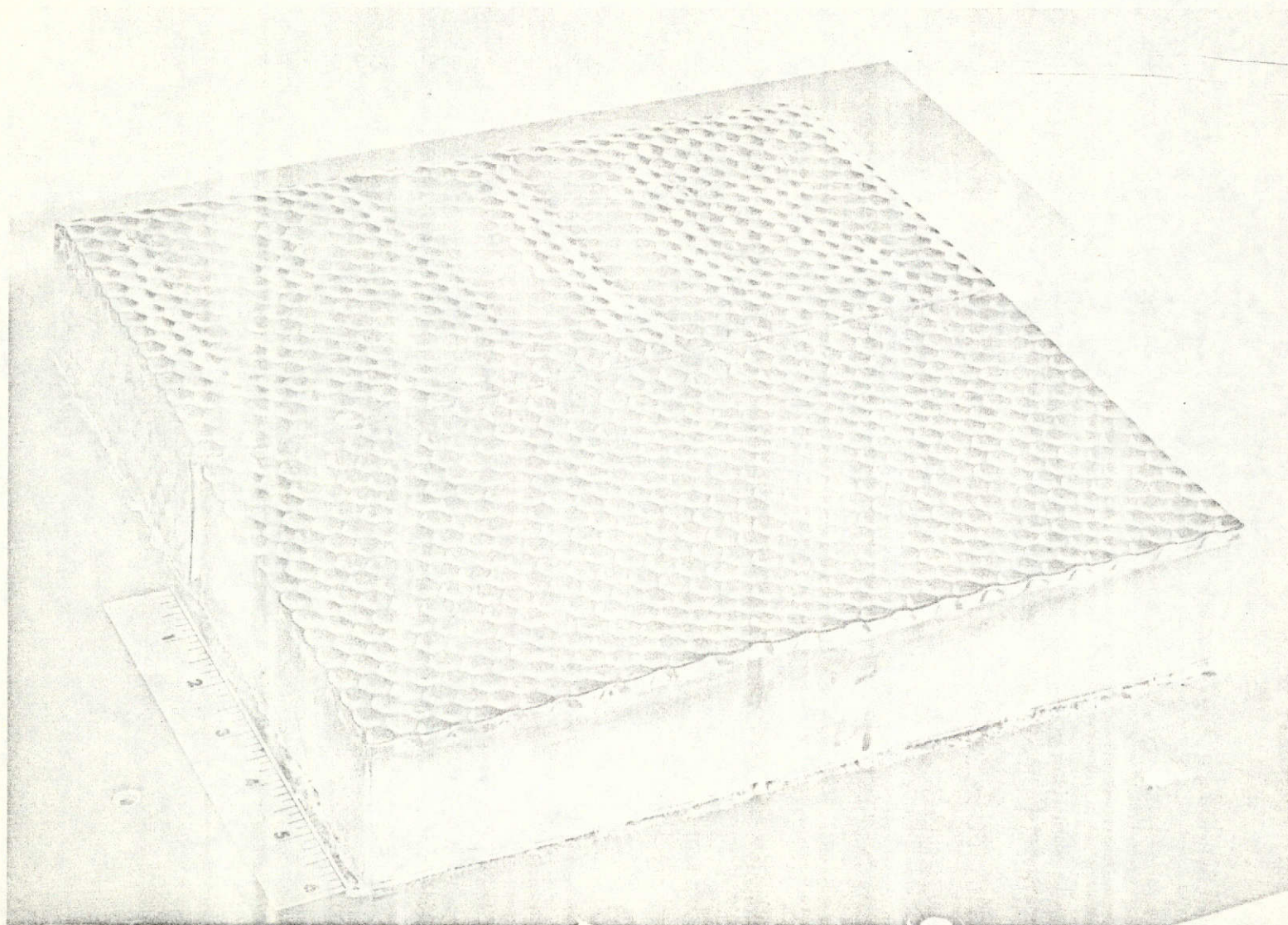


Figure 4.12 POST TEST APPEARANCE OF FLOATING TOP AND REFERENCE SPECIMENS
AFTER FOUR THERMAL CYCLES (1200°, 1400°, 1600°, 1800° F)
(SPECIMENS 7 AND 8)

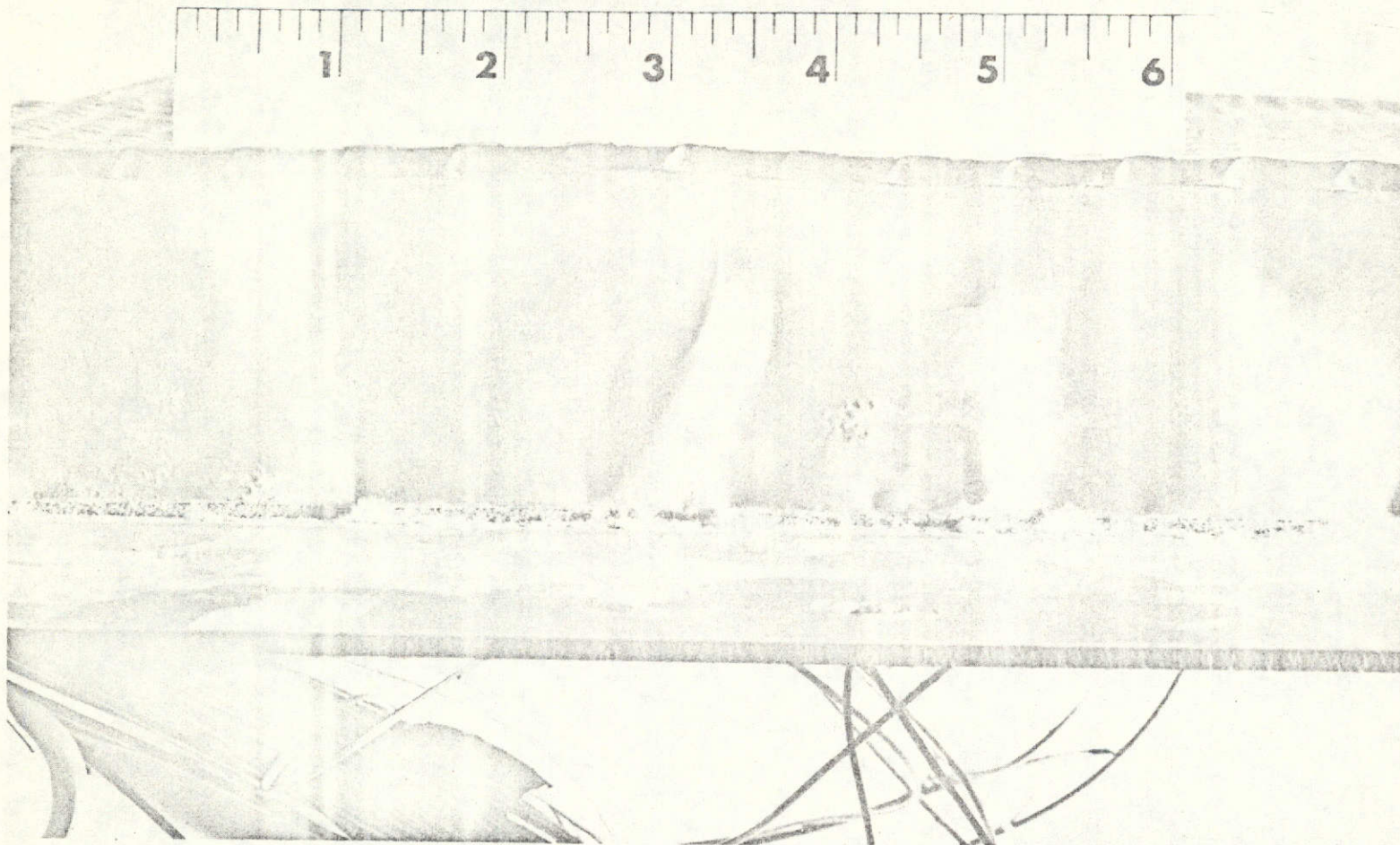


Figure 4.13 COMPRESSIVE CRIPPLING OF SIDE OF FLOATING TOP SPECIMEN
(SPECIMEN 7)

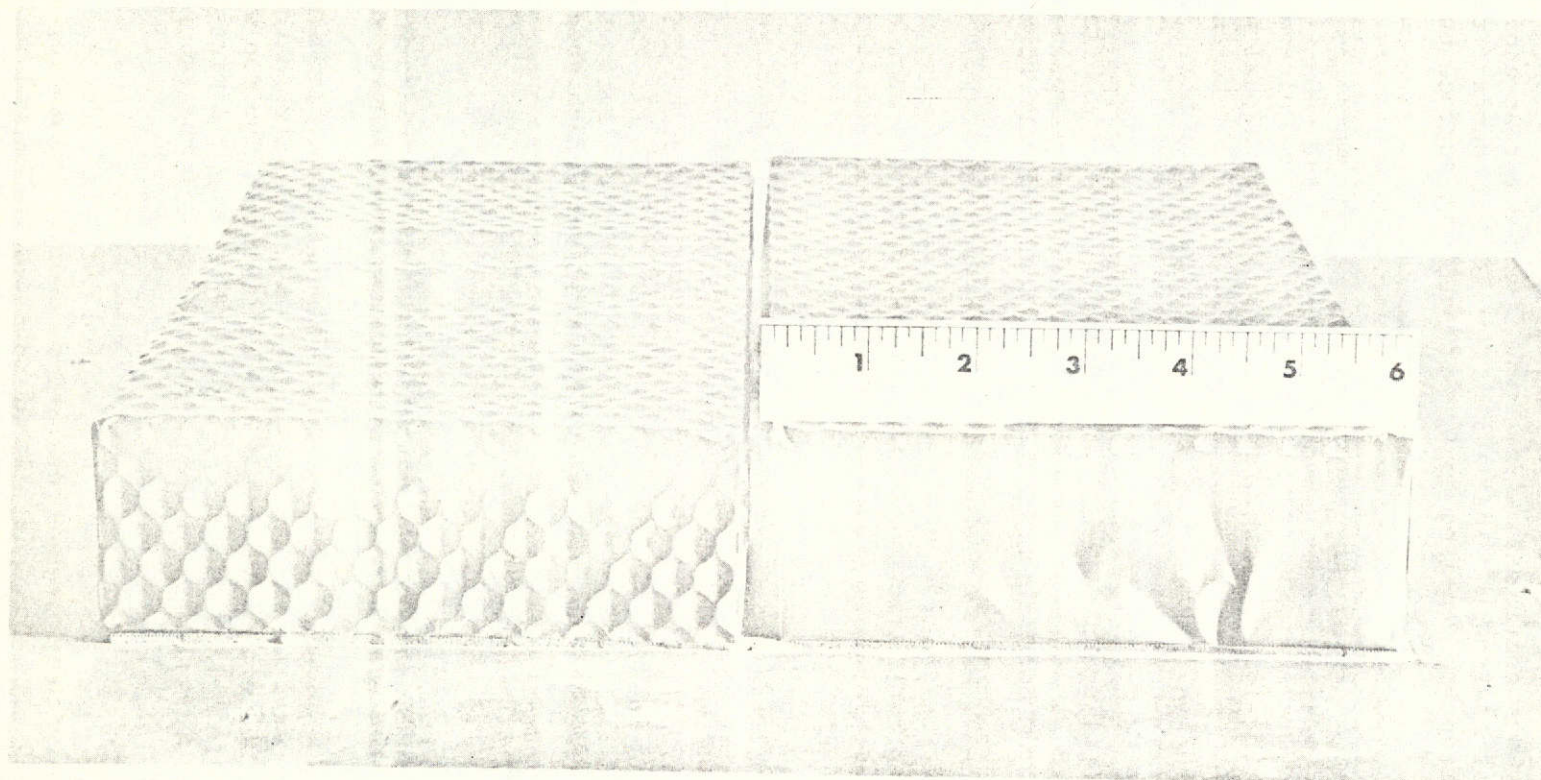


Figure 4.14 END VIEW OF SPECIMENS 7 AND 8 SHOWING COMPRESSIVE
CRIPPLING OF SPECIMEN 7

Thermal testing was continued on Specimens 7 and 8 for an additional ten cycles in the ambient environment test fixture at 1800° F surface temperature with no further degradation becoming apparent beyond the surface buckling noted after the initial test series at four temperature levels (Figure 4.15).

Further evidence of the effectiveness of the texturing for alleviating the thermal strains may be deduced from the behavior of the ends of the sample textured box. As discussed in Section 3.3, the effective modulus of the textured foil is lower for loading across the flats of the hexagonal pattern. For the simple textured box specimens, the orientation of the texture pattern on the ends is necessarily opposite that on the sides of the box. The "flats" of the texture pattern run vertical on the ends and horizontal in the sides. It would appear that the texture pattern should elongate more freely when exposed to loading applied in a direction perpendicular to the "flats". Because the sides of the textured box consistently suffered crippling during the thermal tests while the ends did not, it appears that the more favorable pattern orientation was indeed on the ends.

As discussed in Section 3.3, the temperature gradient in the sides and ends tends to develop tensile stresses near the bottom which must be balanced by compressive stresses near the top. These stresses are sufficient to cause compressive crippling near the upper edge of the box. The design problem appeared to be that of increasing the compressive stability of the top edge and/or decreasing the apparent elastic modulus in the side panel to reduce the compressive load at the edge.

Accordingly, three specimens were fabricated incorporating different methods for relieving the crippling problem (Figure 4.16). All three designs included an angle bracket welded into the top (hot surface) perimeter of the specimen to improve the buckling stability of this edge. Each specimen utilized a different method to flexibilize the side panels and limit the compressive load in the stiffened edge to a manageable level.

Specimen 9 re-oriented the texture pattern to provide maximum flexibility of the sides of the box in the direction parallel to the top surface. It was necessary to splice the ends of the box by welding the end to the top surface as shown in Figure 4.16.

Specimen 10 is detailed in Figure 4.17. It used untextured foil with a beaded pattern running vertically on the sides and ends. The top was stiffened with hat sections which also contained a rod to which the tie wires were attached. Figures 4.18 and 4.19 illustrate two stages in the fabrication of this design.

Specimen 11 had vertical slots incorporated into the sides and ends at three inch intervals with pleated covers welded over the slots for sealing. Figures 4.20 and 3.19 illustrate details of this design.

All three specimens were subjected to thermal exposure in the room ambient heating facility with peak surface temperatures of nominally 1800° F. All three designs successfully eliminated the edge and side crippling problems

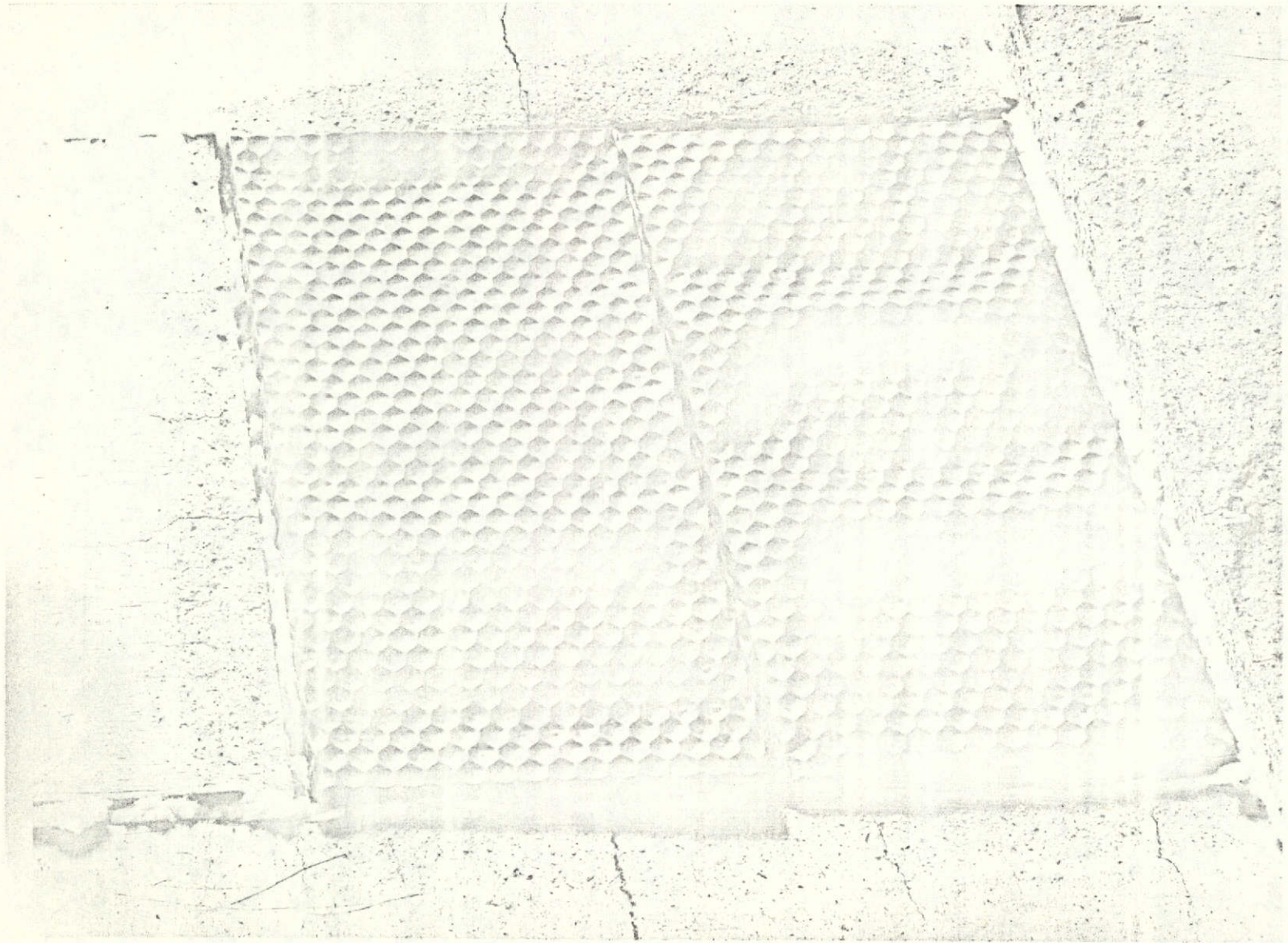
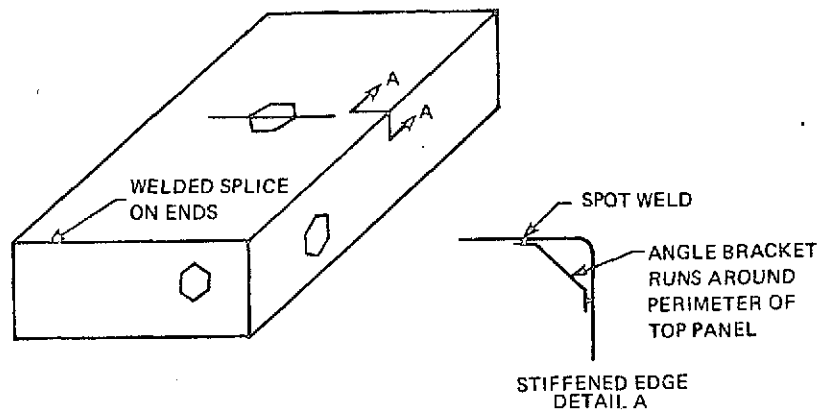
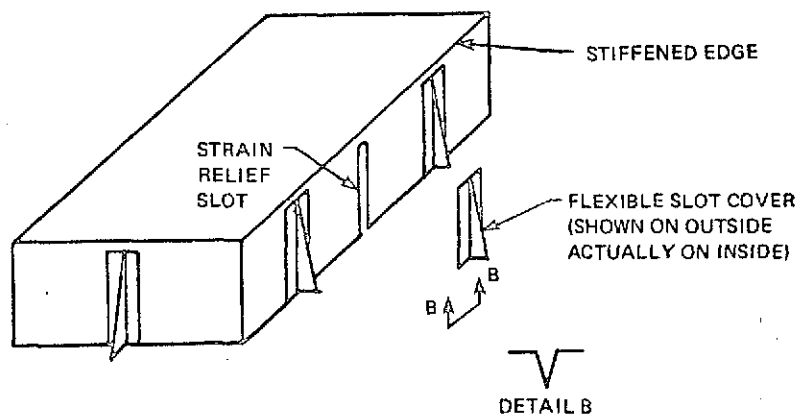


Figure 4.15 POCT TEST APPEARANCE OF FLOATING TOP AND REFERENCE SPECIMENS
AFTER TEN THERMAL CYCLES TO 1800° F (SPECIMENS 7 AND 8)

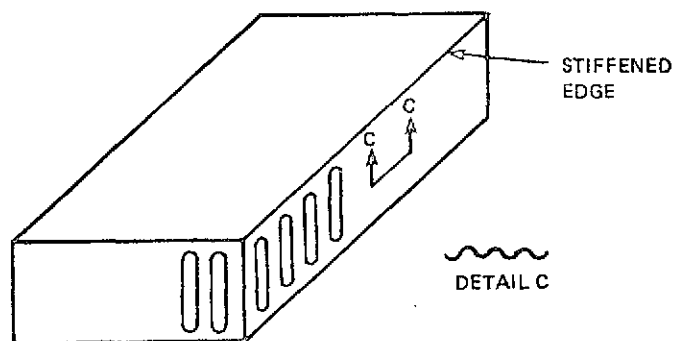
SPECIMEN 9
TEXTURE PATTERN
ORIENTED FOR
MINIMUM SIDE
STIFFNESS



SPECIMEN 11
PLEATED SIDE
CONFIGURATION

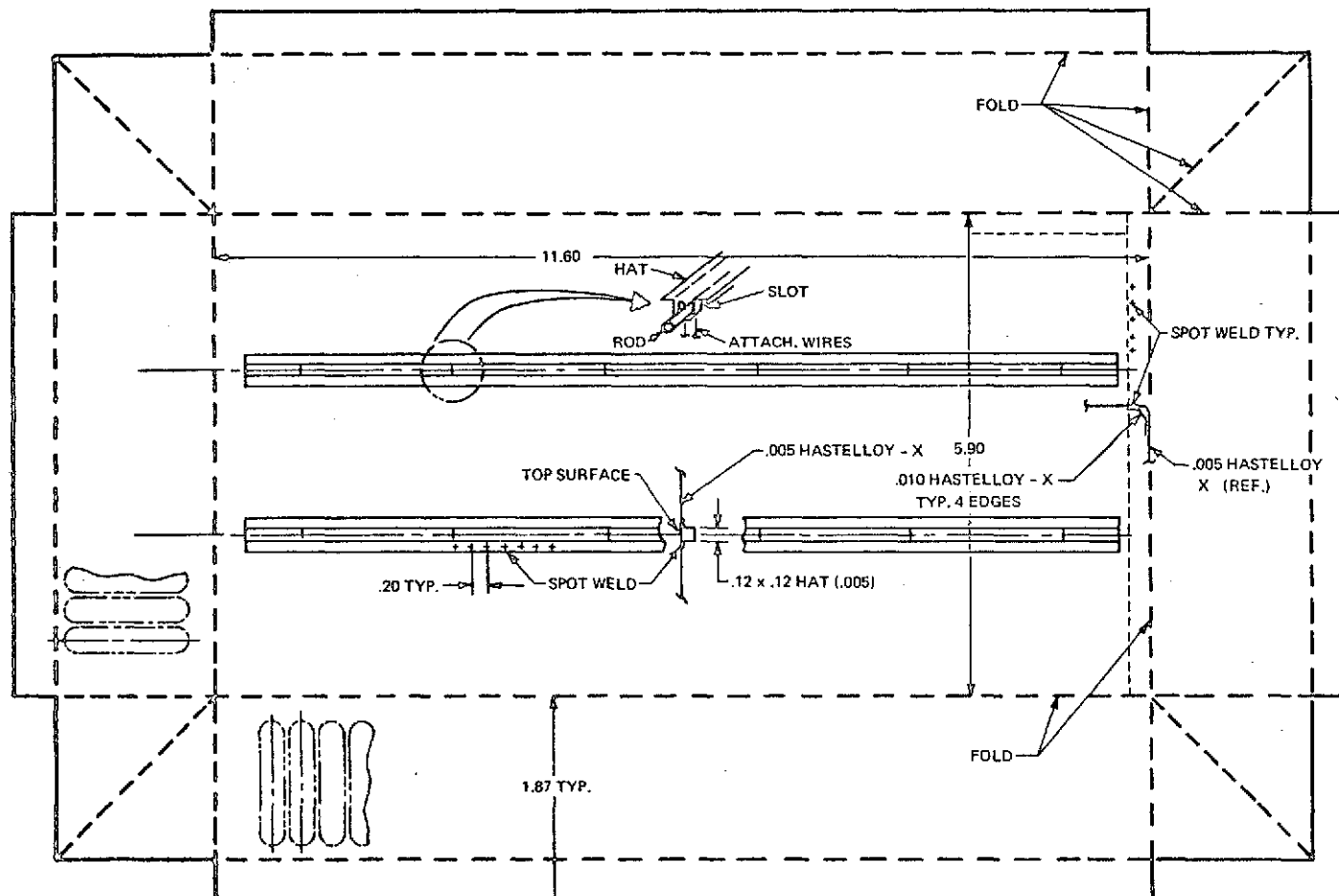


SPECIMEN 10
BEADED SIDE
CONFIGURATION



83-1424

Figure 4.16 MODIFIED CONFIGURATIONS WITH STIFFENED EDGES AND FLEXIBLE SIDES



83-1425

Figure 4.17 DETAIL OF BEADED DESIGN (SPECIMEN 10)

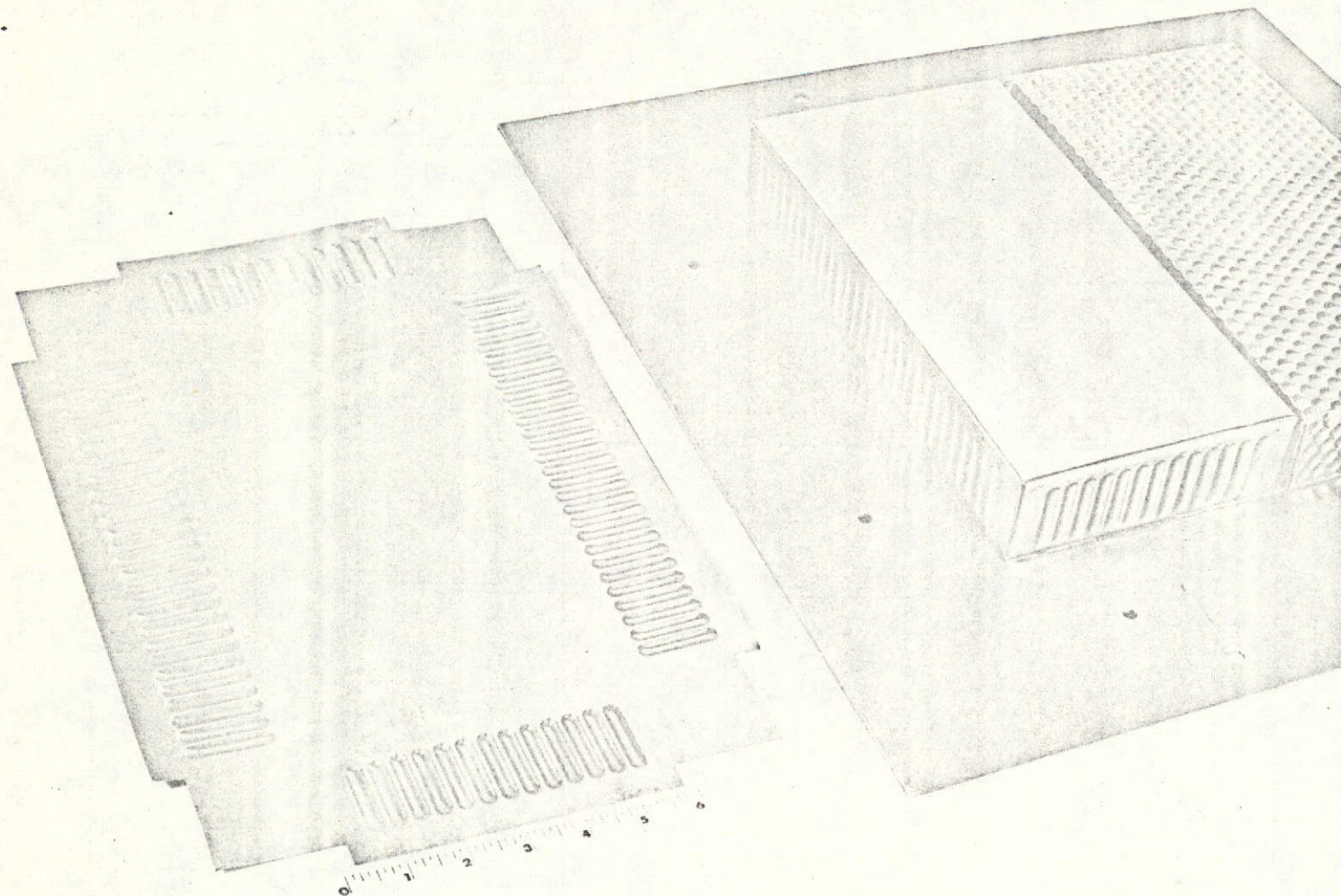


Figure 4.18 BEADED DESIGN FLAT LAYOUT AND FINISHED SPECIMEN
(SPECIMEN 10)

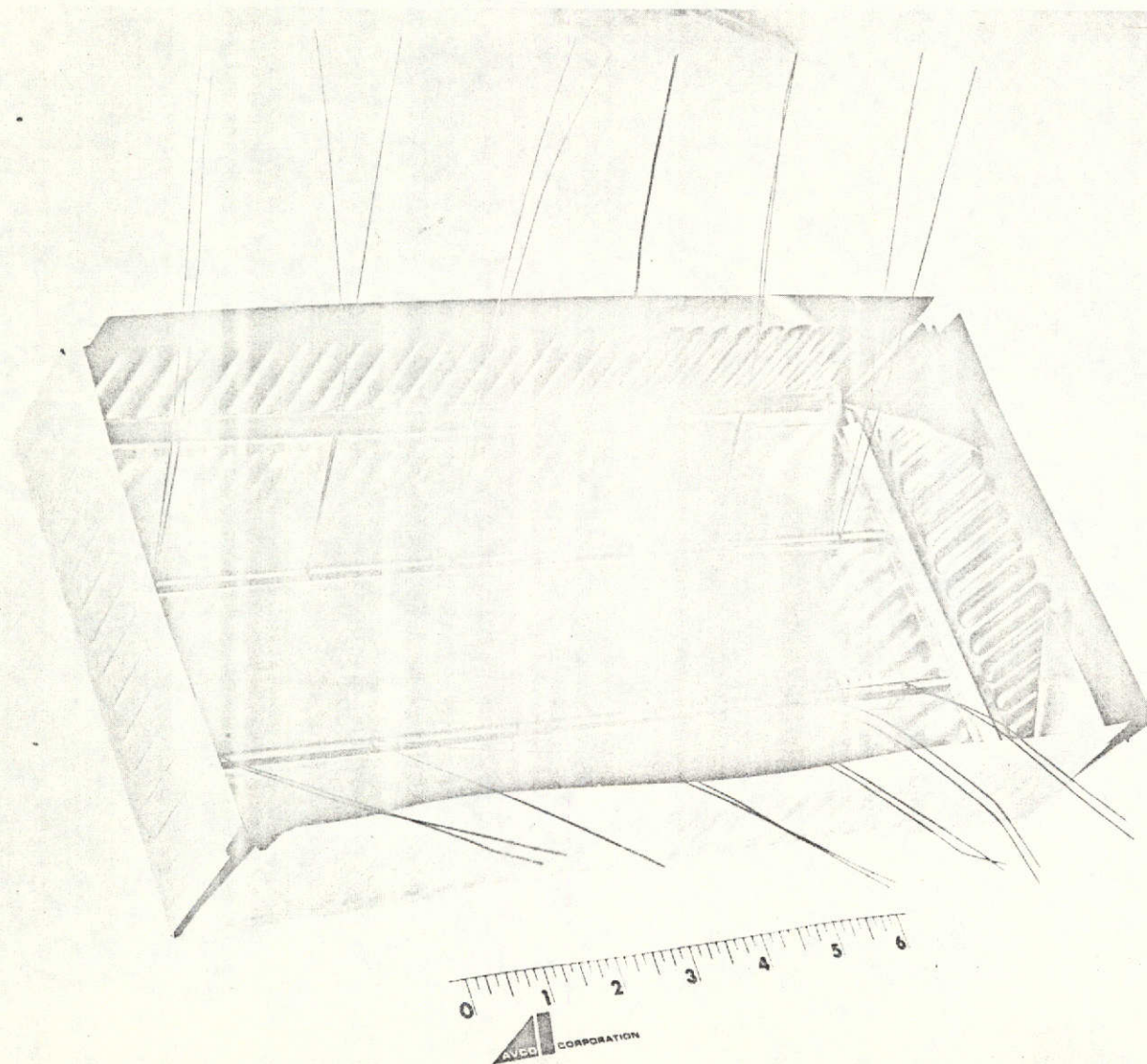


Figure 4.19 BEADED DESIGN PRIOR TO INSTALLATION OF 3DSX INSULATION
(SPECIMEN 10)

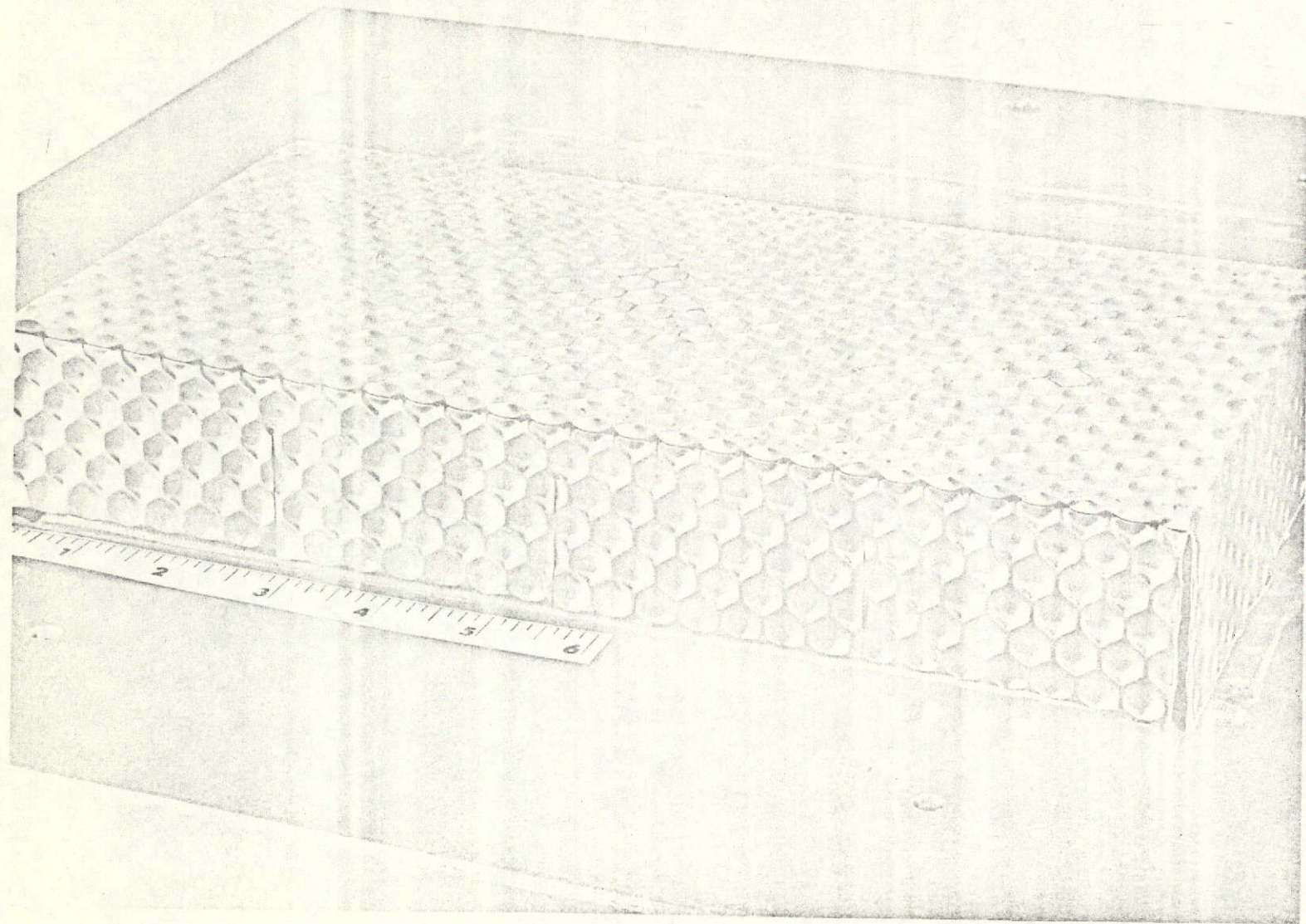


Figure 4.20 PLEATED SIDE DESIGN (SPECIMEN 11)

experienced in thermal testing of the earlier textured box specimens, however, all three specimens still experienced non-catastrophic buckling (not crippling) of the top surface after the first thermal cycle. Specimens 9 and 10 were exposed to ten thermal cycles to 1800° F with no further degradation being apparent (Figure 4.21). Specimen 11 was accidentally exposed to a transient overheat pulse in excess of 2300° F which caused incipient melt of the top surface. Therefore, testing of this specimen was terminated after one thermal cycle.

A "third-generation" set of two specimens was fabricated which were designed to eliminate the top buckling problem (Specimens 12 and 13). Specimen 12 (Figures 4.22 and 4.23) has a textured floating top similar to Specimen 7, but with beaded sides and a stiffened upper edge similar to Specimen 10.

Specimen 13 is a "tension-top" design which is basically similar to Specimen 10 except the top edge stiffeners are installed on the outside of the box rather than inside (Figures 4.24 and 4.25). As discussed in Section 3.3, the thermal stress loading of the internally stiffened edges of Specimens 9 through 12 is such to cause bending of the triangular cross section edge member toward the interior of the box. This loads the top panel compressively causing buckling. By placing the edge stiffener on the outside of the box the thermal loading tends to bend the edge member outward thus applying a tensile stress to the top panel.

Specimens 12 and 13 were subjected to a single thermal cycle to 1800° F. Post-test photos are shown in Figures 4.26 and 4.27. The thermo-structural behavior of both specimens was much superior to the previous designs. The sides and ends of both specimens were completely free of crippling and bending. The floating top of Specimen 12 remained flat and free of buckles. The tension top of Specimen 13 had some slight shear buckles which propagated into the stiffening beads causing several small local buckles in the beads. However, the specimen proved the general concept that the thermal environment can be used to tension the top surface and prevent the relatively large top surface buckling deformations observed in the earlier box specimens. The floating top design apparently remains essentially stress-free in the thermal environment.

The 3DSX/foil specimens were instrumented with thermocouples welded to the foil and to the substructure at the locations indicated in Figure 4.28. The top surface thermocouples were used to monitor and control the input heating required to achieve the desired surface temperature history. Temperature gradients measured by the thermocouples attached to the foil sides were of interest because of their possible use in modeling the thermal stresses which resulted in the crippling failures observed in several of the designs. Back-face structure temperature response was monitored to evaluate any degradation of insulation performance with thermal cycling.

Figure 4.29 presents typical temperature response data obtained during the ten cycle reuse demonstration test of Specimen 7. A plot of predicted backface response is also presented for comparison. The apparently better than predicted performance as the structure temperature increased was due to poor

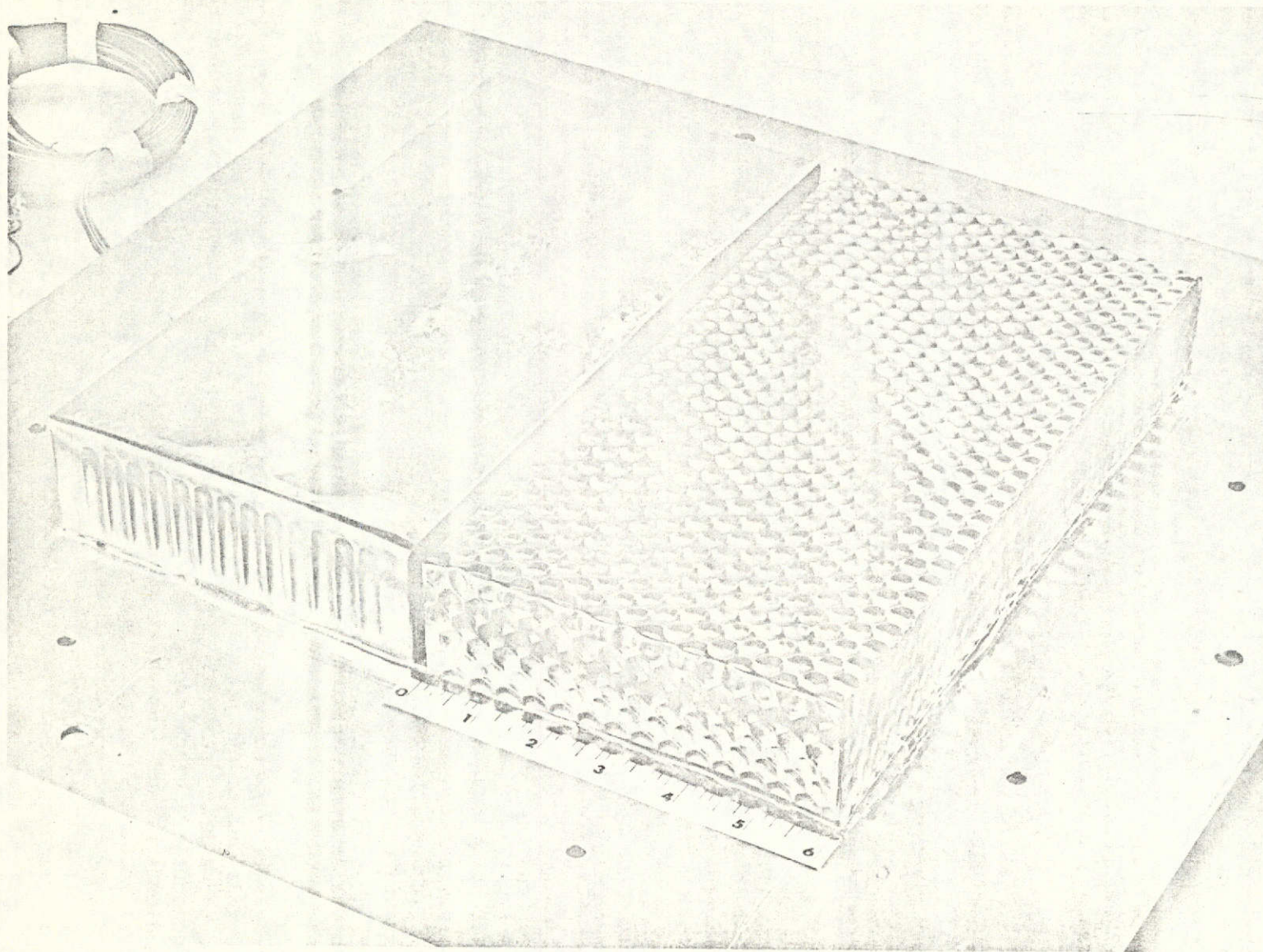
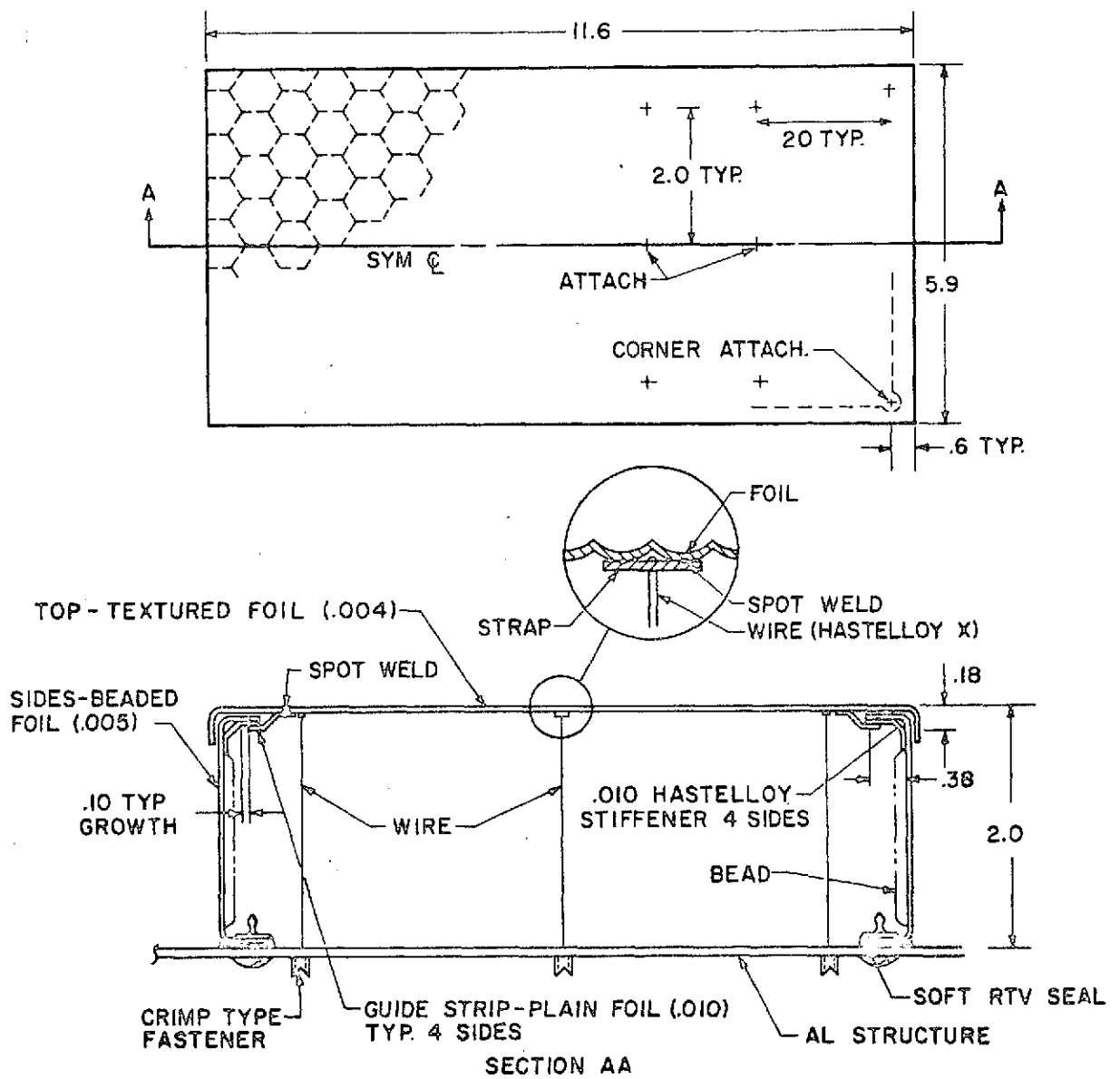


Figure 4.21 SPECIMENS 9 AND 10 AFTER TEN THERMAL CYCLES TO 1800° F



83-1267

Figure 4.22 DETAIL OF SECOND FLOATING TOP DESIGN (SPECIMEN 12)

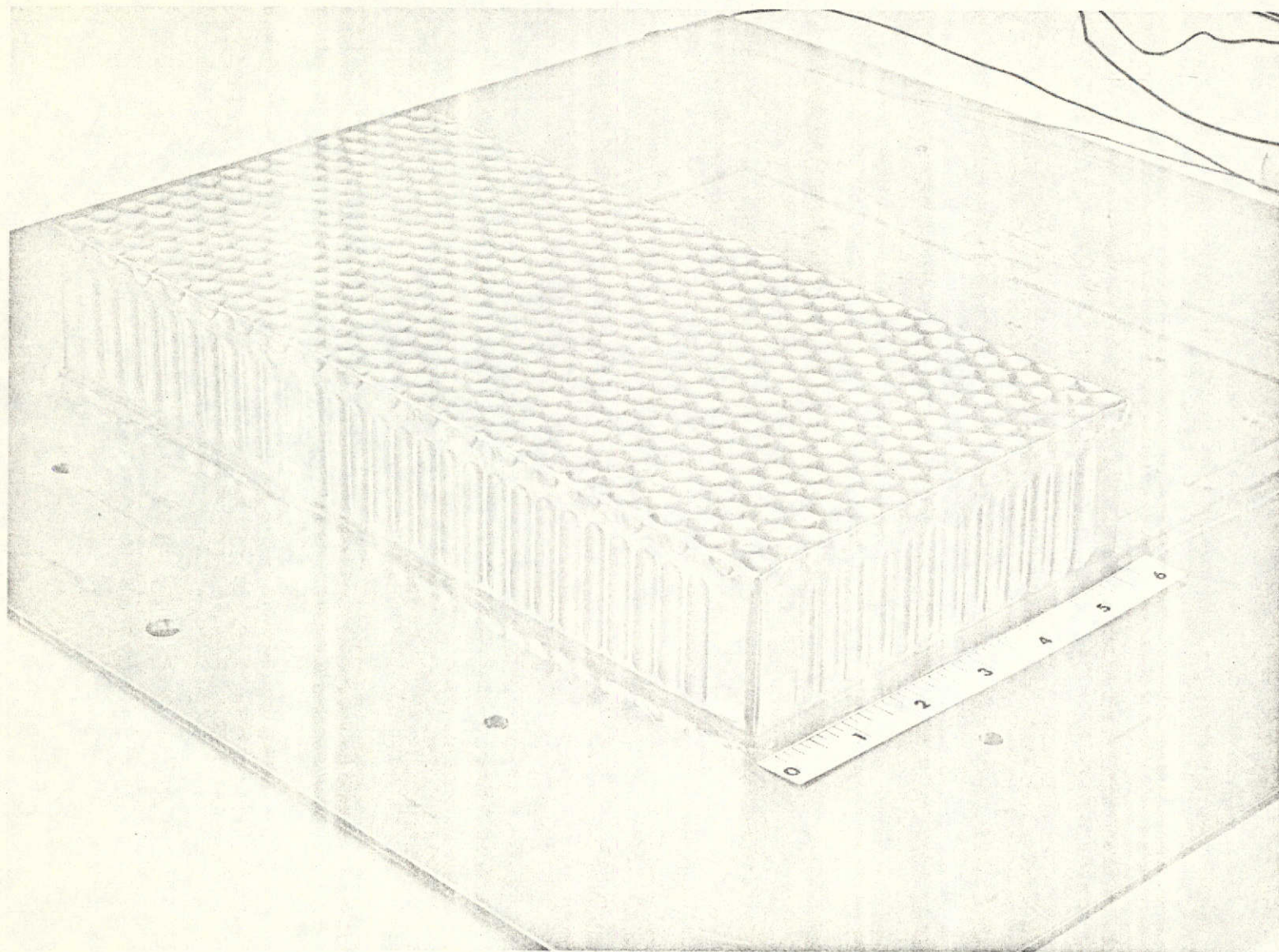
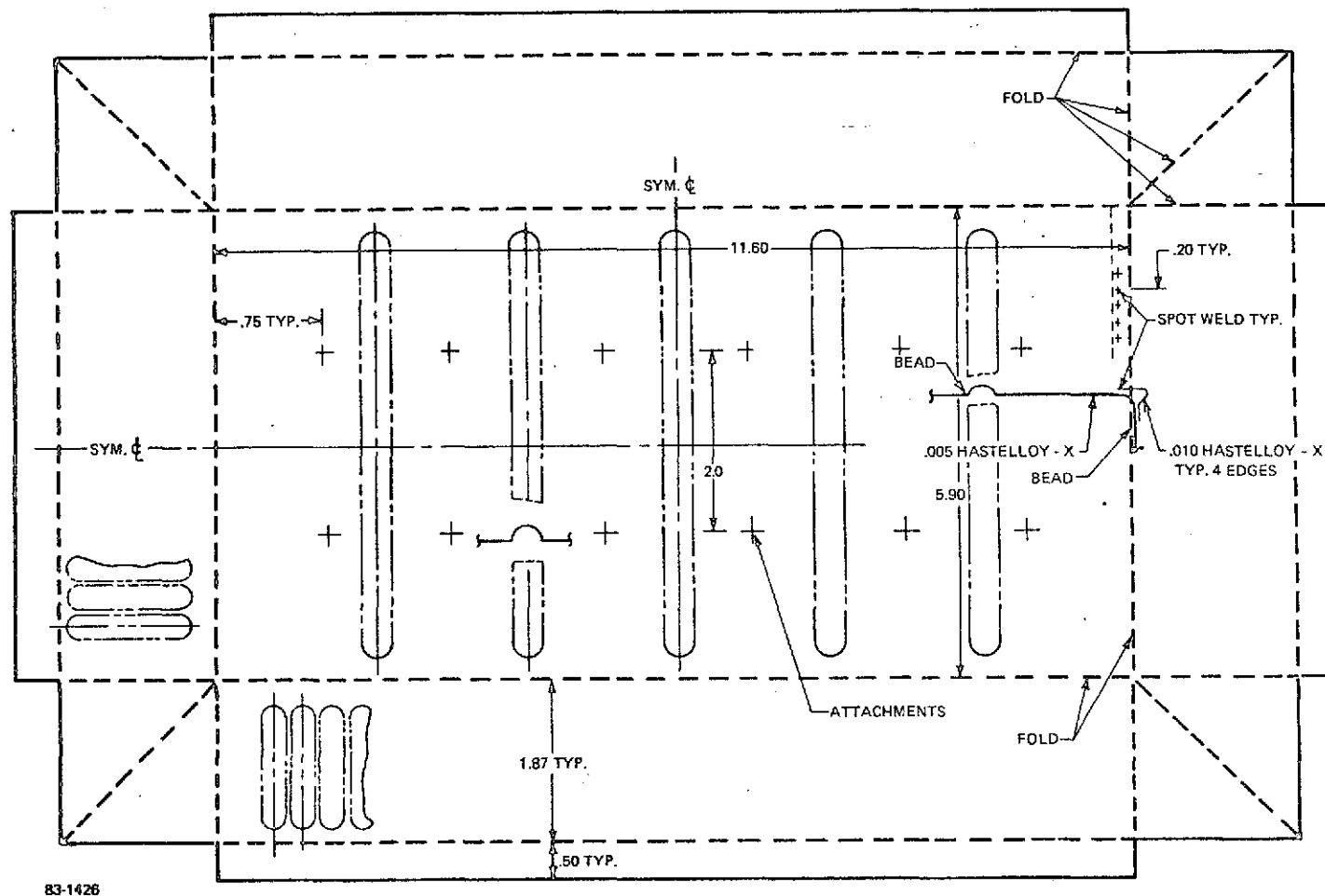


Figure 4.23 SECOND FLOATING TOP SPECIMEN (SPECIMEN 12)



83-1426

Figure 4.24 DETAIL OF TENSION TOP DESIGN (SPECIMEN 13)

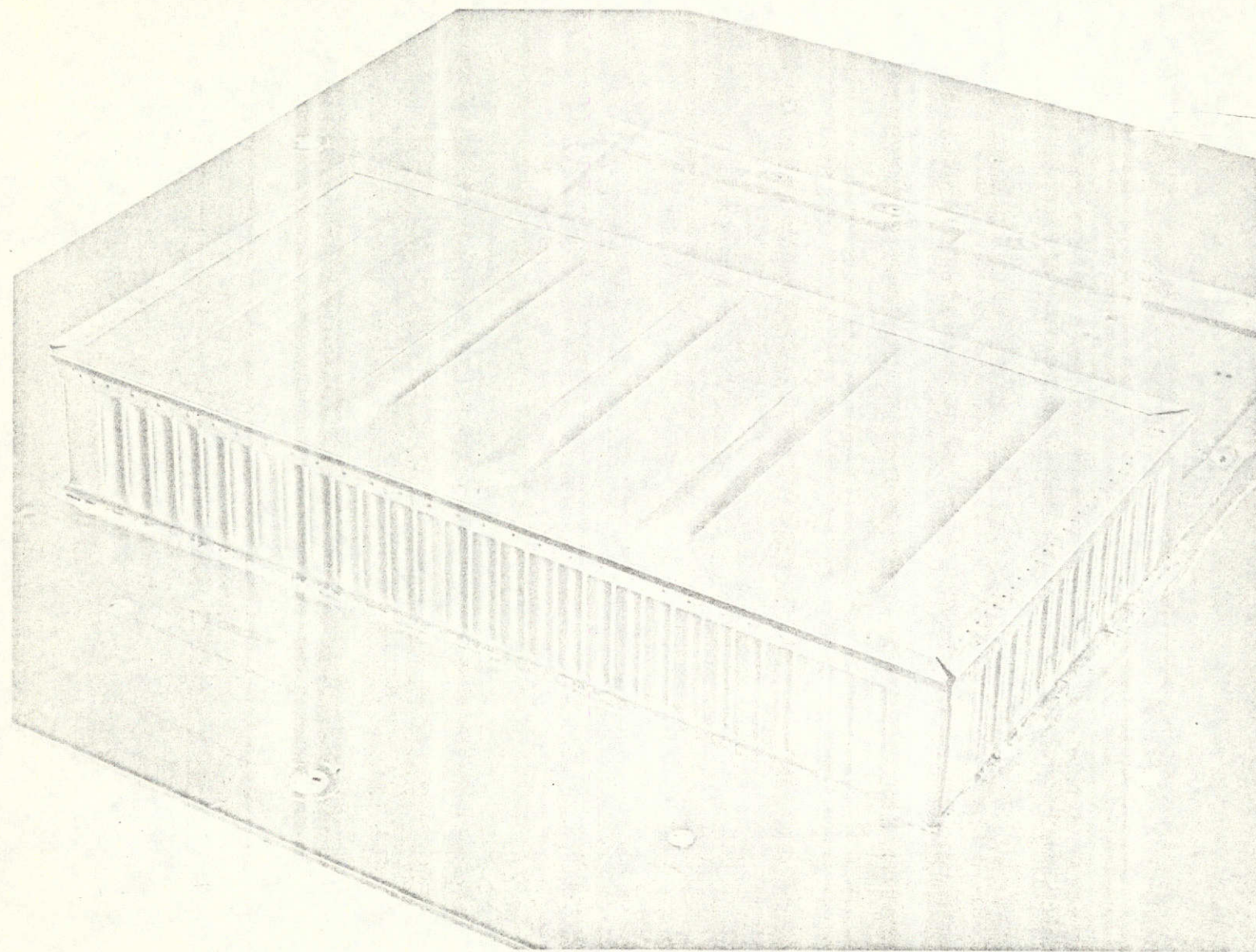


Figure 4.25 TENSION-TOP SPECIMEN (SPECIMEN 13)

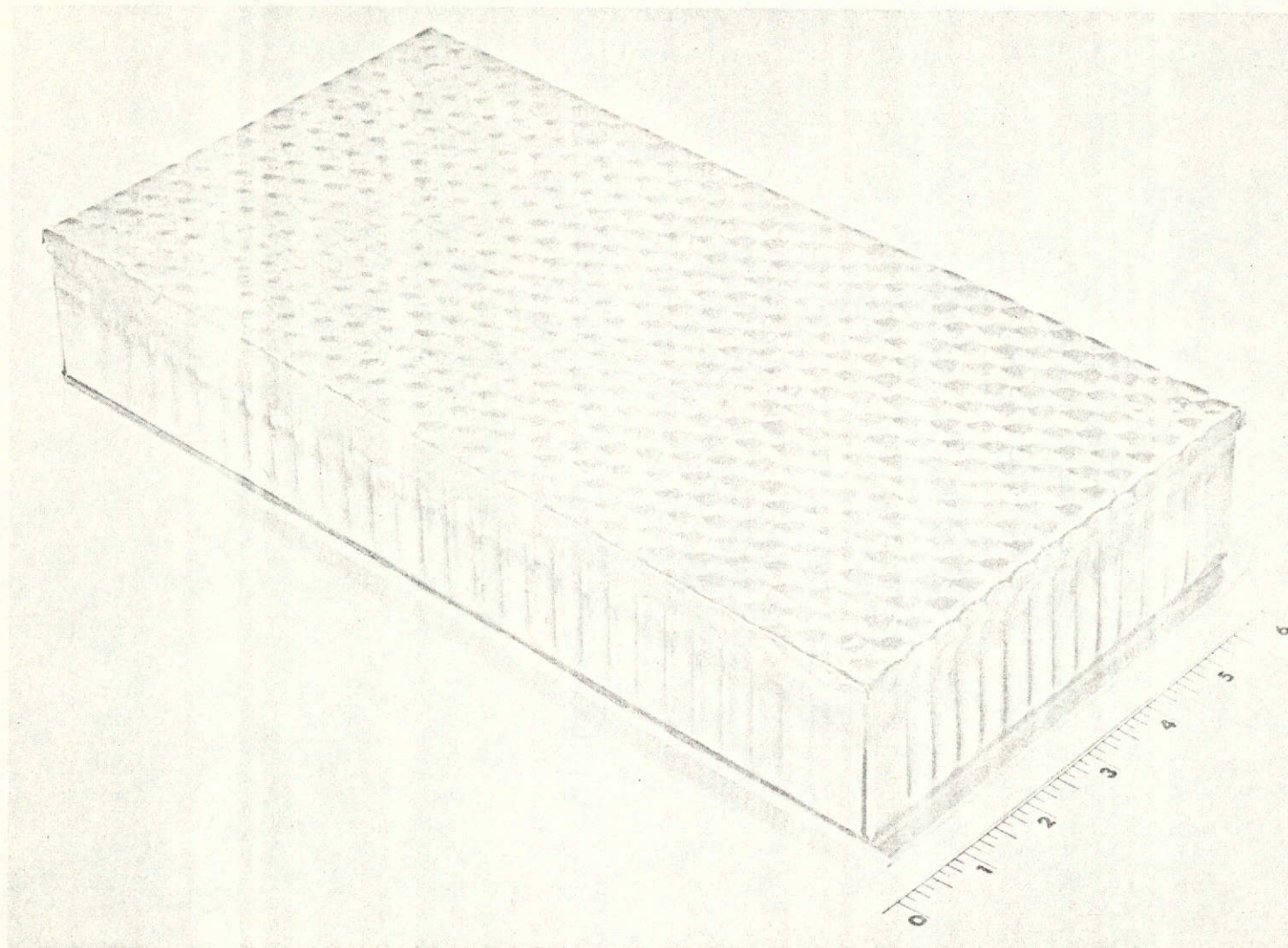


Figure 4.26 POST TEST APPEARANCE OF SECOND FLOATING TOP SPECIMEN
AFTER ONE 1800° F THERMAL CYCLE (SPECIMEN 12)

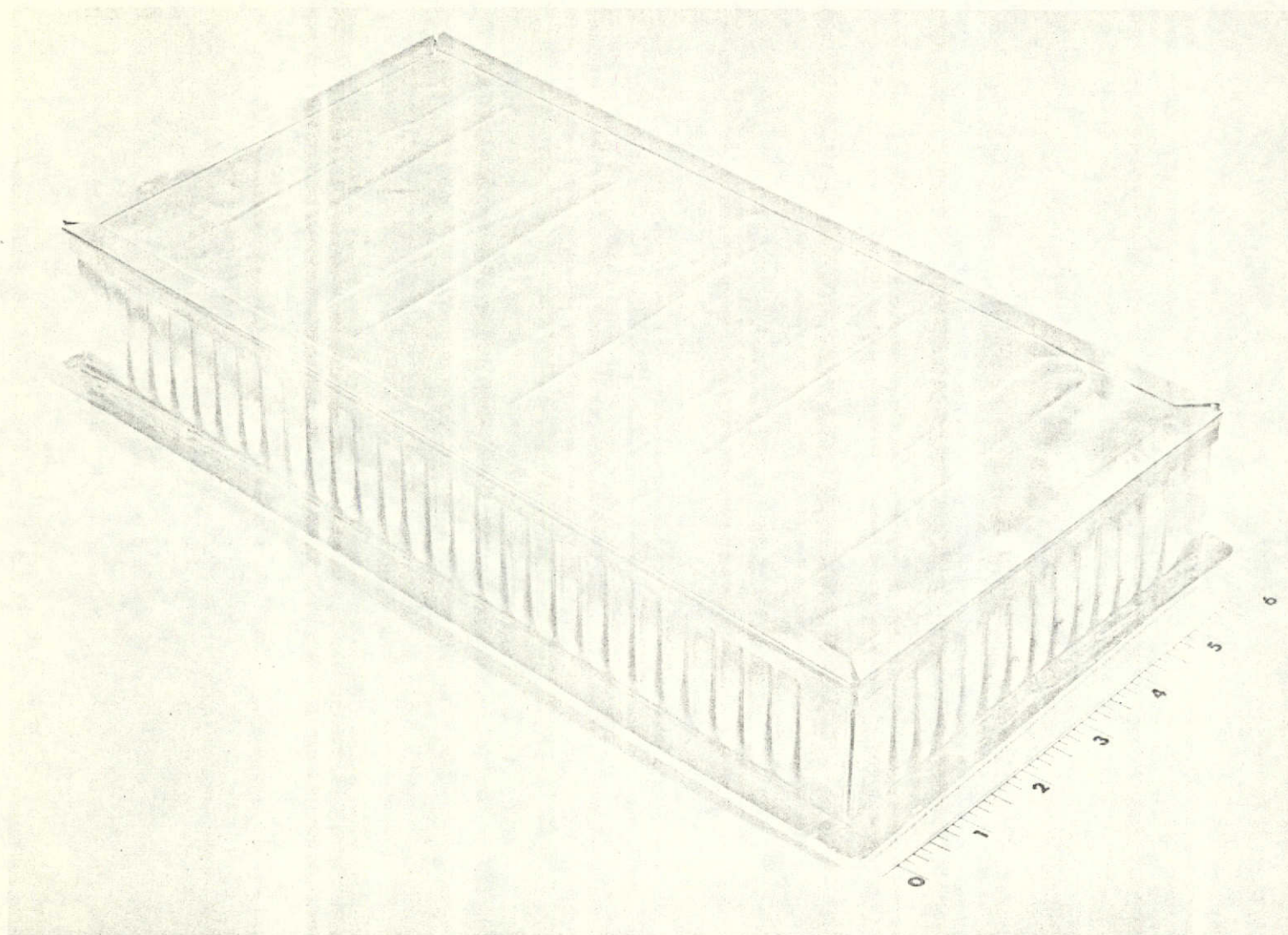
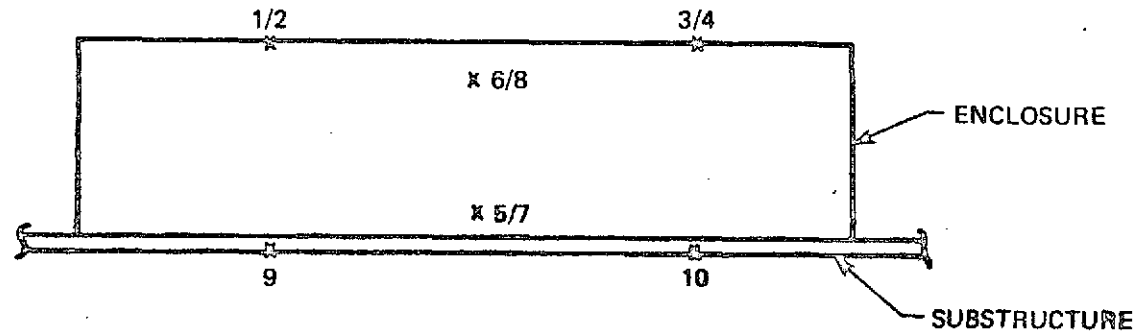
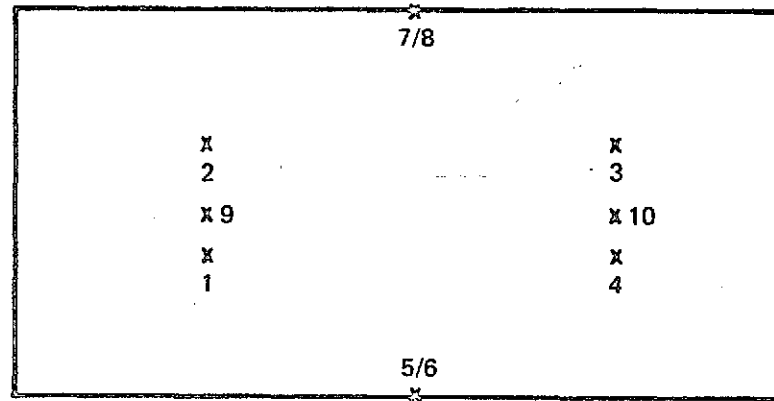
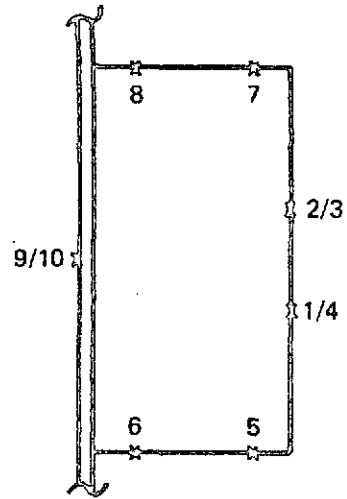


Figure 4.27 POST TEST APPEARANCE OF TENSION TOP SPECIMEN AFTER
ONE 1800° F THERMAL CYCLE (SPECIMEN 13)



83-1427

Figure 4.28 THERMOCOUPLE LOCATIONS

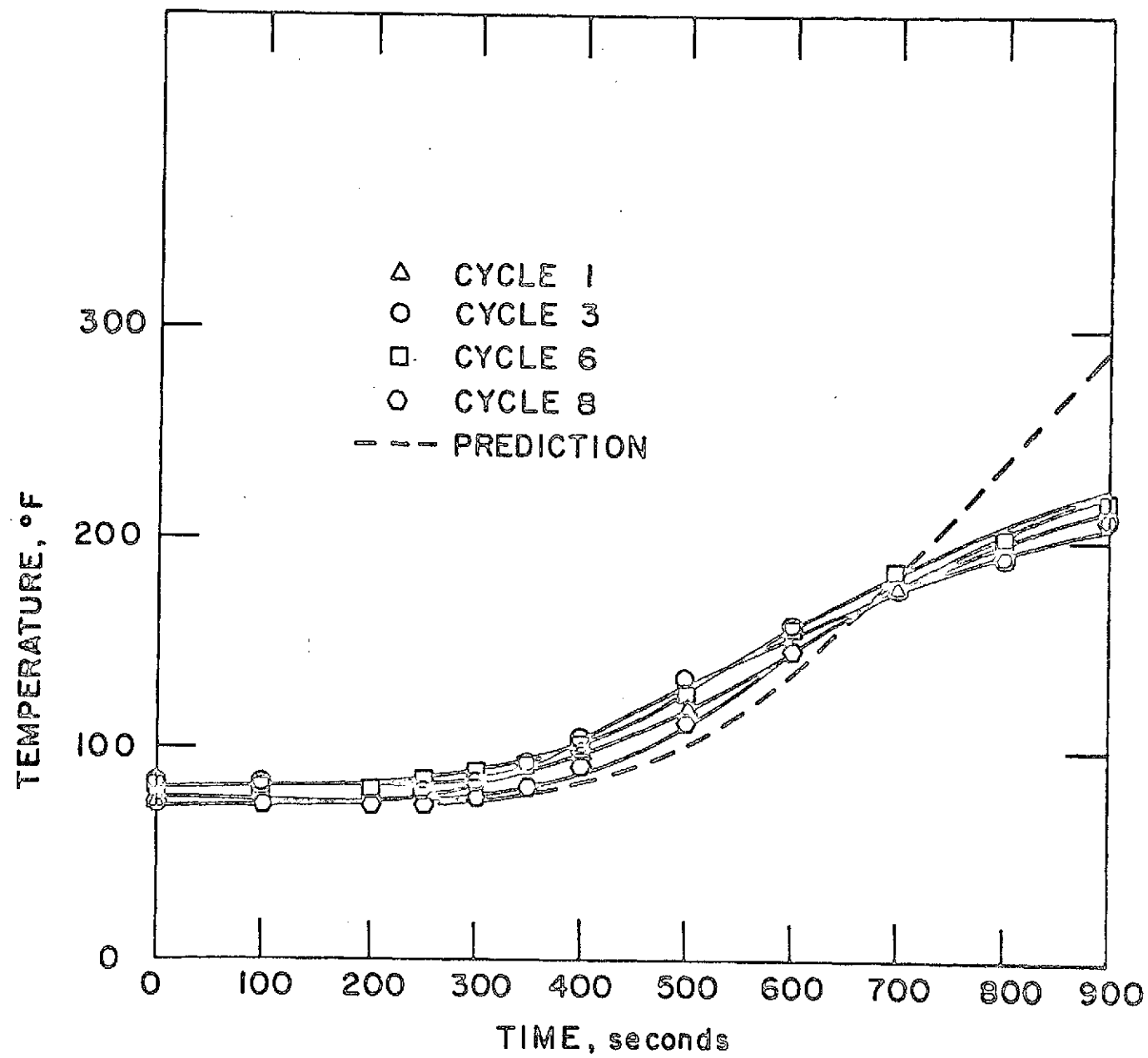


Figure 4.29 STRUCTURE TEMPERATURE RESPONSE DATA (SPECIMEN 7)

thermal isolation of the structure and to three-dimensional heat transfer effects in the structure and mounting system. At early times, while backface temperatures and heat losses are low, the comparison is good. The low heat rates through the two-inch thickness of insulation made the structure response very sensitive to non-isothermal effects at the rear of the specimen. Thermal testing adequate for verification of transient response analysis would require larger specimens and more careful control of thermal losses than was feasible in these tests.

4.2 Acoustic Testing

Four acoustic tests, each of five minutes duration (simulating ten launches), were performed at the facilities of Noise Unlimited, Inc., Somerville, N. J. Figure 4.30 shows the configuration of the panel prior to the first acoustic exposure. It is the same panel subjected to the single 1800° F thermal exposure in the closed chamber with the reduced oxygen partial pressure described in Section 4.2 and Figure 4.31, except that the 3-mil Hastelloy-X specimen (Specimen 3) was replaced by the first floating top specimen (Specimen 7) and Specimen 2 was replaced by Specimen 8 which was of the same configuration (simple textured box). Specimens 7 and 8 were of particular interest because they had previously undergone single thermal cycles at 1200°, 1400°, and 1600°; and ten cycles at 1800° F surface temperature in the room ambient heating facility. The other four specimens were all the simple textured box design and had been previously exposed only to the single 1800° F thermal cycle.

The test environment was an overall sound pressure level of 154 dB with the spectral distribution indicated in Table XIII. Following the test, all six specimens were visually examined for fatigue cracks with the aid of Zyglo. The only apparent degradation which could be attributed to the acoustic exposure was a slight propagation of existing cracks in the 5-mil Haynes 25 specimens (Specimens 5 and 6), which had been previously initiated during the thermal exposure.

The second 5 minute acoustic exposure (also 154 dB) was performed on the same panel but with Specimens 4 and 5 replaced by two of the second generation Hastelloy-X specimens (Specimens 9 and 10). These two specimens incorporated stiffened top/side edges and flexible sides and had each been exposed to ten thermal cycles at 1800° F prior to the second acoustic test. No further thermal exposure of the other four specimens (1, 2, 7, and 4) was performed between the first and second acoustic tests.

No further damage was incurred by five of the six specimens subjected to the second acoustic exposure. However, Specimen 9 did show evidence of an incipient fatigue failure. A number of the individual hexagons in the texture pattern developed surface cracks. These were consistently oriented in the same location in the hexagon as shown in Figure 4.31 and appeared to extend approximately halfway through the foil thickness. It should be noted that six other specimens textured with the same pattern did not show this type of damage. The consistent location of the cracks relative to the hexagon pattern

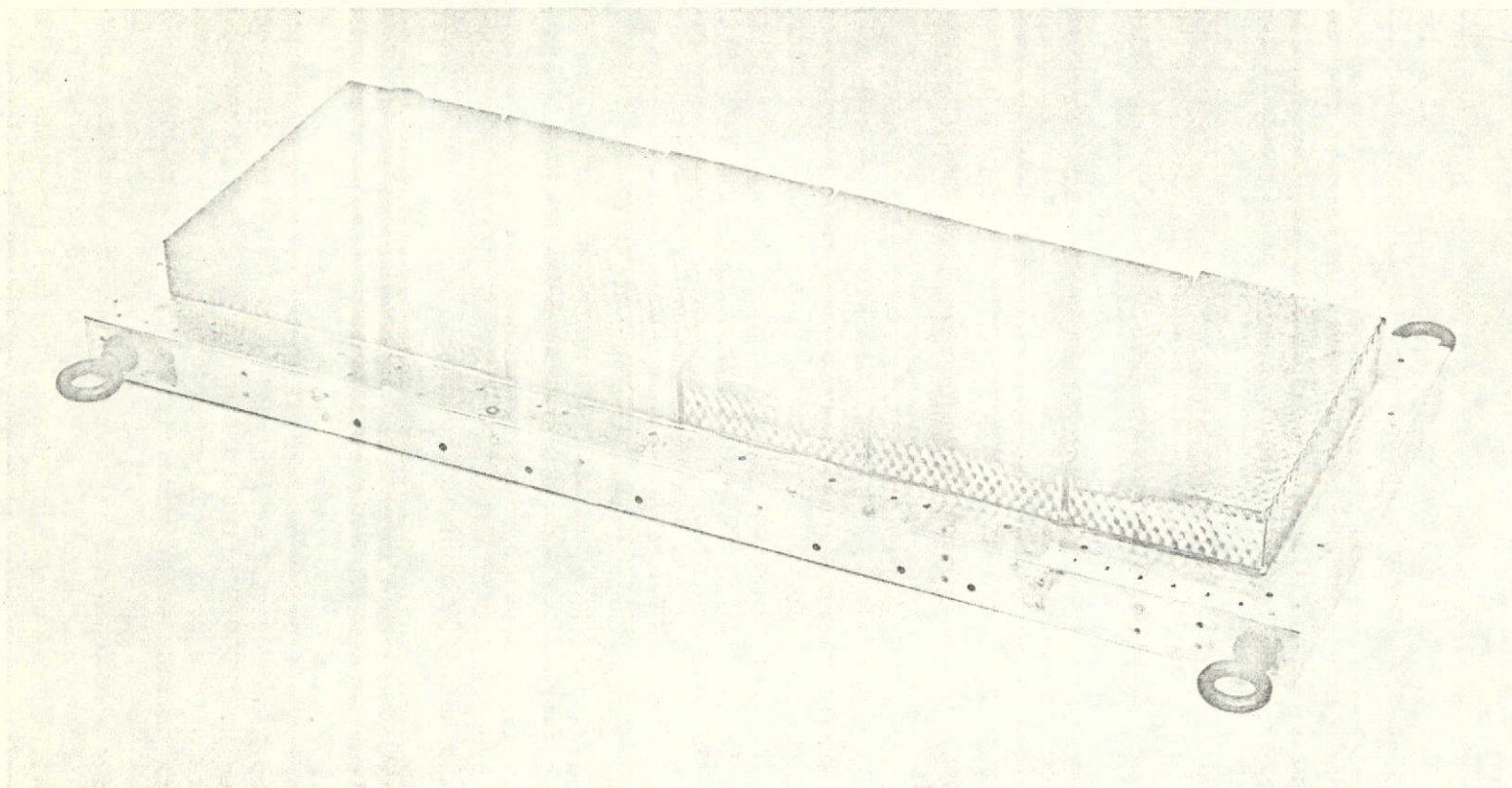


Figure 4.30 ACOUSTIC/THERMAL TEST PANEL PRIOR TO FIRST ACOUSTIC TEST

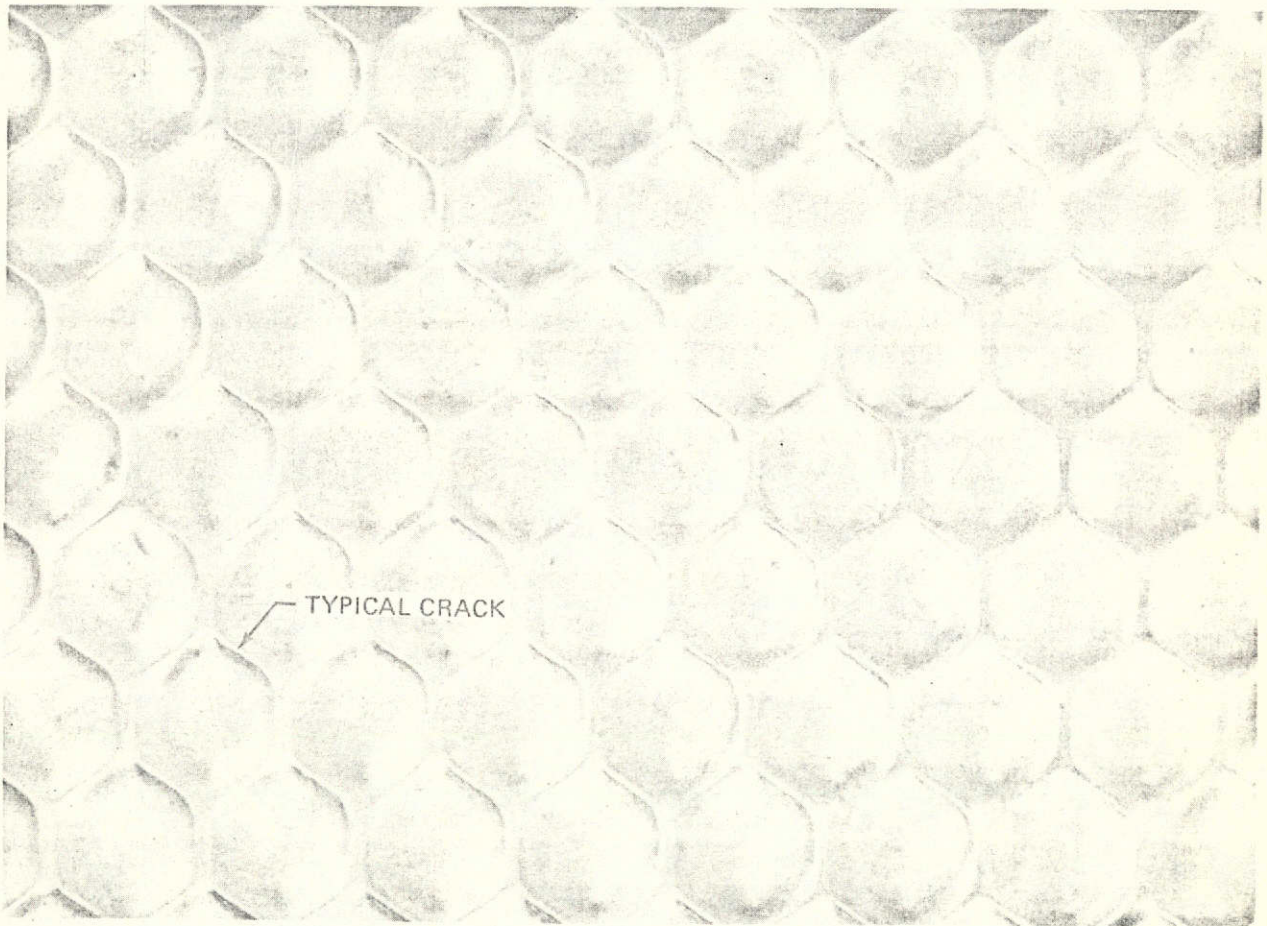


Figure 4.31 FATIGUE CRACK LOCATION IN HEX PATTERN ON TOP OF SPECIMEN 9

TABLE XIII

ACOUSTIC CALIBRATION DATA

Octave Band Centerline (Hz)	Sound Pressure Level for First Test (1 May) (dB)	Sound Pressure Level for Second Test (24 May) (dB)	Sound Pressure Level for Third Test (13 July) (dB)
31.5	134	135	146
63	138	138	146
125	142	147	162
250	149	146	161
500	151	150	158
1000	146	146	158
2000	140	143	154
4000	134	137	147
Overall	154	154	168
Test Duration*	5 min.	5 min.	10 min.

*.5 minute is equivalent to 1 mission.

suggests that the individual dimples in the texture may have had natural frequencies which were excited by the acoustic environment.

Several parameters are slightly different for the damaged specimen which may contribute to a difference in critical frequency and resulting acoustic damage susceptibility. The material was from a different batch, purchased and textured at a different time. The depth of the texture was also slightly greater (inadvertantly) than in the undamaged specimens.

The third and fourth acoustic exposures were at a level of 168 dB overall, again for 5 minutes each on Specimens 6, 7, 8, and 9. The spectral distribution is indicated in Table XIII. The overall level and the distribution were obtained from Reference 10 and represents the current design environment for the base heating region of the shuttle orbiter.

Inspection of the four specimens following the first five minute exposure at 168 dB revealed that two of the tie wires attaching the surface foil to the structure were loosened. No further damage was apparent to any of the specimens. Again, no further damage was apparent in any of the four specimens during the second five minute exposure at 168 dB.

Disassembly of the specimens following the acoustic exposure revealed that the tie wire loosening in the floating top specimen was caused by tie strap failures around the weld where the strap is attached to the surface foil. The tie straps, which are made of 3-mil foil, were badly oxidized. This probably contributed greatly to the observed failure and should be easily remedied by increasing the thickness of the tie strap foil.

The 3DSX insulation was in good condition with no evidence of thermal or structural degradation, even where it contacted the hot surface foil. Some trivial damage in the form of local fiber breakage occurred at the location of the tie wire penetrations. No further damage was observed in the cracked areas of the texture pattern of Specimen 9 which were originally observed after the 154 dB test.

It is concluded that the two five minute exposures to the 168 dB acoustic environment introduced no significant damage beyond that already in the specimens prior to exposure. As observed in the previous tests, the panel design must be such to prevent edge crippling since the crippled areas are susceptible to fatigue in both the thermal and acoustic environments. The stiffened edge designs used in Specimens 9 through 13 were demonstrated effective in eliminating the crippling problem.

REFERENCES

1. High Temperature Insulation Materials for Reradiative Thermal Protection Systems, McDonnell Douglas Astronautics Company for NASA/MSFC (Contract NAS-8-26115).
2. Fabrication of Avco 3DSX Silica-ceramic Material, Avco Systems Division for NASA/MSFC, July-November 1971 (Contract NAS-9-10921).
3. AVSD-0419-72-RR Development and Fabrication of Low Density Fiber Reinforced Silica Ceramic Materials, Avco Systems Division for NASA/MSFC, November 1972 (Contract NAS-9-12490).
4. Timashenko, et al., Theory of Plates and Shells, 2nd Edition, McGraw-Hill, New York, 1959.
5. Kordes, E. E., et al., Flutter Research on Skin Panels, NASA TN D-459 Sept. 1970.
6. Dixon S. C., and C. P. Shore, State of the Art for Panel Flutter as Applied to Space Shuttle Heat Shields, NASA TMX-52876 Vol II, pp. 199-221, 1970.
7. McElman, J. A., "Flutter of Two Parallel Plates Connected by an Elastic Medium". AIAA J. (2), pp. 377-379, 1964.
8. Kordes, E. E., et al., Flutter Research on Skin Panels, NASA TND-459 Sept. 1970.
9. Sundra Raja Iyengar, K. T., et al., "Thermal Stresses in Restrained Rectangular Plates" Journal of the Engineering Mechanics Division, ASCE, February 1968.
10. Specification No. MC364-0006, Insulation, High Temperature Reusable Surface, Shuttle Orbiter, 12 February 1973, Space Division, North American Rockwell Corporation.